

Near Infrared Determination of Lactate in Biological Fluids and Tissues

Denis Lafrance

Department of Chemistry

McGill University,

Montreal, Quebec

Canada

January, 2003

*A thesis submitted to the Faculty of Graduate Studies and Research in partial
fulfillment of the requirements of the degree of Doctor of Philosophy*



Library and
Archives Canada

Bibliothèque et
Archives Canada

Published Heritage
Branch

Direction du
Patrimoine de l'édition

395 Wellington Street
Ottawa ON K1A 0N4
Canada

395, rue Wellington
Ottawa ON K1A 0N4
Canada

Your file Votre référence

ISBN: 0-612-98401-X

Our file Notre référence

ISBN: 0-612-98401-X

NOTICE:

The author has granted a non-exclusive license allowing Library and Archives Canada to reproduce, publish, archive, preserve, conserve, communicate to the public by telecommunication or on the Internet, loan, distribute and sell theses worldwide, for commercial or non-commercial purposes, in microform, paper, electronic and/or any other formats.

The author retains copyright ownership and moral rights in this thesis. Neither the thesis nor substantial extracts from it may be printed or otherwise reproduced without the author's permission.

AVIS:

L'auteur a accordé une licence non exclusive permettant à la Bibliothèque et Archives Canada de reproduire, publier, archiver, sauvegarder, conserver, transmettre au public par télécommunication ou par l'Internet, prêter, distribuer et vendre des thèses partout dans le monde, à des fins commerciales ou autres, sur support microforme, papier, électronique et/ou autres formats.

L'auteur conserve la propriété du droit d'auteur et des droits moraux qui protègent cette thèse. Ni la thèse ni des extraits substantiels de celle-ci ne doivent être imprimés ou autrement reproduits sans son autorisation.

In compliance with the Canadian Privacy Act some supporting forms may have been removed from this thesis.

Conformément à la loi canadienne sur la protection de la vie privée, quelques formulaires secondaires ont été enlevés de cette thèse.

While these forms may be included in the document page count, their removal does not represent any loss of content from the thesis.

Bien que ces formulaires aient inclus dans la pagination, il n'y aura aucun contenu manquant.


Canada

Abstract

Lactate is a key metabolite of glycolytic activity and as such, can be used as an indicator of the energy production of the whole organism, for the assessment of tissue perfusion and oxidative capacity. Estimating lactate levels in biological fluids allows the determination of anaerobic threshold during physical exercise. Likewise, lactate is of significant importance in several clinical situations, where a rapid and easy method is needed for diagnostic assessment and survival rate increase of the patient.

To achieve this objective, the potential of Near Infrared Spectroscopy (NIRS) to quantify lactate in biological fluids and tissues was evaluated. Initially, the project focused on quantifying of lactate in plasma samples taken from exercising humans. Using Partial Least Squares (PLS) and a leave-*N*-out cross validation routine, it was found that lactate concentration in human plasma could be estimated with a standard error of cross validation of 0.51 mmol/L.

To minimize sample preparation and reduce the time of analysis, NIRS was then evaluated as a technique for rapid analysis of lactate in whole blood from exercising rats and humans. Furthermore, standard addition method was used to expand the lactate concentration range and therefore cover a greater part of the physiological lactate concentration range. Regression analysis provided standard

errors of cross validation of 0.29 mmol/L and 0.65 mmol/L for rats and humans respectively.

To improve precision, referenced lactate measurements were calculated. In this method, baseline spectra of subjects were subtracted from all collected spectra before chemometric routines were used. An improvement of the standard error of cross validation to 0.21 mmol/L was found by applying this procedure.

In vivo measurement of lactate during exercise in humans by NIRS was also evaluated. Using diffuse reflectance and 2D correlation spectroscopy, lactate was identified as the primary constituent monitored by *in vivo* measurements. Regression analysis resulted in a substantial error of 2.21 mmol/L for absolute measurements. However, results for referenced lactate measurements provided a significant improvement of the standard error of cross validation to 0.76 mmol/L. This finding suggests that NIRS may provide a valuable tool to assess *in vivo* physiological status for both research and clinical needs.

Résumé

Le lactate est un métabolite clé de l'activité glycolytique et peut donc être utilisé comme indicateur de la production d'énergie d'un organisme vivant, l'évaluation de la perfusion d'un tissu ou la capacité oxydante de l'organisme. La capacité d'estimer la concentration de lactate dans les fluides biologiques permet la détermination du seuil anaérobie lors d'exercice physique. De plus, la concentration de lactate est souvent critique dans plusieurs situations cliniques, où une méthode d'analyse rapide et simple est nécessaire pour poser rapidement un diagnostic et ainsi accroître les chances de survie du patient.

Pour atteindre cet objectif, la possibilité d'utiliser la spectroscopie proche infrarouge (SPIR) pour quantifier le lactate a été évaluée. Initialement, le projet se penchait sur la quantification du lactate dans des échantillons de plasma humain après un exercice physique. En utilisant la méthode de *Partial Least Squares* et une routine de validation croisée, il a été démontré que la concentration de lactate pouvait être estimée avec une erreur de 0.51 mmol/L.

Afin de minimiser la préparation des échantillons et de réduire le temps d'analyse, SPIR a été évalué pour l'analyse du lactate dans des échantillons de sang provenant de rats et d'humains après exercice. De plus, afin d'étendre la plage de concentration du lactate et couvrir une plus large portion de la plage physiologique, des ajouts dosés ont été utilisés. L'erreur standard obtenue a été de 0.29 mmol/L et 0.65 mmol/L chez les rats et les humains respectivement.

Afin d'améliorer la précision de l'analyse, une méthode de mesure du lactate par référencement a été élaborée. Cette méthode consiste à soustraire le spectre au repos de chaque individu à chacun des autres spectres. En utilisant cette méthode, l'erreur standard a été ramenée à 0.21 mmol/L.

Finalement, le potentiel de SPIR a été évalué pour des mesures *in vivo* du lactate durant un exercice chez l'humain. En utilisant la réflectance diffuse et la spectroscopie de corrélation 2D, il a été démontré que le lactate était le principal constituant du sang mesuré par les analyses *in vivo*. L'analyse procure une erreur standard de 2.21 mmol/L. Par contre, la méthode par référencement permet d'atteindre une erreur standard de 0.76 mmol/L. Ce résultat suggère que SPIR puisse permettre d'évaluer l'état physiologique *in vivo* d'un patient et ainsi répondre aux besoins de la recherche et des situations cliniques.

Table of Contents

<i>Foreword</i>	<i>ix</i>
<i>Contribution of Authors</i>	<i>xi</i>
<i>Contribution to Original Knowledge</i>	<i>xv</i>
<i>Acknowledgements</i>	<i>xvi</i>
<i>List of Figures</i>	<i>xviii</i>
<i>List of Tables</i>	<i>xx</i>
CHAPTER 1 <i>Introduction</i>	<i>1</i>
1.0 Project Overview and Research Objectives	1
 CHAPTER 2 <i>Background to Near Infrared Spectroscopy of Metabolism</i>	<i>5</i>
2.0 Introduction to Near Infrared Spectroscopy.....	5
2.1 Near Infrared Spectroscopy for Metabolic Measurements	8
2.1.1 Overview.....	8
2.1.2 Metabolic Measurements	9
2.1.3 Conclusion	34
2.1.4 References.....	36
 CHAPTER 3 <i>Near Infrared Spectroscopic Measurement of Lactate in Human Plasma</i>	<i>57</i>
3.1 Abstract	58
3.2 Introduction	59
3.3 Experimental	61
3.3.1 Instrumentation	61
3.3.2 Reagents.....	62
3.3.3 Procedures.....	62
3.4 Results and Discussion.....	64
3.4.1 Spectral Features.....	64
3.4.2 Experimental Protocol for Minimal Covariance with Plasma Constituents	67
3.4.3 Optical Pathlength.....	68
3.4.4 PLS Calibration Models.....	68

3.5	Conclusion	73
3.6	References	74

CHAPTER 4 *Lactate Measurement in Whole Blood using Near Infrared Spectroscopy.....77*

4.1	Abstract	78
4.2	Introduction	79
4.3	Materials and Methods.....	80
4.3.1	Instrumentation	80
4.3.2	Reagents.....	81
4.3.3	Procedure	82
4.3.4	Partial Least Squares Analysis.....	82
4.4	Results and Discussion.....	84
4.4.1	Spectral Features.....	84
4.4.2	Optical Pathlength.....	84
4.4.3	PLS Calibration Models.....	87
4.5	Conclusion	92
4.6	References	93

CHAPTER 5 *Measurement of Lactate in Whole Human Blood with Near-Infrared Transmission Spectroscopy.96*

5.1	Abstract	97
5.2	Introduction	98
5.3	Experimental	100
5.3.1	Instrumentation	100
5.3.2	Sample Collection.....	100
5.3.3	Sample Preparation	101
5.3.4	Data Collection	103
5.3.5	Data analysis.....	103
5.4	Results and Discussion.....	105
5.5	Conclusion	111
5.6	References	114

**CHAPTER 6 *In vivo Lactate Measurement in Human tissue by
Near- Infrared Diffuse Reflectance Spectroscopy...*** 116

6.1 Instrument Configuration	118
6.2 Abstract	122
6.3 Introduction	122
6.4 Materials and Methods.....	124
6.4.1 Sample Collection.....	124
6.4.2 Data Collection	125
6.4.3 Data analysis	126
6.5 Results and Discussion.....	128
6.6 Conclusion	141
6.7 References	142

CHAPTER 7 *Conclusion*..... 146

7.1 Results	146
7.2 Future directions.....	149
7.3 References	154

***Appendix A: Partial Least Squares Analysis*.....** 155

References	157
------------------	-----

***Appendix B: 2D Correlation Spectroscopy*.....** 158

References	161
------------------	-----

***Appendix C: Ethic Committee Approval*.....** 162

***Appendix D: Copyright Clearance*.....**160

Foreword

In accordance with section C of the "Guidelines for Thesis Preparation" (Faculty of Graduate Studies and Research), the following text is cited:

"As an alternative to the traditional thesis format, the dissertation can consist of a collection of papers of which the student is an author or co-author. These papers must have a cohesive, unitary character making them a report of a single program of research. The structure for the manuscript-based thesis must conform to the following:

Candidates have the option of including, as part of the thesis, the text of one or more papers submitted, or to be submitted, for publication, or the clearly-duplicated text (not the reprints) of one or more published papers. These texts must conform to the "Guidelines for Thesis Preparation" with respect to font size, line spacing and margin sizes and must be bound together as an integral part of the thesis. (Reprints of published papers can be included in the appendices at the end of the thesis.)

The thesis must be more than a collection of manuscripts. All components must be integrated into a cohesive unit with a logical progression from one chapter to the next. In order to ensure that the thesis has continuity, connecting texts that provide logical bridges between the different papers are mandatory.

The thesis must conform to all other requirements of the "Guidelines for Thesis Preparation" in addition to the manuscripts. The thesis must include the

following: (a) a table of contents; (b) an abstract in English and French; (c) an introduction which clearly states the rationale and objectives of the research; (d) a comprehensive review of the literature (in addition to that covered in the introduction to each paper); (e) a final conclusion and summary;

As manuscripts for publication are frequently very concise documents, where appropriate, additional material must be provided (e.g., in appendices) in sufficient detail to allow a clear and precise judgement to be made of the importance and originality of the research reported in the thesis.

In general, when co-authored papers are included in a thesis the candidate must have made a substantial contribution to all papers included in the thesis. In addition, the candidate is required to make an explicit statement in the thesis as to who contributed to such work and to what extent. This statement should appear in a single section entitled "Contributions of Authors" as a preface to the thesis. The supervisor must attest to the accuracy of this statement at the doctoral oral defense. Since the task of the examiners is made more difficult in these cases, it is in the candidate's interest to clearly specify the responsibilities of all the authors of the co-authored papers.

When previously published copyright material is presented in a thesis, the candidate must include signed waivers from the co-authors and publishers and submit these to the Thesis Office with the final deposition, if not submitted previously."

Contribution of Authors

Listed below are the articles included as part of this dissertation and an outline of the responsibility of each author. Overall, Dr. Burns was both thesis supervisor and critical reviewer to Mr. Lafrance.

Chapter 2

Lafrance D.; Burns, D.H. Near Infrared Spectroscopy for Metabolic Measurements, in: Useful and advance information in the field of NIR spectroscopy, Publisher Research Signpost, in press Fall of 2002

This review article was written as a contribution to: Useful and advance information in the field of NIR spectroscopy. The literature review was done by Mr. Lafrance. The manuscript prepared for publication was written by Mr. Lafrance and edited by Dr. Burns.

Chapter 3

Lafrance D.; Lands L.C.; Hornby L.; Burns D.H. Near Infrared Spectroscopic Measurement of Lactate in Human Plasma, *Appl. Spectrosc.* **2000**, *54*, 300-304.

Mr. Lafrance co-designed along with Drs. Burns and Lands the experimental procedure to quantify lactate in human plasma. Mr. Lafrance designed the thermostated sample holder for the FT-NIR instrument. Mrs Hornby did the sample preparation and the enzymatic lactate measurements using the YSI SPORT Model

1502 instrument. Mr. Lafrance collected the FT-NIR spectra of plasma samples, measured pH of the samples and analyzed all experimental data. Dr. Lands designed and developed the isokinetic cycle. Dr. Burns proposed the leave-N-out cross validation method to estimate lactate in human plasma. The manuscript prepared for publication was written by Mr. Lafrance and edited by Drs. Burns and Lands.

Chapter 4

Lafrance D.; Lands L.C.; Hornby L.; Rohlicek C.; Burns D.H. Lactate Measurement in Whole Blood using Near Infrared Spectroscopy, *Can. J. Anal. Sci. Spectrosc.* **2000**, *45*, 36-40.

Dr. Rohlicek provided the blood samples. Mrs Hornby did the sample preparation and the enzymatic lactate measurements using the YSI SPORT Model 1502 instrument. Mr. Lafrance designed the experimental procedure to quantify lactate in whole blood from exercising rats and the thermostated sample holder for the FT-NIR instrument. Mr. Lafrance collected the FT-NIR spectra of blood samples and analyzed all experimental data. The manuscript prepared for publication was written by Mr. Lafrance and edited by Drs. Burns and Lands.

Chapter 5

Lafrance D.; Lands L.C.; Burns D.H. Measurement of Lactate in Whole Human Blood with Near-Infrared Transmission Spectroscopy, *Talanta*, accepted January 2003.

Mr. Lafrance designed the experimental procedure to quantify lactate in human blood and collected the FT-NIR spectra of blood samples, measured pH of the samples and analyzed all experimental data. Mr. Lafrance suggested the use of standard addition method to extend the lactate concentration range of the samples. Dr. Burns suggested the use of referenced measurements of lactate. The manuscript prepared for publication was written by Mr. Lafrance and edited by Drs. Burns and Lands.

Chapter 6

Lafrance D.; Lands L.C.; Burns D.H. *In vivo* Lactate Measurement in Human tissue by Near-Infrared Diffuse Reflectance Spectroscopy, *Journal of Applied Physiology*, submitted June 2002.

Mr. Lafrance designed the experimental procedure to quantify lactate in human tissue, assembled the instrument, designed the sample holder, collected the FT-NIR spectra through fingernail and analyzed all experimental data. Dr. Lands designed and developed the isokinetic cycle. Dr. Burns suggested the use of 2D correlation spectroscopy to assess the species mostly changing in the NIR spectra. The 2D correlation algorithm originally written by Dr. Burns was expanded upon by Mr. Lafrance. The manuscript prepared for publication was written by Mr. Lafrance and edited by Drs. Burns and Lands.

Contribution to Original Knowledge

1. Quantification of lactate in plasma from exercising humans with a standard error within the range needed for real-time monitoring of lactate.
2. Use of the standard addition method in biological samples to allow development of a calibration model that emphasizes the contribution of lactate over other blood species.
3. Quantification of lactate in whole blood from exercising humans with a standard error within the range needed for real-time monitoring of lactate.
4. Use of referenced lactate measurements to improve the precision of the method and minimizing the error due to baseline variations at low lactate concentration.
5. First reported *in vivo* measurements of lactate through fingernail in exercising human.

Acknowledgements

This project has spread over several years and has involved a lot of hard work at night and during most of the weekends. I have many people to thank for their support, patience and assistance throughout this entire project.

I would like first to thank my supervisor Professor David H. Burns, for his support and good advise during my work at McGill. Dave was always there to bring me “back on track” when it was needed and for telling me “I want to make sure you will graduate”. Thanks Dave.

I also thank Larry Leonardi, William Long, He Xiao, Ania Fafara and Claudia Gributs who made my days spent at McGill very interesting.

A very special thank for all those valiant volunteers whom by the blood samples they provided, some of you more than once, have made this work possible. So thank you Dave, Larry, Xiao, Anny, Adolfo, Aurelio, Mario, Brigitte, Suzanne (at least you tried), Simon, Olivier, Gilles, Claude, Margaret and Claudia.

Une pensée très spéciale à mes deux enfants, Paola et Thomas, qui, à travers leur émerveillement à découvrir et apprendre le monde les entourant, m’ont insufflé le désir et l’énergie de poursuivre mon travail, me permettant ainsi d’atteindre l’objectif que je m’étais fixé.

Finalmente, quiero agradecer a mi esposa Brigitte, por su paciencia, su apoyo y su amor. Tu apoyo fue incondicional durante todo estos años, aunque varios fines de semana y noches fueron dedicadas a completar el trabajo necesario a esta tesis. Te dedico el resultado de “nuestro” trabajo y esfuerzos. Te amo.

List of Figures

Figure 2.1: Overview of Molecules Important for Respiration.	10
Figure 2.2: Visible and Near Infrared Spectra of Hemoglobin and Myoglobin in the oxygenated and deoxygenated states between 500 nm and 800 nm wavelength range.	12
Figure 2.3: Near Infrared Spectra of Cytochrome aa ₃ in its oxidized (—) and redox (--) states between 700 and 950 nm.	21
Figure 2.4: Near Infrared Spectra of Glucose between a)1500 and 1850 nm b)2000 and 2400 nm after water subtraction.	24
Figure 2.5: Near Infrared Spectra of Lactate between a)1600 and 1750 nm b)2050 and 2400 nm.	31
Figure 3.1: NIR absorbance spectra of human plasma specimens and 10 mmol/L lactate standard in aqueous buffered solution after water subtraction. Lactate standard spectrum has been offset for clarity.	65
Figure 3.2: Second derivative of NIR absorbance spectra of human plasma specimens.	66
Figure 3.3: PRESS plot for lactate cross-validation model based on the 2050 to 2400 nm spectral range.	69
Figure 3.4: Linear regression coefficient plot using 6 PLS factors for the NIR determination of lactate in human plasma.	71
Figure 3.5: NIRS estimated vs. YSI Lactate Analyzer values for human plasma samples for each of the ten subjects. Cross-validation model: 6 PLS factors based on 2050-2400 nm spectral segment.; n=30, r ² =0.995, RMSCV=0.51 mmol/L using a leave-3-out cross-validation procedure.	72
Figure 4.1: NIR absorbance spectra of rat whole blood specimens and 10 mmol/L lactate standard in aqueous buffered solution after water subtraction. Lactate standard spectrum has been offset and identified for clarity.	85
Figure 4.2: Second derivative of NIR absorbance spectra of rat whole blood specimens. Arrows indicate the regions where changes in lactate concentration are contributing.	86

Figure 4.3: PRESS plot for lactate cross-validation model based on the 2050 to 2400 nm spectral range.	88
Figure 4.4: Linear Regression Coefficient plot using 3 PLS factors for the NIR determination of lactate in rat whole blood. Regions where lactate contributes are identified.....	89
Figure 4.5: NIRS estimated vs YSI Lactate Analyser values for rat whole blood samples for each of the three subjects. Cross-validation model: 3 PLS factors based on 2050-2400 nm spectral segment; $n=10$, $r^2=0.984$, RMSCV=0.29 mmol/L using a leave 2 out cross-validation procedure.....	91
Figure 5.1: Second derivative (a) and second derivative difference between spiked and unspiked samples (b) of NIR absorbance spectra of human whole blood specimens from each of the five subjects.....	107
Figure 5.2: Cumulative PRESS plot for lactate cross-validation model based on the 2050 to 2400 nm spectral range.	108
Figure 5.3: NIRS estimated vs. YSI Lactate Analyzer values for whole human blood samples for each of the five subjects. Cross-validation model: 7 PLS factors based on 2050-2400 nm spectral segment; $n=45$, $r^2=0.978$, RMSCV= 0.65 mmol/L using a leave-9-out cross-validation procedure.....	109
Figure 5.4: NIRS estimated vs. lactate referenced values for whole human blood samples for each of the five subjects. Cross-validation model: 6 PLS factors based on 2050-2400 nm spectral segment; $n=40$, $r^2=0.992$, RMSCV= 0.21 mmol/L using a leave-9-out cross-validation procedure.....	112
Figure 6.1: NIR transmittance spectrum of a typical human nail of 0.75 mm thickness.....	117
Figure 6.2: Schematic diagram of the modified Nicolet Magna-IR 550 FT-NIR spectrometer to allow diffuse reflectance spectroscopy. M1, M4 and M5 mirrors were added to the original setting of the instrument.....	119
Figure 6.3: Front and left side view of the sample holder (with a finger) designed to minimize finger movement during diffuse reflectance measurements of the fingernail bed.	121
Figure 6.4: Correlation coefficient plot based on diffuse reflectance spectra from the fingernails of each of the subjects.	129

Figure 6.5: 2D-NIR correlation spectra (synchronous and asynchronous) based on diffuse reflectance spectra from the fingernails of each of the subjects.....	131
Figure 6.6: PRESS plot for lactate cross-validation model based on the 1500 to 1750nm spectral range.	135
Figure 6.7: Calibration coefficient plot using 4 PLS factors for the <i>in vivo</i> determination of lactate.....	136
Figure 6.8: NIRS estimated vs. Kodak Vitros values for <i>in vivo</i> lactate measurements for each of the ten subjects. Cross-validation model: 4 PLS factors based on 1500-1750nm spectral segment; n=40, $r^2=0.74$, RMSCV= 2.21 mmol/L using a leave-4-out cross-validation procedure.....	138
Figure 6.9: NIRS estimated vs. lactate referenced values for <i>in vivo</i> lactate measurements for each of the ten subjects. Cross-validation model: 5 PLS factors based on 1500-1750 nm spectral segment; n=30, $r^2=0.97$, RMSCV= 0.76 mmol/L using a leave-4-out cross-validation procedure.....	140
Figure 7.1: Second derivative of an average NIR absorbance spectrum from ten healthy human fingernail beds.	152
Figure 7.2: NIRS estimated vs. lactate referenced values for <i>in vivo</i> lactate measurements using the average spectrum method. Cross-validation model: based on 1500-1750 nm spectral segment; n=30, RMSCV= 1.04 mmol/L using a leave-4-out cross-validation procedure.....	153

List of Tables

Table I: Lactate and glucose concentration changes over the course for each of the ten individuals.....	130
Table II: Correlation coefficients (R) calculated between lactate and other measured meters.....	133

Chapter 1 Introduction

1.0 Project Overview and Research Objectives

The goal of this research was to investigate and develop a method for non-invasive *in vivo* quantification of lactate. Continuous monitoring of lactate is of significant importance, because lactate is a marker for the assessment of tissue perfusion and oxidative capacity. However, most of the standard clinical methods for lactate analysis are not adapted for continuous lactate monitoring. Current techniques are often time-consuming, since there are many steps involved in the analysis. Samples have to be prepared, which lead to cost-inefficiency and often biased results. Near infrared spectroscopy (NIRS) represents an interesting alternative to conventional techniques for *in vivo* measurements ⁽¹⁻⁵⁾, since it is non-invasive and requires little or no sample preparation.

The potential of NIRS as a rapid method to quantify lactate in biological fluids and tissues was investigated. Towards this goal, the research was divided in three phases, each representing increased complexity in the sample systems. In the first phase, lactate is quantified in plasma from exercising humans, to cover a larger part of the physiological range of lactate concentration. This medium represents a relatively low scattering media, but a very complex matrix. Estimates of lactate are made using Partial Least Squares and are compared to a clinical method based on an electrochemical enzymatic reaction. Moreover, to avoid wasting data when building traditional calibration, prediction and validation sets, a special leave-one out

calibration routine is used to correlate lactate concentration with spectral changes in plasma. In this routine, all data related to one individual, rather than just one at a time, are removed from the data set and used as the prediction set in iteration. This is an extension of previous studies where simulated biological matrices were used to estimate lactate.⁽⁶⁻⁹⁾

In the second phase of the research, lactate was estimated in whole blood. Blood represents a much more complex matrix, since red cells induce scattering of the light. Blood samples from exercising rats and PLS, with a leave- N out cross validation routine, are first used to estimate lactate in this scattering medium. With this knowledge gained, standard additions to human whole blood samples are used to extend the lactate concentration range. This was done to cover a broader part of the human physiological range and increase the data set, while minimizing possible covariance with other blood constituents. In addition, the significance of parameters that may impact the spectra baseline and the correlation between the calculated model and the data is studied using referenced measurements of lactate against a baseline spectrum.

In the final phase, *in vivo* measurement of lactate during exercise in humans is investigated by NIRS. To determine the primary constituent that is monitored by the *in vivo* measurements, 2D correlation spectroscopy is used. Furthermore, to improve the precision of the method, referenced measurements of lactate concentration are calculated. The work presented in this section demonstrates the feasibility of *in vivo*

lactate measurements for physiological or clinical use and represents a faster and nondestructive alternative to current enzymatic methods.

This dissertation is presented in seven chapters, which develop the three phases of the research. A brief overview of the project is given in Chapter 1. Chapter 2 provides an introduction to Near Infrared Spectroscopy and a review on the application of Near Infrared Spectroscopy for metabolic measurements. In Chapter 3, the quantification of lactate in human plasma is investigated using PLS which is described in Appendix A. The quantification of lactate in rat whole blood is investigated in Chapter 4, followed by the determination of lactate from human whole blood and the introduction of the referenced measurement method in Chapter 5. The determination of lactate from *in vivo* tissue measurements using diffuse reflectance spectroscopy is described in Chapter 6. In this chapter, the concept of 2D correlation spectroscopy is introduced and described in Appendix B. Finally, Chapter 7 is a summary of the thesis and presents directions for future work related to *in vivo* lactate measurements.

1.1 References

1. F.F. Jobsis, *Science*, **198**, 1264-1267 (1977).
2. F.F. Jobsis, J.H. Keizer, J.C. LaManna and M. Rosenthal, *J. Appl. Physiol.*, **43**, 858-872 (1977).
3. V.W. MacDonald, J.H. Keiser and F.F. Jobsis, *Arch. Biochem. Biophys.*, **184**, 423-430 (1977).
4. J.M. Colacino, B. Grubb and F.F. Jobsis, *Neurol. Res.*, **3**, 17-31 (1981).
5. C.A. Piantadosi, A.L. Sylvia and F.F. Jobsis, *J. Clin. Invest.*, **72**, 1224-1233 (1983).
6. H. Chung, M.A. Arnold, M. Rhiel, and D.W. Murhammer, *Appl. Spectrosc.*, **50**, 270-276 (1996).
7. M.J. McShane, G.L. Coté, and C.H. Spiegelman, *Appl. Spectrosc.*, **52**, 878-884 (1998).
8. M.J. McShane and G.L. Coté, *Appl. Spectrosc.*, **52**, 1073-1078 (1998).
9. K.H. Hazen, M.A. Arnold, and G.W. Small, *Anal. Chim. Acta*, **371**, 255-267 (1998).

Chapter 2 **Background to Near Infrared Spectroscopy of Metabolism**

In this chapter, the application of Near Infrared Spectroscopy to the field of metabolic measurements is reviewed. This review article was written as a contribution to "Useful and advance information in the field of NIR spectroscopy". Before this review, a brief introduction to the field of Near Infrared Spectroscopy is provided for a better understanding of the technique involved.

2.0 *Introduction to Near Infrared Spectroscopy*

The astronomer William Hershel was the first to identify in 1800 the infrared region of the electromagnetic spectrum, when he was conducting an experiment to determine which color of the visible spectrum was responsible for the heat in sunlight. By positioning a thermometer at each color coming from the decomposition of sun's white light using a glass prism, he noticed that not much happened. It was only after the thermometer was positioned below the red end of the spectrum that a temperature change was noticed.⁽¹⁾ This invisible light was named infrared, which means "below red".

For many years, the infrared spectrum remained a curiosity, mostly because it was more difficult to extract information from this region than from the visible region, where lines and bands could be seen. Furthermore, the invention of the photographic plate made it even easier to study visible and also ultraviolet. It took

the development of radiation dispersion and detection methods and later the development of the first infrared spectrometer in 1900 by Coblentz ⁽²⁾ to see the first recordings of infrared spectra of some organic compounds. However, the first commercial infrared instruments for routine analysis were not available until World War II and were based on the design of those used in the synthetic rubber program in the United States.⁽³⁾

Although instrumentation was now available to record near-infrared spectra, only a few spectroscopists were ready to explore this region. Most of them preferred mid-infrared, since it was found that many compounds exhibited a unique spectrum or "fingerprint" in this region.⁽⁴⁾ In the infrared region, the absorption of radiation causes the molecules to vibrate according to a model similar to an anharmonic oscillator. The energy levels between vibrational transitions in this model can be approximated by:

$$E_v = (v + \frac{1}{2}) \hbar\omega - (v + \frac{1}{2})^2 x_e \hbar\omega + (v + \frac{1}{2})^3 y_e \hbar\omega \dots \quad (v = 0, 1, 2, \dots) \quad 1.1$$

where x_e and y_e are the anharmonicity constants and $\hbar = h/2\pi$. For polyatomic molecules, the equation can be generalized as: ⁽⁵⁾

$$E(v_1, v_2, v_3, \dots) = \sum_{i=1}^{3N-6} (v_i + \frac{1}{2}) \hbar\omega_i \dots \quad (v_1, v_2, v_3, \dots = 0, 1, 2, \dots) \quad 1.2$$

where the transition of energy state is from 0 to 1 in any vibrational states (v_1, v_2, v_3, \dots), the transition is called a *fundamental*. Because anharmonicity allows infringement to the selection rule (where $\Delta v = \pm 1$, as predicted by quantum

mechanics assuming harmonic motion), transitions from ground state to $v_i = 2, 3, \dots$ are allowed and are called *overtones*. Finally, transitions from ground state to a state for which $v_i=1$ and $v_j=1$ simultaneously are known as *combinations*. Results of these “forbidden” transitions can be seen in the Near-Infrared region, which exhibits overlapping and shoulder peaks originating from overtones and combination bands of C-H, N-H and O-H stretching and bending vibrational modes. There are no sharp peaks, often loss of baseline resolution and routinely peaks are between 100 and 1000 weaker than the fundamentals seen in the mid-infrared region. For this reason, the development of Near-Infrared spectroscopy only happened at the end of the 1960s with the work of Karl Norris who was the first to demonstrate that diffuse reflectance spectra of complex biological samples could be obtained.⁽⁶⁾ He was also the first to apply multivariate analysis for making quantitative measurements from complex near-infrared spectra. The four principal advantages offered by this technique are speed, ease of sample preparation, multiplicity of analyses from a single spectrum and the intrinsic non-consumption of the sample.⁽⁷⁾ Following the important findings by Norris and the advantages of the technique, a revived interest in Near-Infrared spectroscopy led to the foundation of a technique that is now used as an analytical tool in a wide variety of fields from agriculture to medicine. Indeed, the result of technical progress and increasing demands for medical treatment and non-invasive diagnostic methods has led to a rapid increase in the use of NIR spectroscopy for biomedical applications. Some of these applications are described in the next section.

2.1 Near Infrared Spectroscopy for Metabolic Measurements

2.1.1 Overview

The term metabolism generally refers to the chemical changes in living cells by which energy is provided for vital processes. Substances, both endogenous and exogenous, that intervene or are by-products of the metabolic processes are called metabolites.

Ability to continuously monitor metabolic activities or metabolites is of importance in critical care or in physiological assessment studies, where measurements are of prognostic significance. Analyses have to be performed by rapid and robust methods to provide real time information to the clinician and, as such, improve diagnosis in critical situations. However, most of the standard clinical methods for metabolite analysis are based on enzymatic assays using photometric or electrochemical detection and not easily adapted for continuous monitoring.

Among the many methods which have been used for clinical measurements, the Near Infrared (NIR) region, which was long thought to be too complex to be useful for analyses, has been found to be useful for monitoring the brain, muscles, the liver and other organs. Furthermore, important advantages such as simplicity and the low cost of instrumentation have made NIR spectroscopy an accepted method for routine monitoring at the patient's bedside.

2.1.2 Metabolic Measurements

Oxygenation and anaerobic metabolites are key parameters of metabolism under various conditions. Noninvasively, NIR spectroscopy is useful to monitor several steps in the metabolic processes of the living organisms (Figure 2.1). Intrinsic indicators such as hemoglobin, myoglobin, cytochrome c oxidase, glucose and lactate have spectral properties that can be observed between 700 and 2500 nm and allow the O_2 supply and consumption to be measured. Likewise, since these molecules are found in various location of the organism, assessment of the respiration can be provided at a system level where organ, tissue and cellular function are monitored simultaneously.

2.1.2.1 Oxygenation

2.1.2.1.1 Hemoglobin/Myoglobin

To monitor metabolic oxygenation by Near Infrared Spectroscopy, both hemoglobin and myoglobin measurements can be used. While hemoglobin is the most abundant and readily detected oxygen-carrying molecule in tissue, myoglobin is present in all skeletal and heart muscle as both an oxygen reservoir and oxygen carrier between hemoglobin and mitochondria.⁽⁸⁾

Oxyhemoglobin (HbO_2) and deoxyhemoglobin (Hb) are the main forms of hemoglobin present in living systems. When the hemes are oxidized to Fe^{3+} , the molecule does not bind oxygen and is termed methemoglobin (metHb). As with hemoglobin, myoglobin can be present in living organisms in three distinct forms: oxymyoglobin (MbO_2), deoxymyoglobin (Mb) and metmyoglobin (metMb).

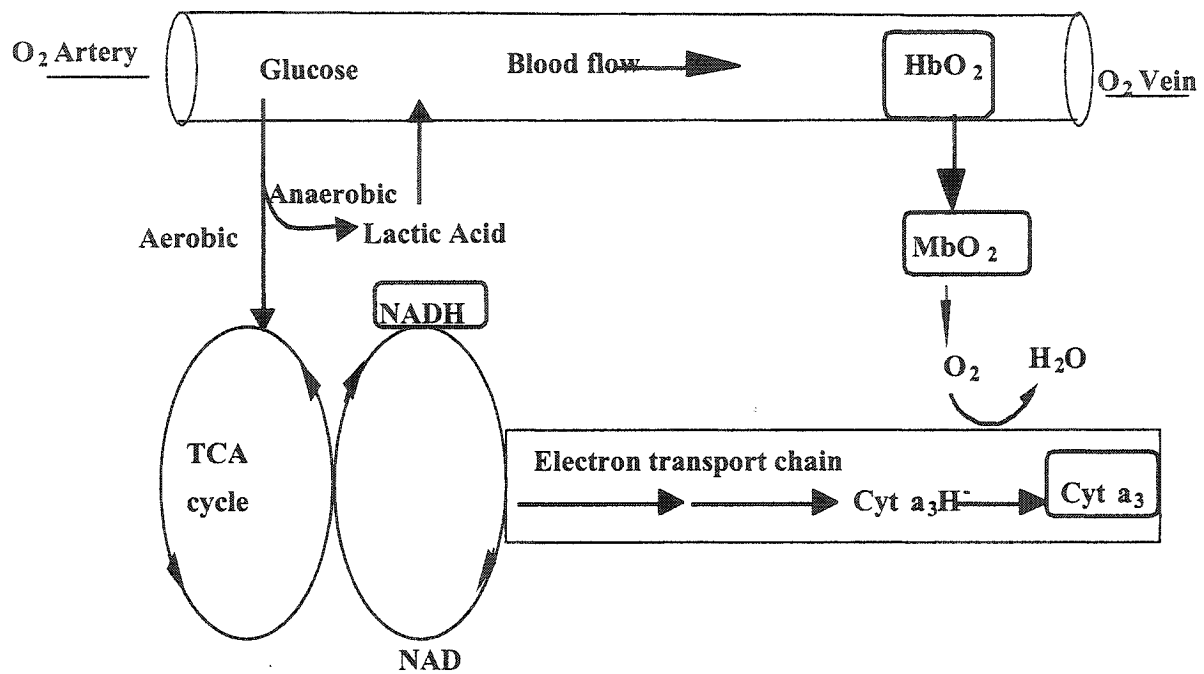


Figure 2.1: Overview of Molecules Important for Respiration.

However, as in methemoglobin, this last form of myoglobin is usually low in living systems due to the presence of reducing enzymes.

The near infrared spectra of oxy and deoxyhemoglobin are dominated by the electronic transitions of the hemes (Figure 2.2). Deoxyhemoglobin has an absorption at 750 nm and oxyhemoglobin is characterized by a broad absorption between 800 and 1000 nm.⁽⁸⁾ In solution, the oxy and deoxy forms of hemoglobin have an isosbestic point at 810 nm. The absorption bands due to electronic transitions in Mb and MbO₂ are different than those obtained from hemoglobin. Deoxymyoglobin has a similar absorption to deoxyhemoglobin but is shifted to 760 nm, whereas MbO₂ is less distinct from the HbO₂ at 900 nm.^(8, 10)

2.1.2.1.1.1 Oxygen Saturation Measurement Techniques

Oxygen saturation, which is related to the oxygen concentration in a sample, can be determined by the ratio of the oxyhemoglobin to the total hemoglobin. The development of the first oximeters was made in the early 1940's, based on dual wavelength measurements.⁽¹¹⁻¹³⁾ The technique had however some important drawbacks. Transferring techniques from isolated fluids directly to tissues was challenging. Background from other constituents in tissue was difficult to eliminate and limited the accuracy of quantification.

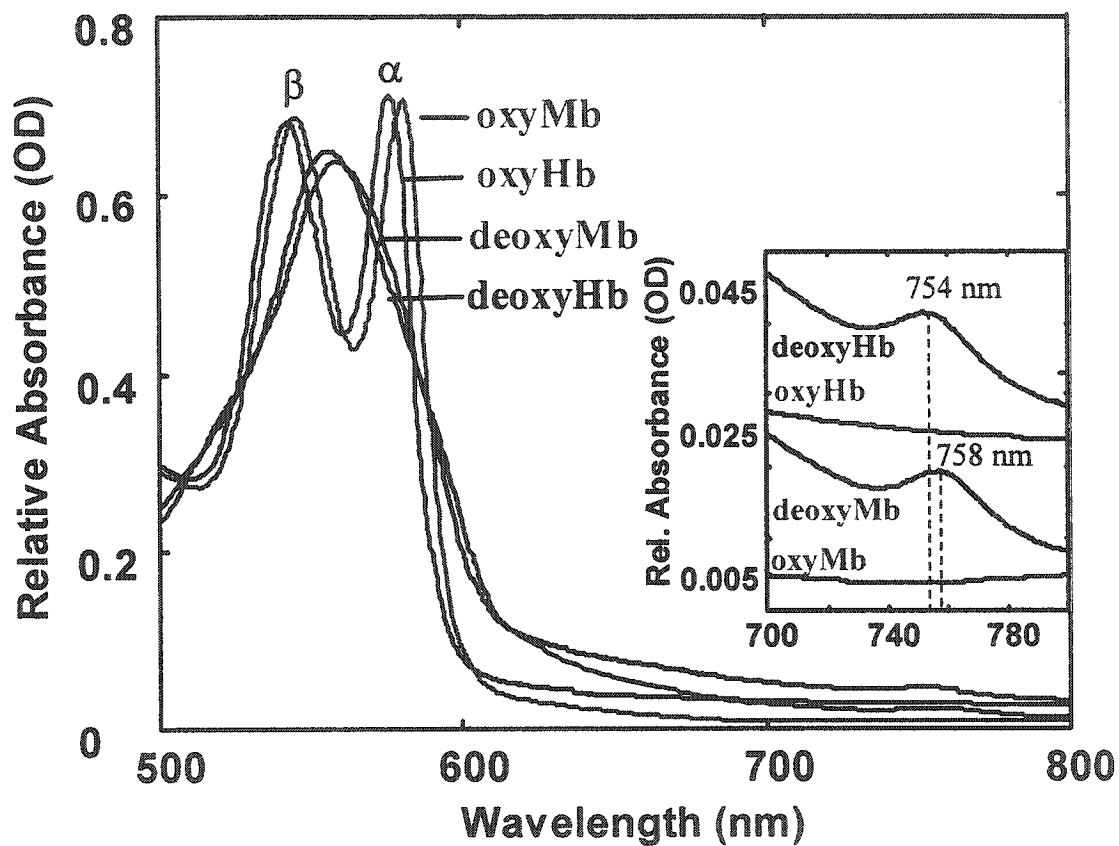


Figure 2.2: Visible and Near Infrared Spectra of Hemoglobin and Myoglobin in the oxygenated and deoxygenated states between 500 nm and 800 nm wavelength range. Both molecules are indistinct above 1000 nm.

To minimize some of these limitations, pulse oximetry was developed for arterial oxygen saturation measurements. With this technique, the pulsatile portion of the signal is used to isolate the contribution caused by the blood volume increase of the arterial component during the cardiac cycle.⁽¹⁴⁾ Because venous blood and tissue absorption do not change as significantly during a pulse, their contributions can be subtracted when measurements are synchronized. Pulse oximetry is based on continuous wave spectroscopy (CWS) in which a certain intensity light is given to the system and an attenuated output is measured. Among various near-infrared methods, it is the simplest and is especially suitable for real-time measurement. However, there are certain limitations that should be considered.⁽¹⁵⁻¹⁷⁾ Low signal-to-noise ratio (SNR), motion artifacts, interference by ambient light, application of probes and changes in scattering can influence the oxygen saturation measurement. To minimize these limitations some technical improvements have been proposed.⁽¹⁸⁻²⁵⁾ It has been shown that the probe geometry has a great influence on the sensitivity of the measurement.⁽¹⁸⁾ By increasing the separation between the light source and detector, improvement of sensitivity is achieved. However this improvement is limited by the decrease of the signal-to-noise ratio.⁽¹⁸⁾ Technical improvements have also been proposed by scanning a wide spectral range from 700 nm to 1000 nm rather than just the conventional 2-wavelengths.⁽¹⁹⁻²⁰⁾ Likewise, other alternatives using a higher sampling rate⁽²¹⁻²²⁾, new probe designs⁽²³⁾ or more intense light source have been developed to allow deeper probing of tissue.⁽²⁵⁾

Besides technical modifications, new algorithms to analyze data and improve overall results have been proposed.⁽²⁶⁻³³⁾ However, most of the quantification algorithms for CWS are inaccurate due to inhomogeneous tissue structure which affects measurements sensitivity and because almost all algorithms were experimentally determined.⁽²⁸⁾ To circumvent these problems, linear and nonlinear algorithms have been developed using mean optical pathlengths^(26,29) where fat layers were taken into account.^(28,30) Likewise, the feasibility of using partial least-squares analysis of near-infrared spectra to optically separate Hb and Mb and determine Mb saturation in a blood-perfused beating heart has been demonstrated.⁽³⁴⁻³⁵⁾

To overcome the CWS limitations such as SNR, other techniques have been developed to evaluate oxygenation. Phase modulation spectroscopy (PMS) introduces a sinusoidal wave into the system, and the magnitude and the phase shift at the nanosecond delay of the output, compared to the input, are measured and analyzed for system characterization.⁽³⁶⁻³⁹⁾ Although this technique has many improvements as compared to CWS, some factors still introduce inaccuracies in the data analysis and the measurements. If only a limited number of wavelengths are monitored, PMS techniques are not capable of accounting for absorption of chromophores besides oxy- and deoxy hemoglobin, such as water.⁽³⁶⁾ Likewise, approximations made in the derivation of light propagation diffusion model, voltage to phase conversion and initial phase calibration can result in inconsistent and unreliable calculations.⁽³⁶⁾

Time-resolved spectroscopy (TRS) is another technique that can be used to monitor tissue oxygenation.⁽⁴⁰⁻⁴³⁾ A sharp pulse of light input to the system is used, and an attenuated and broadened output time response is measured and analyzed.⁽³⁶⁾ Time of flight or photon counts are the usual way of analyzing a time domain TRS spectrum. One of the main advantages of TRS spectroscopy is the capability to measure the absorption (μ_a) and scattering (μ_s) coefficients of tissues, thus providing the potential absolute measurements of tissue oxy- deoxy and total hemoglobin rather than qualitative ones.

2.1.2.1.1.2 *Patents*

Because oxygen saturation measurement has clinical applications for diagnostics, several patents were granted between 1980 and 2001 for hemoglobin myoglobin measurements based on NIR techniques. One patent was granted for an algorithm.⁽³³⁾ The constituents of cerebral tissues that mostly contribute to light absorbency and a component for characterizing light loss due to scattering were used to construct a model that emulates cerebral tissue reflectance spectra in various conditions. Using the model system in a reverse mode, the spectra collected from brain tissue were decomposed into individual spectra features and the values for features attributable to oxy- and deoxy- Hb were used to calculate a ratio that corresponds to the percentage of total Hb that contained oxygen.⁽³³⁾ Likewise, four patents were granted for instruments based on near-infrared spectroscopy to non-invasively measure tissue oxygenation.⁽⁴⁴⁻⁴⁷⁾ While one measured the reflectance of a blood sample at a wavelength at which the absorbance of oxyHb was not altered,⁽⁴⁶⁾

the three others used two wavelengths for their measurements. One used a reference and measuring wavelengths at 815 nm and 760 nm respectively,⁽⁴⁷⁾ while the other one used a ratio of the reflectance of red light and near-infrared light.⁽⁴⁵⁾ Another patent has reported to measure changes in absorbance at two different wavelengths that were both specified to be > 700 nm.⁽⁴⁴⁾ Finally, one patent was granted for a method to determine myoglobin oxygen fractional saturation *in vivo* in muscle tissue and intracellular oxygen tension pO_2 in the presence of hemoglobin using second derivative spectra and Partial Least Squares (PLS) algorithm.⁽⁴⁸⁾

2.1.2.1.1.3 *Physiological Studies*

Brain

Oximetry techniques have been largely used to gain crucial knowledge of cerebral tissue metabolism and major advances in the understanding of brain function.⁽⁴⁹⁻⁶²⁾ A review was made on noninvasive optical spectroscopy and imaging of human brain function.⁽⁶³⁾ The technique was useful by providing information non-invasively on cerebral oxidative metabolism and hemodynamics.^(49-50,52,54) Near infrared spectroscopy was found to be a sensitive indicator of hemoglobin oxygenation changes in the absence of hypoxia or with extreme hypoxia followed by recovery.⁽⁶⁰⁾ Likewise, based on cerebral hemoglobin oxygenation state and blood volume measured during various mental tasks, it was possible to show that there are regional variations of the oxygen delivery and oxygen utilization during activation of the brain.⁽⁵⁹⁾ Furthermore, several studies used oximetry to measure hemoglobin

oxygenation changes in cerebral tissue on patients with a disease,^(53,56-58,61) with mitochondrial dysfunction,⁽⁵⁵⁾ or with depression.⁽⁵¹⁾

Oximetry has found some application in monitoring cerebral tissue oxygenation after drug delivery⁽⁶⁴⁻⁷²⁾ and blood flow changes under various conditions assuming scattering does not change during the course of the study.^(64,73-75) Studies suggested that NIRS is capable of detecting the relative changes in cerebral hemodynamics induced by acetazolamide⁽⁶⁴⁾, caffeine and aminophylline⁽⁷⁶⁾, surfactant administered by bolus administration to very low birth weight infants⁽⁶⁷⁾, ibuprofen⁽⁵⁸⁾, kainic acid-induced seizures⁽⁶⁹⁾, normovolemic hemodilution⁽⁷¹⁾, but also net effects of nitric oxide on cerebral metabolic recovery after deep hypothermic circulatory arrest.^(65,69) The role of opioids during brain injury was also studied.⁽⁷⁰⁾ It was found that NIR measurements of cerebral blood flow and cerebral oxygenation were useful in ascertaining the contribution of cerebral opioids to arteriolar constriction which may play a role in causing ischemia after brain injury.⁽⁷⁰⁾

Cerebral circulation and oxygen metabolism were also studied by NIR spectroscopy during surgery⁽⁷⁵⁻⁸¹⁾ or birth procedures^(74,77,84-88), two situations where the information provided by this technique can contribute to prevent brain damage.⁽⁸⁴⁻⁸⁵⁾ It was shown that changes in oxyhemoglobin levels monitored by NIRS reflected cerebral oxygen metabolism during cardiopulmonary bypass without the effect of variability of hemoglobin concentration due to hemodilution.⁽⁷⁶⁾ NIRS indicated that dynamic changes occur in cerebral circulation and oxygenation as part

of the physiological changes taking place soon after birth.⁽⁸³⁾ Likewise, uterine contractions were associated with detectable changes from baseline in cerebral oxy-deoxy- hemoglobin and in cerebral blood volume.⁽⁸⁸⁾

Muscle/Tissues

The spectral overlap between hemoglobin and myoglobin has resulted in monitoring a combined signal for most muscle oxygenation studies. Monitoring Hb and Mb simultaneously has been used to follow oxygenation during both exercise and ischemia.⁽⁸⁷⁻¹¹¹⁾ The analysis of oxidative phosphorylation and utilization of oxygen at rest, during exercise and post exercise by near infrared spectroscopy were valuable in diagnosis of mitochondrial disorders^(94,97) and development of edema.⁽⁹³⁾ Likewise, the study of the effect of alcohol on muscle energy metabolism in chronic alcoholics has led to the conclusion that abnormality of aerobic metabolism exist for chronic alcoholics with neurological signs owing to muscle mitochondrial dysfunction.⁽⁹²⁾

Measurement of dynamic changes in blood oxygenation by NIR was found to be a valuable tool for tumor prognosis⁽¹¹³⁻¹¹⁸⁾ and provided insight into tumor vascular development.^(113,115) NIR was used to monitor hemoglobin oxygen state during surgery^(119-120,125) and organ transplantation.⁽¹²¹⁻¹²⁴⁾ It was shown that nitrosyl-Hb, an end-product of nitric oxide (NO), showed good correlation with recipient survival time⁽¹²²⁻¹²³⁾ and that NIRS was able to provide some information on the kinetics of reperfusion in the transplanted organs.⁽¹²⁴⁾ Furthermore, tissue pH has been estimated based on shifts of the oxygen saturation calculated by NIR. This

information provided a noninvasive measure of ischemia during heart and plastic surgery which is useful as an early indicator of shock in ICU patients.⁽¹²⁵⁾

Oxygen consumption was monitored in non-exercising skeletal muscle after aerobic exercise. It was found that a significant correlation existed between the increase in $VO_{2\text{nonex}}$ and the increase in lactate concentration. This suggested that lactate concentration was an important stimulant factor of $VO_{2\text{nonex}}$.⁽¹²⁶⁾ Finally, muscle deoxygenation during submaximal workload was found to significantly correlate with blood lactate concentration.^(104,127) Building on this fact, an attempt was made to use NIR spectroscopy to determine lactate threshold by identifying particular trends in the rate of muscle deoxygenation.⁽¹²⁷⁾

Fatigue felt during illness was examined by comparing the Hb+Mb oxygenation in leg muscle of healthy subjects to patients suffering from cardiac disease.⁽¹¹⁰⁻¹¹¹⁾ $\Delta(\text{Hb}+\text{Mb})$ was used to determine the diagnosis of chronic compartment syndrome.⁽¹¹²⁾ Although trends in the data collected by this method are observed when Hb and Mb are measured together, it is not possible to measure the intracellular oxygenation component as indicated by myoglobin. To address this limitation, methods to optically separate Mb and Hb in the NIR have been proposed.⁽³⁴⁾ Spectra taken on beating living dog hearts were examined by second differential processing and partial least squares analysis in the 660 to 840 nm range. Using *in vitro* calibration spectral data, *in vivo* myoglobin oxygen saturation could be

estimated with an accuracy of 6%.⁽³⁴⁾ Useful information on oxygen limitation in clinical investigations could be provided by the application of this technique.

2.1.2.1.2 Cytochrome oxidase

Cytochrome oxidase (Cyt) is the terminal electron acceptor of the mitochondrial chain (see Figure 2.1), responsible for the majority of oxygen consumption in the body and essential for the efficient generation of cellular ATP.⁽¹²⁸⁾ Cytochrome c oxidase is composed of four redox active metal centers: Cu_A, heme a, heme a₃ and Cu_B.⁽¹²⁹⁾ Only the first three have absorption bands in the NIR region of the spectrum. The oxidized binuclear copper center Cu_A has the strongest absorption in the near infrared region centered at around 820-840 nm,⁽¹³⁰⁾ whereas oxidized heme a and a₃ absorb weakly with a broad band at approximately 780 nm⁽¹³¹⁾ as shown in Figure 2.3. These spectral features are not present in the reduced form of the enzyme.

2.1.2.1.2.1 Cytochrome Measurement Techniques

Because the cytochrome concentration is less than 10% of that of Hb in tissue, detection is not straightforward. To isolate the absorption due to cytochrome oxidase, algorithms using four wavelengths⁽¹³²⁻¹³³⁾ or the entire spectrum between 500 and 900 nm have been employed.^(49,60,134-139) Likewise, to avoid the interference from the spectral overlap of cytochrome with hemoglobin, a fluorocarbon oxygen carrier has been used to replace blood.^(137,140) Furthermore, because the oxidative state is dependent on the amount of oxygen present, the intracellular oxygenation state of

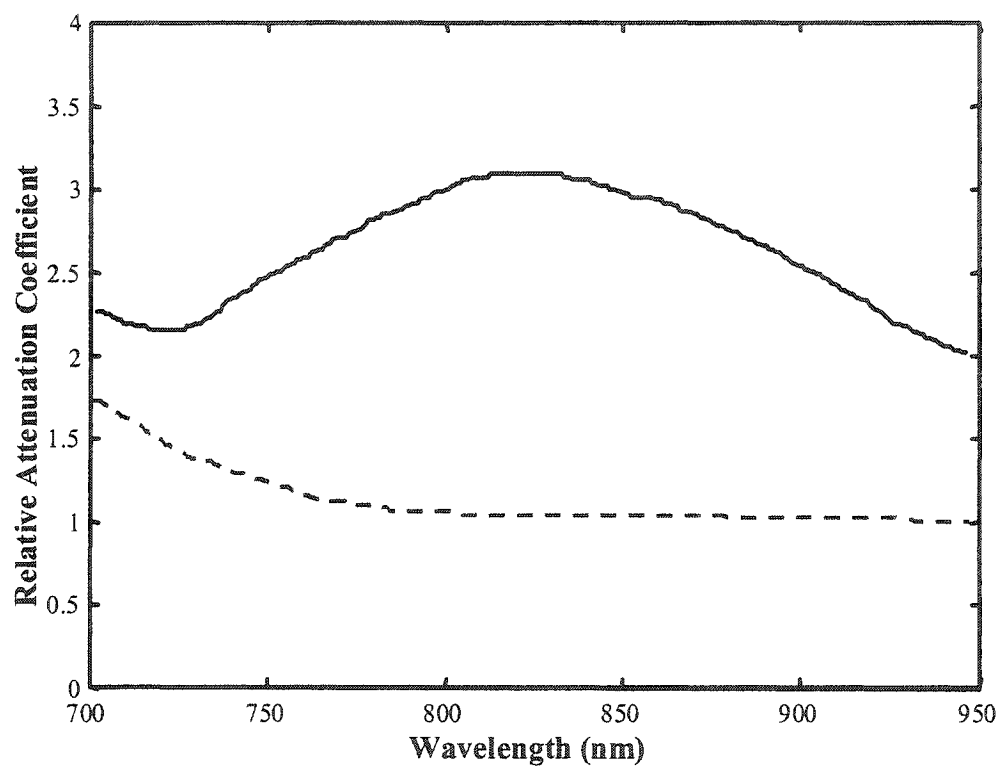


Figure 2.3: Near Infrared Spectra of Cytochrome aa_3 in its oxidized (—) and redox (--) states between 700 and 950 nm.

mitochondria-rich tissue can then be examined using the cytochrome signal.^(49, 138, 141) For this reason, cytochrome oxidase may be a more useful marker than Hb for lack of oxygen.^(80,128)

2.1.2.1.2.2 *Patents*

One patent was granted between 1980 and 2001 for monitoring cellular metabolism by noninvasive, *in situ* measurement of redox state of cytochrome aa₃ using NIR spectroscopy. The instrument reference and measuring wavelengths are at 815 nm and 840 nm respectively.⁽⁴⁷⁾

2.1.2.1.2.3 *Physiological Studies*

Redox changes monitoring of cytochrome oxidase have been used as an indicator of the mitochondrial energetics breakdown⁽⁴⁹⁾, which is known to be directly responsible for brain damage.^(80,143) Changes in Cyt has been used as an indicator of changes in brain perfusion and oxygenation during neonatal hypoxia (73,145-146) and heart surgery (147) to prevent neurological dysfunction. Furthermore, it has been found that Cyt may be an indicator of critical neuronal hypoxia prior to a significant impairment of the cellular energy state caused by cerebral ischemia,⁽¹⁴²⁾ or mitochondrial dysfunction,^(55,97,144) and could indicate hypoxic-ischaemic damage to the brain if the oxidation state does not return to initial level.⁽⁷³⁾ Near Infrared spectroscopy can also detect recovery of oxidative phosphorylation during

recirculation, which can not be observed by electro-encephalograms⁽¹⁴²⁾ or ^{31}P NMR⁽¹³⁷⁾ and oxygen consumption in tumors.⁽²⁴⁾

In clinical practice, cytochrome measurements have only been partially successful for patient management. Results obtained for studies on Cyt often show discrepancies⁽¹³⁸⁾ that arise either from differences or errors in the algorithm employed.⁽¹⁴⁸⁾ In many cases, the reason for this is that the photon pathlengths are unknown since ischemia causes a change in the tissue scattering properties.⁽⁵⁵⁾ Nitric oxide, sometimes present in tissue, will also affect cytochrome oxidase state by impacting pH.⁽¹⁴⁶⁾ Overall, the reliability of monitoring the redox state of cytochrome c oxidase by NIRS is promising, though not conclusive.⁽⁷³⁾

2.1.2.2 Anaerobic Metabolites

Glucose and lactate are two molecules that play an essential role in cell metabolism and are linked to the respiration. Because of the importance in anaerobic conditions, both are routinely measured in critical care units. Likewise, the control of diabetes mellitus and the potential of measuring glucose non-invasively by NIR spectroscopy have lead to intense efforts towards the development of glucose monitoring systems. Several recent reviews are available.⁽¹⁴⁹⁻¹⁵²⁾

2.1.2.2.1 Glucose

There are several wavelength regions that have been examined for sensitivity to glucose. The three absorption bands seen in Figure 2.4a at 1613, 1689, and

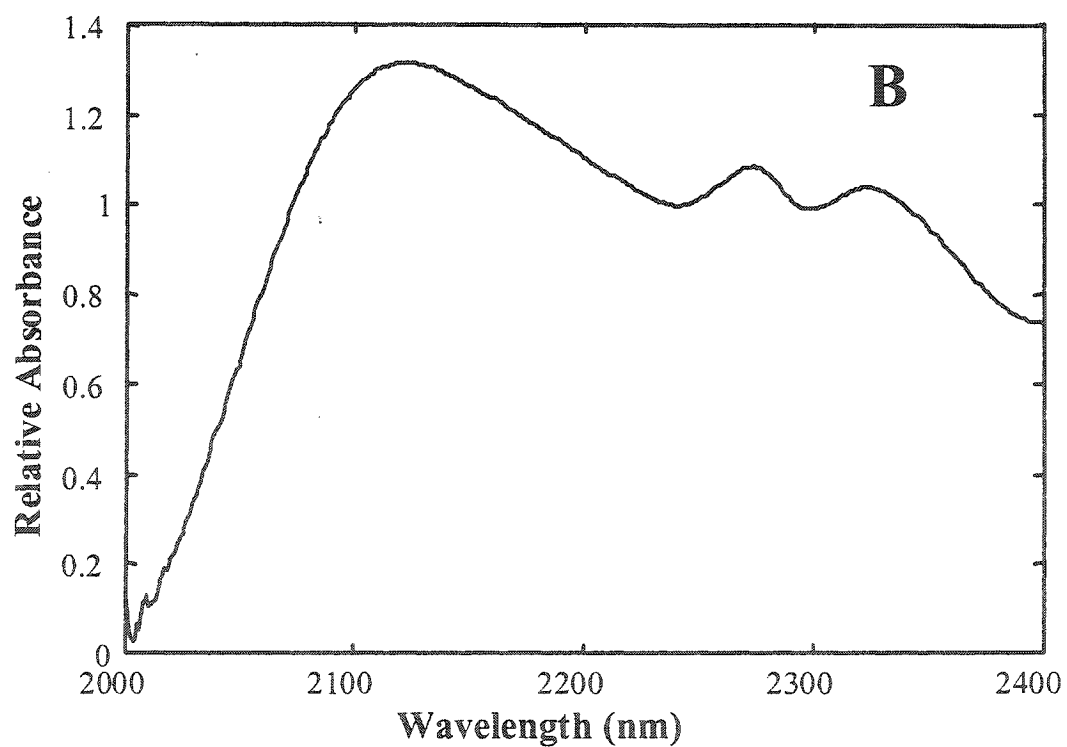
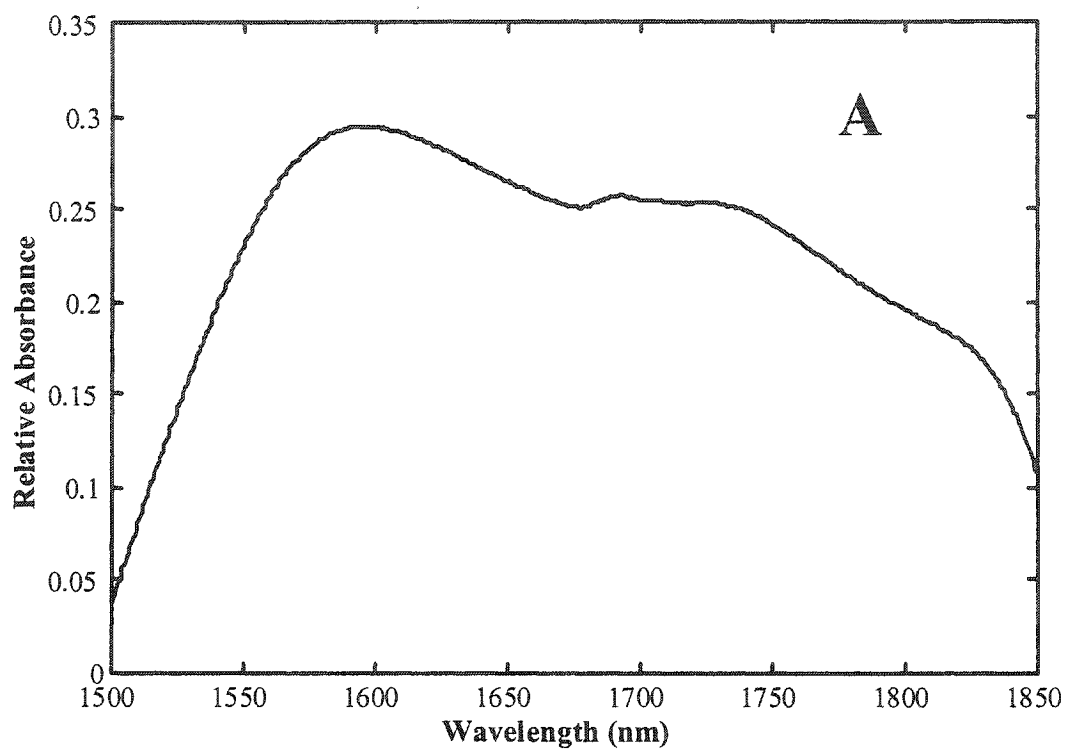


Figure 2.4: Near Infrared Spectra of Glucose between a)1500 and 1850 nm b)2000 and 2400 nm after water subtraction.

1732 nm,⁽¹⁵³⁾ have been associated with overtone bands of O-H and C-H stretching in glucose.⁽¹⁵⁴⁾ The wavelength range from 2000 nm to 2400 nm has been also studied, since this range provides more intense signal from glucose.⁽¹⁵⁵⁾ Three absorption bands seen in Figure 2.4b at 2105, 2273 and 2326 nm are assigned to glucose in this spectral range. However, the low signal-to-noise ratio (SNR) and large spectral overlap from water associated with glucose measurement in either range is a major obstacle to spectral determination. Since glucose concentration in tissue is almost 1000 time lower than that of water in tissue (3.5 to 6.1 mmol/L)⁽¹⁵⁵⁾, the weak signal of glucose is hidden by stronger, spectrally overlapping water absorption bands. Furthermore, background signal resulting from water absorption is known to vary with changes in pH and temperature, complicating analyses. Likewise, protein and fat, being at higher concentration levels, also interfere with glucose measurements to some extent. To minimize background signal impact on spectral determination, multi-wavelengths analyses and multivariate calibrations have been used. Dual beam systems have also been suggested as a means of reducing the sensitivity to background variations.⁽¹⁵⁸⁾ However, as the properties of the “sample” vary over time, a possible bias may be introduced to the data. For robust models, integration of this bias into the calibration is needed to achieve accurate results. However, because they are based only on few replicates, most of the data models published have not shown long term stability.⁽¹⁵⁴⁾ Collecting data with a good SNR and constructing a robust analysis model is the limitation of the current methods.⁽¹⁵¹⁾

2.1.2.2.1.1 Glucose Measurement Techniques

Noninvasive determination of blood glucose is of importance for diabetic patients, in intensive care or during surgery. To examine the feasibility of glucose *in vivo* measurements, several attempts have been made using different *in vitro* and *ex vivo* assays.⁽¹⁵⁹⁻¹⁸³⁾ Reported studies for *in vitro* glucose measurements were made on progressively more complex simulated matrices ranging from buffered glucose solutions,^(155,159-168) to protein solutions,^(165,169-172) tissue-like phantoms,^(156,173) plasma,⁽¹⁷⁴⁻¹⁷⁸⁾ urine⁽¹⁷⁹⁾ and whole blood.^(175,177,180-181) Likewise, *ex vivo* studies on glucose were done using microdialysis and ATR spectroscopy for continuous on-line monitoring.⁽¹⁵⁹⁾

Since blood serves as the main metabolic transport system in the body, several capillary-rich locations are the preferred choice for *in vivo* glucose analysis by NIR. Transmission measurements through the skin,^(153,157,187,189) tongue,^(153,185) lower and upper lips, cheek, nasal septum, the eye and webbing tissue between the thumb and the forefinger⁽¹⁵³⁾ have all been proposed as useful measurement sites. It was found that from all proposed sampling sites, the tongue provided spectra with the highest SNR.⁽¹⁵³⁾ The small concentration of fat in the tongue, which leads to a relatively low scattering and spectral interference, is suggested as the reason for the improved estimations. A model built from a series of transmission spectra collected through the tongues of five human subjects with type 1 diabetes achieved a standard error of prediction for glucose of 3.4mmol/L.⁽¹⁸⁵⁾ The magnitude of the prediction error was related to spectral quality and reproducibility of the tongue-to-spectrometer interface. spectral SNR and sample thickness.

To evaluate more convenient systems for patients, measurements through the skin have also been proposed. To minimize variations resulting from sensor positioning and when applicable skin pigment, reflectance methods rather than transmission approach have been suggested.^(153,185,190-191) NIR spectra of the inner lip between 9000 cm^{-1} and 5450 cm^{-1} (1100 nm – 1800 nm) measured by diffuse reflectance were used to construct a PLS model.⁽¹⁵³⁾ The error in glucose estimation was in the range of 2.6 to 3.2 mmol/L, the major contribution to the prediction uncertainty being the variations in lip position and contact pressure.⁽¹⁵⁴⁾ NIR pulsed photoacoustic technique have also been used to measure glucose concentration^(186,188) and a prediction error of 4.0mmol/L was achieved. However, this is slightly too high for a continuously working sensor in a clinical environment.⁽¹⁸⁸⁾

Care must be taken when considering results on *in vivo* glucose measurements reported in the literature. Indeed, published reports on *in vivo* measurements of glucose appeared to be mostly correlated with time.⁽¹⁵⁵⁾ The study suggested that calibration models built from phantom glucose spectra are not capable of estimating glucose values when glucose assignments to phantom spectra are made randomly. However, errors of the calibration models, when glucose assignments are made in a non-random, time-dependent manner, are close to those published as evidence of successful non-invasive blood glucose measurements. This time-dependent bias of the data explains why, although promising, NIR technique is still not the reference method for clinical measurement of glucose.

2.1.2.2.1.2 *Patents*

The potential of non-invasive measurement by NIR has led to an important commercial effort in development of glucose monitors. Twenty-two patents have been granted between 1989 and 2001 for non-invasive monitoring of glucose by NIR.⁽¹⁹²⁻²¹²⁾ The instruments described have used mostly fingers as the sampling site,⁽¹⁹³⁻²⁰³⁾ but also eyes⁽²⁰⁴⁻²⁰⁵⁾ and skin surface,⁽¹⁹²⁾ using a NIR light source. Likewise, methods using pulse light⁽²¹¹⁾ or photoacoustic⁽²¹⁰⁾ to measure blood glucose have also been proposed. Some algorithms are also presented where two wavelengths calibration with one wavelength being taken as reference,⁽²⁰⁹⁾ three wavelengths calibration corrected for temperature and using second derivative spectra⁽²⁰⁶⁻²⁰⁷⁾ and multi wavelengths calibration.⁽²⁰⁸⁾ Spectral clusters^(198,212) was another algorithm used to determine blood glucose concentration. Likewise, most of the instruments described used transmission spectra to determined blood glucose, while some claimed to work using diffuse reflectance⁽²⁰⁴⁻²⁰⁵⁾ or a combination of both transmission and reflectance data.^(195,203)

2.1.2.2.1.3 *Physiological Studies*

A review of new developments in the treatment of type 1 diabetes mellitus has discussed systems that measure blood glucose by NIR spectroscopy.⁽²¹³⁾ It was shown that glucose in the aqueous humor correlated linearly with plasma glucose in rabbits when blood glucose rose above 11 mM, even though aqueous humor glucose concentration exceeded blood glucose concentration at normoglycemic levels.⁽²¹⁴⁾

Likewise, glucose was measured in serum collected during hemodialysis treatments with a SNR high enough to distinguish glucose spectral features from those of other matrix components.⁽²¹⁵⁾ The effects of physiological factors like temperature fluctuations, tissue water content and other analytes concentration in the determination of glucose concentration was compared to Monte Carlo computer simulation.⁽²¹⁶⁾ It was found that interference from tissue parameters in the glucose measurements were significant and contribute to the difficulty to achieve accurate glucose measurements.

Near Infrared Spectroscopy was also identified as a good technique for noninvasive measurement of concentration of important nutrients and metabolic byproducts in cell cultures.⁽²¹⁷⁻²²⁸⁾ The ultimate goal was to minimize human intervention by using computer system to control the growth process and improve efficiency and repeatability of experiments. The non-invasive measurements by NIR were attractive because it reduces the risk of contamination of culture environment while monitoring important parameters as compared to conventional methods. Furthermore, the optimization of cell culture growth in bioreactors require continuous monitoring of the process.⁽²¹⁹⁾ To develop the data model, several systems were studies in the 2000-2500 nm range. Conditions similar to cell culture were first used to determine the potential of the technique ^(220-221,224-228) and glucose could be measured with a standard error of prediction of 1.3mmol/L using PLS regression.⁽²²²⁾ This level of error is encouragingly low considering the changes of the growth media

due to shifting levels of amino acids, carbohydrates, yeastolate, proteins and cell debris.⁽²²²⁾

2.1.2.2.2 Lactate

Lactate is another important component of glycolytic activity in tissue, where it is used as a marker for the assessment of tissue perfusion and oxidative capacity during surgery or in emergency trauma situations. Lactate measurements can also be used to determine the anaerobic threshold during physical exercise.⁽²²⁹⁾ While the human physiological range of lactate extends from 0.3 to 25 mmol/L, a lactate concentration of less than 2 mmol/L is considered as normal. However, concentrations higher than 4 mmol/L are often found in association with general circulatory failure. Likewise, the change in pattern or the trend towards an increase of blood lactate is a good indicator of survival.⁽²³⁰⁻²³¹⁾ In all these cases, measurements of lactate levels are of prognostic significance.

2.1.2.2.2.1 Lactate Measurement Techniques

Lactate has three broad absorption bands in the 2000-2500 nm wavelength range at 2166 nm, 2254 nm and 2300 nm, as shown in Figure 2.5b.⁽²²⁶⁻²²⁷⁾ Three absorption bands can also be seen in the 1500-1750 nm wavelength range at 1675, 1690 and 1730 nm, as shown in Figure 2.5a. This wavelength range has not yet been used for lactate studies, despite the fact that scattering is reduced for *in vivo* lactate determination.

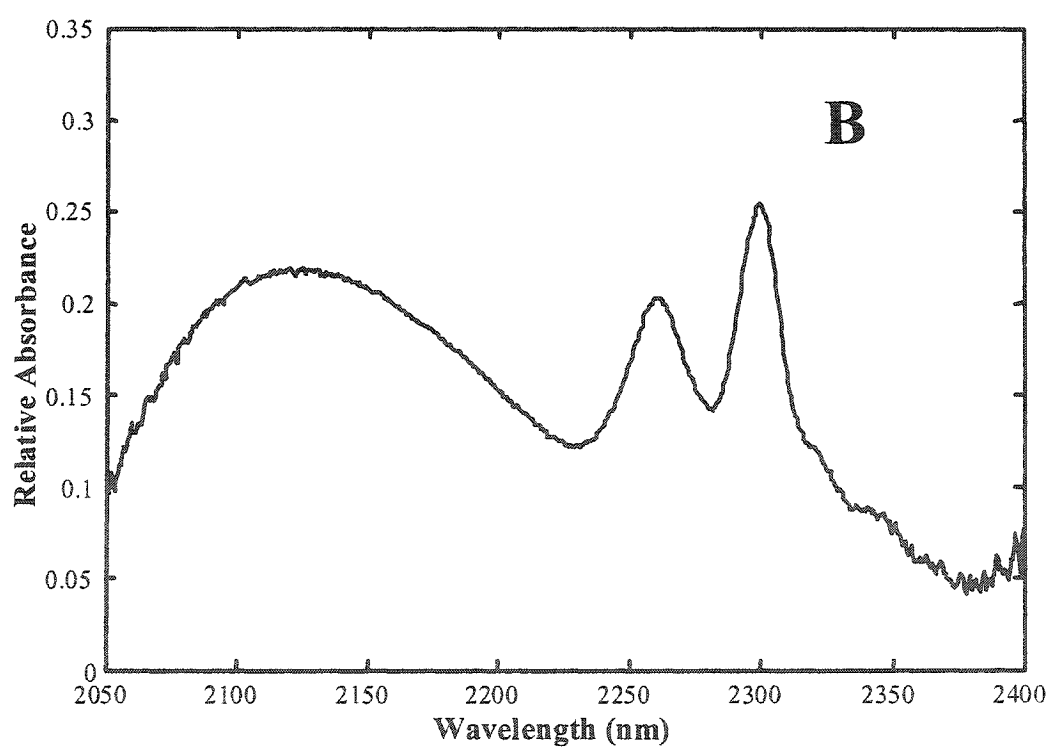
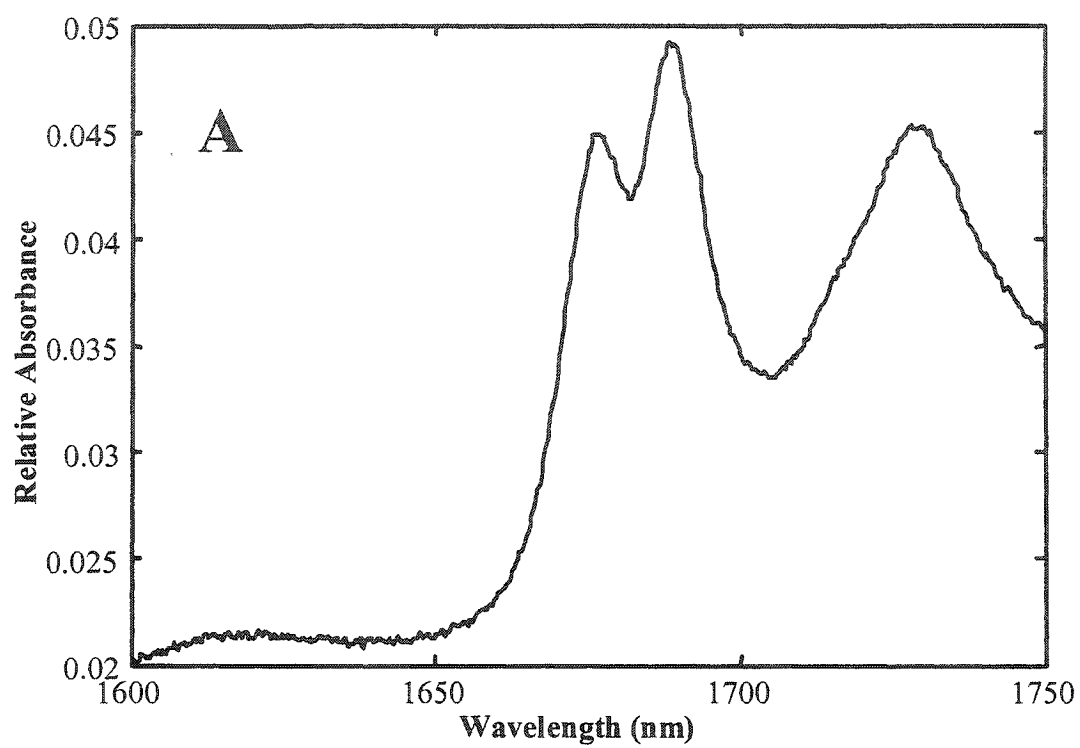


Figure 2.5: Near Infrared Spectra of Lactate between a)1600 and 1750 nm b)2050 and 2400 nm.

The first absorptions (2000-2500 nm) have been associated with combinations of C-H vibrational transitions, the second ones (1500-1750) were associated with 1st overtone of C-H vibrational transitions. In both cases, they overlap with other species such as glucose, glutamate and glutamine. Because of the severe overlap with other constituents, multivariate analysis has been required to estimate lactate in all of the studies.

Like for glucose determination, reported studies for *in vitro* lactate measurements were made on progressively more complex simulated matrices ranging from buffered lactate solutions,^(166,223,228,234) to protein solution,⁽¹⁷⁰⁾ cell culture media,^(218,220-221,223-225,227) plasma,^(178,233) and whole blood.⁽²³²⁾ Lactate was monitored with a standard error of 0.5 mmol/L in cell culture media (227) and human plasma, (178, 233) although the error was too significant to measure lactate at rest.⁽¹⁷⁸⁾ However, measurements on a wider human physiological range of lactate concentrations induced by exercise were successful.⁽²³³⁾ Likewise, good correlation between estimated and reference lactate concentrations were found in rat blood samples.⁽²³²⁾ The reported standard error of 0.29 mmol/L is well within the range needed for real-time monitoring of lactate in blood for exercising studies. This approach, which could have significant impact in clinical situations or exercise physiological studies, represents a faster and nondestructive alternative to current enzymatic methods.

2.1.2.2.2.2 *Patents*

Since the beginning of my research work, one patent was granted for monitoring lactate in an organism using NIR spectroscopy. The proposed instrument used a probe that comes in contact with a finger or an arm and brought light to the tissue. The selected wavelengths for the measurements were the ones in the 1580 to 1850 nm and 2080 to 2380 nm ranges with a correlation coefficient of at least 0.8 between lactate concentration and absorbance in an aqueous lactate solution.⁽²³⁵⁾ However, no results were presented in the patent as to the accuracy of the proposed instrument. Indeed, the multivariate methods proposed used a calibration curve made from aqueous lactate solution with concentration levels ranging from 100mM to 400mM. The human physiological range is 0.3 to 25mM. It is then unlikely that the statistical model built using the proposed calibration curve led to an accurate quantification of *in vivo* lactate concentration. The aqueous lactate solution samples used to build the calibration curve are too different from tissue and the concentration range too far apart to allow an extrapolation of that magnitude.

2.1.2.2.2.3 *Physiological Studies*

As previously discussed for glucose, NIR Spectroscopy was identified as a good technique for noninvasive measurement of lactate in cell cultures.^(218,220-221,233-234,227) To develop the data model, several systems were studied in the 2000-2500 nm range. Conditions similar to cell culture were first used to determine the potential of the technique.^(220-221,223-225) However, to reduce the development time of the

calibration set, simulated spectra of multi-component system were proposed as calibration set to quantify analytes in experimentally collected spectra.⁽²²¹⁾ By this technique, the prediction error for lactate was 0.45 mmol/L, which is similar to the error obtained with full experimental calibration at 0.35mmol/L, both using PLS regression. The main advantage of simulated spectra is the significant reduction in time required to generate an accurate calibration. Since time is one of the limiting factors in the application of NIR spectroscopy to monitor biological processes, this improvement may lead to a wider use of the technique.

Lactate is a byproduct of the respiratory chain process. For this reason, it can be used as a marker to assess tissue perfusion and oxidative capacity. The potential that NIR spectroscopy may provide a noninvasive method to measure continuous changes in tissues could allow insights into controversial issues related to blood lactate concentration.

2.1.3 Conclusion

Near infrared analysis has yielded a number of useful methods for metabolic measurements. Noninvasively, this technique allows the monitoring of living systems, which in some case can lead to the assessment of the tissue oxidative capacity, tissue damage prognostic and the diagnosis of a disease. If some applications such as monitoring hemoglobin oxygenation by pulse oximetry are well established and used routinely for clinical purposes, others applications such as quantification of glucose and lactate still need development work mainly to improve

accuracy of the measurements between patients and over time. What is currently identified, as the main obstacle to metabolic measurements is the very nature of tissue. Because tissue is not a homogeneous material, uncertainty in the light path length exists, which makes absolute concentrations difficult to obtain. Furthermore, near infrared absorption bands are broad and overlapped, where it is sometimes difficult to distinguish between the spectra arising from the different chromophores present in tissue. However, advances in time-of-flight and multivariate statistical analysis methods have brought solutions to the difficulties described above, making metabolic measurements by near infrared spectroscopy a growing field for tissue assessment and clinical monitoring.

2.1.4 References

1. W. Herschel, *Philos. Trans. R. Soc. Lond.*, **90**, 293-236 (1800).
2. W.W. Coblentz, Carnegie Institution of Washington Publications: Washington D.C., 5 (1905).
3. R.B. Barnes, *Ind. Eng. Chem. Anal. Ed.*, **15**, 659-709 (1943).
4. J.D. Ingle and S.R. Crouch, 'Spectrochemical Analysis'. Prentice Hall: New Jersey, 408 (1988).
5. E. W. Ciureczak, 'Handbook of Near-Infrared Analysis', D.A. Burns and E.W. Ciureczak Eds, Marcel Dekker: New York, 9 (1992).
6. D.R. Massie and K.H. Norris, *Trans. Am. Soc. Agr. Eng.*, **8**, 598-600 (1965).
7. K.H. Norris, 'Agricultural Handbook: 2nd ed.'. G.C. Martens, J.S. Shenk and F. E. Barton Eds, U.S. Government Printing Office, Washington D.C., 6 (1989).
8. K.A. Schenkman, 'Determination of Myocardial Intracellular Oxygen Partial Pressure by Optical Spectroscopy'. Unpublished Ph.D. Dissertation, University of Washington, Seattle, WA (1996).
9. H. Ohdan, S. Suzuki, M. Kanashiro, H. Amemiya, Y. Fukuda, and K. Dohi, *Transplantation*, **57**(11), 1674-1677 (1994).
10. K.A. Schenkman, D.A. Marble, D.H. Burns, and E.O. Feigl, *J. Appl. Physiol.*, **82**(1), 86-92 (1997).
11. J.R. Squire, *Clin. Sci.*, **4**, 331-339 (1940).
12. G.A. Millikan, J.R. Pappenheimer, A.J. Rawson, and J.E. Hervey, *Am. J. Physiol.*, **133**, 390 (1941).
13. E.H. Wood and J.E. Geraci, *J. Lab. Clin. Med.*, **34**, 387-401 (1949).

14. J.W. Severinghaus and Y. Honda, *J. Clin. Monit.*, **3**, 135-138 (1987).
15. A.C. Ralston, R.K. Webb, and W.B. Runciman, *Anaesthesia*, **46**, 202-206 (1991).
16. R.K. Webb, A.C. Ralston, and W.B. Runciman, *Anaesthesia*, **40**, 207-212 (1991).
17. A.C. Ralston, R.K. Webb, and W.B. Runciman, *Anaesthesia*, **46**, 291-295 (1991).
18. F. Wang, H. Ding and F. Lin, *Guangpuxue Yu Guangpu Fenxi*, **20**, 585-588 (2000).
19. T. Kitai, A. Tanaka, A. Tokuka, K. Tanaka, Y. Yamaoka, K. Ozawa and K. Hirao, *Hepatology*, **18**, 926-936 (1993).
20. D.W. Luebbbers, *Sens. Actuators, B*, **B11**, 253-262 (1993).
21. T. Shiga, E. Chihara, K. Tanabe, Y. Tanaka and K. Yamamoto, *Proc. SPIE-Int. Soc. Opt. Eng.*, **3194** (Photon Propagation in Tissues III), 435-442 (1998).
22. E. Chihara, T. Shiga, K. Tanabe and Y. Tanaka, *Proc. SPIE-Int. Soc. Opt. Eng.*, **3194** (Photon Propagation in Tissues III), 83-91 (1998).
23. D.M. Hueber, S. Fantini, A.E. Cerussi and F.B. Barbieri, *Proc. SPIE-Int. Soc. Opt. Eng.*, **3597** (Optical Tomography and Spectroscopy of Tissue III), 618-631 (1999).
24. F. Steinberg, H.J. Rohrborn, T. Otto, K.M. Scheufler and C. Streffer, *Adv. Exp. Med. Biol.*, **428** (Oxygen Transport to Tissue XIX), 69-77 (1997).
25. H. Sato, S. Wada, M. Ling and H. Tashiro, *Appl. Spectrosc.*, **54**, 1163-1167 (2000).

26. C.E. Copper, C.E. Elwell, J.H. Meek, S.J. Matcher, J.S. Wyatt, M. Cope and D.T. Delphy, *Pediatr. Res.*, **39**, 32-38 (1996).
27. S. Suzuki, S. Takasaki, T. Ozaki and Y. Kobayashi, *Proc. SPIE-Int. Soc. Opt. Eng.*, **3597** (Optical Tomography and Spectroscopy of Tissue III), 582-592 (1999).
28. J. Shao, L. Lin, M. Niwayama, N. Kudo and K. Yamamoto, *Proc. SPIE-Int. Soc. Opt. Eng.*, **4082** (Optical Sensing, Imaging and Manipulation for Biological and Biomedical Applications), 76-86 (2000).
29. F. Wang, W. Li, F. Lin, G. Wang and H. Ding, *Qinghua Daxue Xuebao, Ziran Kexueban*, **39**, 16-19 (1999).
30. M. Niwayama, L. Lin, J. Shao, N. Kudo and K. Yamamoto, *Rev. Sci. Instrum.*, **71**, 4571-4575 (2000).
31. Y. Kobayashi, S. Takasaki, T. Ozaki, M. Ishizuka and S. Suzuki, *Ther. Res.*, **21**, 1528-1532 (2000).
32. H. Sasaki, M. Endo, S. Kisiduti, Y. Matsumoto, Y. Abe, S. Kawashima, Y. Hiranou and T. Ueyama, *Ther Res.*, **21**, 1533-1537 (2000).
33. D.A. Wilson, *PCT Int. Appl.*, 76pp. (2001), Application WO 2000-2000US32830.
34. K.A. Schenkman, D.R. Marble, D.H. Burns and E.O. Feigl, *Appl. Spectrosc.* **53**, 332-338 (1999).
35. K.A. Schenkman, D.R. Marble, E.O. Feigl and D.H. Burns, *Appl. Spectrosc.*, **53**, 325-331 (1999).

36. M.W. Hemelt, J.T. Barnett, D.F. Bruley and K.A. Kang, *Biotechnol. Prog.*, **13**, 640-648 (1997).
37. H. Iwai, T. Urakami, M. Miwa, Y. Yamashita and Y. Tsuchiya, *Ther. Res.*, **21**, 1560-1564 (2000).
38. V. Ntziachristos, N. Brun, B. Feet, G. Gresien and B. Chance, *Proc. SPIE-Int. Soc. Opt. Eng.*, **2979** (Optical Tomography and Spectroscopy of Tissue), 715-723 (1997).
39. E.M. Sevick, B. Chance, J. Leigh, S. Noika and M. Maris, *Anal. Biochem.*, **195**, 330-351 (1991).
40. M. Oda, Y. Yamashita, T. Nakano, A. Suzuki, K. Shimizu, I. Hirano, F. Shimomura, E. Ohmae, T. Suzuki and Y. Tsuchiya, *Proc. SPIE-Int. Soc. Opt. Eng.*, **3597** (Optical Tomography and Spectroscopy of Tissue III), 611-617 (1999).
41. M. Oda, Y. Yamashita, E. Ohmae, F. Shimomura, T. Suzuki and Y. Tsuchiya, *Ther. Res.*, **21**, 1524-1527 (2000).
42. K.L. Worden, Y. Song, X. Jiang, A. Constantinescu, R.P. Mason and H. Liu, *Proc. SPIE-Int. Soc. Opt. Eng.*, **3597** (Optical Tomography and Spectroscopy of Tissue III), 601-610 (1999).
43. D.J. Wallace, B. Michener, D. Choudhury, M. Levi, P. Fennelly, D.M. Hueber and B.F. Barbieri, *Proc. SPIE-Int. Soc. Opt. Eng.*, **3597** (Optical Tomography and Spectroscopy of Tissue III), 300-316 (1999).
44. T. Tamura, M. Tamura and O. Hajiki, *Jpn. Kokai Tokkyo Koho*, (1989) Application JP 87-248590.

45. S. Takatani, *Jpn. Kokai Tokkyo Koho*, (1987), Application JP 86-94614.
46. S. Takatani, *Jpn. Kokai Tokkyo Koho*, (1987), Application JP 86-94615.
47. F.F. Jobsis, Pat. Specif. (Aust.), (1981), Application AU 80-58055.
48. L.S. Arakaki, E. Feigl, M.J. Kushmerick, D. Marble, D.H. Burns, K.H. Schenkman, *U.S.* (1997), Application US 97-870483.
49. R. Springett, M. Wylezinska, E.B. Cady, M. Cope and D.T. Delpy, *J. Cereb. Blood Flow Metab.*, **20**, 280-289 (2000).
50. E.O.R. Reynolds, D.C. McCormick, S.C. Roth, A.D. Edwards and J.S. Wyatt, *Ann. Med.*, **23**, 681-686 (1991).
51. K. Matsuo, T. Kato, M. Fukuda and N. Kato, *J. Neuropsychiatry Clin. Neurosci.*, **12**, 465-471 (2000).
52. D.M. Hueber, M.A. Franceschini, H.Y. Ma, Q. Zhang, J.R. Ballesteros, S. Fantini, D. Wallace, V. Ntziachristos and B. Chance, *Phys. Med. Biol.*, **46**, 41-62 (2001).
53. J.S. Soul, G.A. Taylor, D. Wypij, A.J. Adre and J.J. Volpe, *Pediatr. Res.*, **48**, 445-449 (2000).
54. D.A. Boas, X. Cheng, J.A. Marota and J.B. Mandeville, *Proc. SPIE-Int. Soc. Opt. Eng.*, **3863** (Biomedical Optics (BMO '99)), 81-94 (1999).
55. C.E. Cooper, M. Cope, R. Springett, P.N. Amess, J. Penrice, L. Tyszczuk, S. Punwani, R. Ordidge, J. Wyatt and D.T. Delpy, *J. Cereb. Blood Flow Metab.*, **19**, 27-38 (1999).

56. Y. Oana, C. Wang, A. Hoshika, Y. Takei, M. Kondo, N. Sakaue, N. Hirabayashi, H. Watahiki and M. Kaneko, *Tokyo Ika Daigaku Zasshi*, **56**, 182-189 (1998).
57. C. Hock, K. Villringer, F. Mueller-Spahn, R. Wenzel, H. Heekeren, S. Schuh-Hofer, M. Hofman, S. Minoshima, M. Schwaiger, U. Dirnagl and A. Villringer, *Brain Res.*, **755**, 293-303 (1997).
58. J. Tureen, Q. Liu and L. Chow, *Pediatr. Res.*, **40**, 759-763 (1996).
59. Y. Hoshi and M. Tamura, *Sinkei Kenkyu no Shinpo*, **38**, 301-308 (1994).
60. M.S. Thorniley, N. Livera, Y.A.B.D. Wickramasinghe and P. Rolfep, *Biochem. Soc. Trans.*, **17**, 903-904 (1989).
61. M. Mishio and H. Ogata, *Dokkyo Igakkai Zasshi*, **11**, 35-43 (1996).
62. I. Oda, Y. Ito, H. Eda, T. Tamura, M. Takada, R. Abumi, K. Nagai, H. Nakagawa and M. Tamura, *Proc. SPIE-Int. Soc. Opt. Eng.*, **1431** (Proc. Time-Resolved Spectrosc. Imaging Tissues), 284-93 (1991).
63. A. Villringer and B. Chance, *Trends Neurosci.*, **20**, 435-442 (1997).
64. H. Yamaguchi, H. Yamauchi, S. Hazama, H. Hamamoto and I. N. Hirotsugu, *J. Biomed. Opt.*, **4**, 418-423 (1999).
65. T. Hiramatsu, R.A. Jonas, T. Miura, A. Duplessis, T. Masahiro, J.M. Forbess and D. Holtzman, *J. Thorac. Cardiovasc. Surg.*, **112**, 698-707 (1996).
66. C. Dani, G. Bertini, R. Giovanna, F.M. Reali, M. Tronchin, L. Wiechmann, E. Martelli and F.F. Rubaltelli, *Biol. Neonate*, **78**, 27-32 (2000).
67. C. Roll, J. Knief, S. Horsch and L. Hanssler, *Neuropediatrics*, **31**, 16-23 (2000).

68. F. Mosca, M. Bray, M.R. Colnaghi, M. Fumagalli and G. Compagnoni, *J. Pediatr.*, **135**, 644-646 (1999).
69. Y. Takei, R. Totsuka, Y. Inage, T. Takami, N. Yamada, T. Tasuku and A. Hoshika, *Tokyo Ika Daigaku Zasshi*, **57**, 165-173 (1999).
70. W.M. Armstead and C.D. Kurth, *Brain Res.*, **660**, 19-26 (1994).
71. D.A. Lubarsky, J.A. Griebel, E.M. Camporesi and C.A. Piantadosi, *Resuscitation*, **23**, 45-57 (1992).
72. Y. Morimoto, Y. Morimoto, O. Kemmotsu, S. Gando, T. Shibano and H. Shikama, *Anesth. Analg.*, **91**, 347-352 (2000).
73. M. Shadid, L. Hiltermann, L. Monteiro, J. Fontijn and F. Van Bel, *Early Hum. Dev.*, **55**, 169-182 (1999).
74. M. Ferrari, C. De Marchis, I. Giannini, A. Di Nicola, R. Agostino, S. Nodari and G. Bucci, *Adv. Exp. Med. Biol.*, **200**, 203-211 (1986).
75. J.A. Wahr and K.K. Tremper, 'Pulse Oximetry' in "Monitoring in Anesthesia and Critical Care Medicine", C.D. Blitt and R.L. Hines (Eds.), Churchill Livingstone, New York, pp. 385-405 (1995).
76. T. Honda, *Yonago Igaku Zasshi*, **47**, 42-51 (1996).
77. G. Donzelli, S. Pratesi, S. Fantini and M.A. Franceschini, *New Technol. Reprod. Med. Neonatol. Gynecol., Int. Congr. 2nd*, 451-459 (1999).
78. M. Ishikawa, *Kyorin Igakkai Zasshi*, **30**, 27-36 (1999).
79. M. Tsuji, A. Duplessis, G. Taylor, R. Crocker and J.J. Volpe, *Pediatr. Res.*, **44**, 591-595 (1998).

80. H. Matsumoto, T. Oda, M.A. Hossain and N. Yoshimura, *Anesth. Analg.*, **83**, 513-518 (1996).
81. M.S. Thorniley, I.A. Sammut, S. Simpkin and C.J. Green, *Biochem. Soc. Trans.*, **23**, 525S (1995).
82. K. Isobe, T. Kusaka, Y. Fujikawa, M. Kondo, K. Kawada, S. Yasuda, S. Itoh, K. Hirao and S. Onishi, *J. Biomed. Opt.*, **5**, 283-286 (2000).
83. I.A.A. Hassan, S.A. Spencer, Y.A. Wickramasinghe and K.S. Palmer, *Early Hum. Dev.*, **57**, 211-224 (2000).
84. L. Bennet, S. Rossenrode, M.I. Gunning, P.D. Gluckman and A.J. Gunn, *J. Physiol.*, **517**, 247-257 (1999).
85. H.P. Lehr, Y. Wickramasinghe and P. Rolfe, *Proc. SPIE- Int. Soc. Opt. Eng.*, **2979** (Optical Tomography and Spectroscopy of Tissue), 774-784 (1997).
86. C.W. Yoxall and A.M. Weindling, *Pediatr. Res.*, **39**, 1103-1106 (1996).
87. Y.A.B.D. Wickramasinghe, K.S. Palmer, R. Houston, S.A. Spencer, P. Rolfe, M.S. Thorniley, B. Oeseburg and W. Colier, *Pediatr. Res.*, **34**, 15-17 (1993).
88. D.M. Peebles, A.D. Edwards, J.S. Wyatt, A.P. Bishop, M. Cope, D.T. Delpy, E. Osmund and R. Reynolds, *Am. J. Obstet. Gynecol.*, **166**, 1369-1373 (1992).
89. M. Niwayama, D. Kohata, J. Shao, N. Kudo, T. Hamaoka, T. Katsumura and K. Yamamoto, *Proc. SPIE-Int. Soc. Opt. Eng.*, **4082** (Optical Sensing, Imaging and Manipulation for Biological and Biomedical Application), 48-56 (2000).
90. M.S. Thorniley, R. Houston, Y.A.B.D. Wickramasinghe and P. Rolfe, *Biochem. Soc. Trans.*, **18**, 1195-1196 (1990).
91. K. McCully, B. Chance and U. Giger, *Muscle Nerve*, **22**, 621-627 (1999).

92. M. Haida, K. Yazaki, D. Kurita and Y. Shinohara, *Alcohol. :Clin. Exp. Res.*, **22**, 108S-110S (1998).
93. T. Binzoni, V. Quaresima, E. Hiltbrand L. Gurke, P. Cerretelli and M. Ferrari, *Adv. Exp. Med. Biol.*, **428**, 533-538 (1997).
94. W. Bank, J. Park, G. Lech and B. Chance, *Biofactors*, **7**, 243-245 (1998).
95. R. Boushel and C.A. Piantadosi, *Acta Physiol. Scand.*, **168**, 615-622 (2000).
96. T.K. Tran, N. Sailasuta, U. Kreutzer, R. Hurd, Y. Chung, P. Mole, S. Kuno and T. Jue, *Am. J. Physiol.*, **276**, R1682-R1690 (1999).
97. W. Bank and B. Chance, *Mol. Cell. Biochem.*, **174**, 7-10 (1997).
98. T. Yasuda, *Kanazawa Daigaku Juzen Igakkai Zasshi*, **105**, 2-16 (1996).
99. L. Marcu, J.-M.I. Maarek, A. Bembi and S. Howell, *Proc. SPIE-Int. Soc. Opt. Eng.*, **2387**, 218-224 (1995).
100. K.A. Schenkman and D.H. Burns, *Proc. SPIE-Int. Soc. Opt. Eng.*, **2131** (Biomedical Fiber Optic Instrumentation), 468-474 (1994).
101. T. Sako, T. Hamaoka, H. Higuchi, Y. Kurosawa and T. Katsumura, *J. Appl. Physiol.*, **90**, 338-344 (2001).
102. T. Hamaoka, H. Iwane, T. Shimomitsu, T. Katsumura, N. Murase, S. Nishio, T. Osada, Y. Kurosawa and B. Chance, *J. Appl. Physiol.*, **81**, 1410-1417 (1996).
103. B. Chance, S. Nioka, H. Long, C. Xie, X. Ma, V. Ntziachristos and Q. Luo, *Proc. SPIE-Int. Soc. Opt. Eng.*, **4001** (Optical Technologies in Biophysics and Medicine), 2-13 (2000).
104. B. Grassi, V. Quaresima, C. Marconi, M. Ferrari and P. Cerretelli, *J. Appl. Physiol.*, **87**, 348-355 (1999).

105. T. Nishiyasu, N. Tan, N. Kondo, M. Nishiyasu and H. Ikegami, *Acta Physiol. Scand.*, **166**, 123-130 (1999).
106. M.J. MacDonald, M.A. Tarnopolsky, H.J. Green and R.L. Hughson, *J. Appl. Physiol.*, **86**, 687-693 (1999).
107. T. Hamaoka, H. Iwane, T. Shimonitsu, T. Katsumura, N. Murase, S. Nishio, T. Osada, Y. Kurosawa and B. Chance, *J. Appl. Physiol.*, **81**, 1410-1417 (1996).
108. M.S. Irwin, M.S. Thorniley and C.J. Green, *Biochem. Soc. Trans.*, **21**, 502S (1993).
109. A. Hicks, S. McGill and R.L. Hughson, *Can. J. Appl. Physiol.*, **24**, 216-230 (1999).
110. R. Belardinelli, D. Georgiou and T.J. Barstow, *G. Ital. Cardiol.*, **25**, 715-724 (1995).
111. R. Belardinelli, T.J. Barstow, J. Porszasz and K. Wasserman, *Eur. J. Appl. Physiol.*, **70**, 487-492 (1995).
112. G.A. Breit, J.H. Gross, D.E. Waterpaugh, B. Chance, and A.R. Hargens, *J. Bone Joint Surg.*, **79-A**(6), 838-843 (1997).
113. H. Liu, Y. Song, K.L. Worden, X. Jiang, A. Constantinescu and R.P. Mason, *Appl. Opt.*, **39**, 5231-5243 (2000).
114. D.L. Conover, B.M. Fenton, T.H. Thomas and E.L. Hull, *Phys. Med. Biol.*, **45**, 2685-2700 (2000).
115. E.L. Hull and T.H. Foster, *Proc. SPIE-Int. Soc. Opt. Eng.*, **2979** (Optical Tomography and Spectroscopy of Tissue), 355-364 (1997).

116. A. Mahadevan-Jansen, M.F. Mitchell, N. Ramanujam, A. Malpica, S. Thomsen, U. Utzinger and R. Richards-Kortum, *Photochem. Photobiol.*, **68**, 123-132 (1998).
117. U. Utzinger, D.L. Heintzelman, A. Mahadevan-Jansen, A. Malpica, M. Follen and R. Richards-Kortum, *Appl. Spectrosc.*, **55**, 955-959 (2001).
118. T.O. McBride, B.W. Pogue, E.D. Gerety, S.B. Poplack, U.L. Osterberg and K.D. Paulsen, *Appl. Opt.*, **38**, 5480-5490 (1999).
119. M. Nakagawa, E. Chihara, H. Tohjo and Y. Tanaka, *Biomed. Res.*, **18**, 465-469 (1997).
120. M. Ikeda, *Kanazawa Daigaku Juzen Igakkai Zasshi*, **108**, 410-418 (1999).
121. E. Hatano, T. Kiuchi, A. Tanaka, H. Shinohara, T. Kitai, S. Satoh, T. Inomoto, H. Egawa, S. Uemoto, Y. Inomata, H. Lang, K.J. Oldhafer, B. Ringe, R. Pichlmayr, K. Tanaka and Y. Yamaoka, *Clin. Sci.*, **93**, 81-88 (1997).
122. T. Kakefuda, S. Enosawa, X.-K. Li, M. Kanashiro and S. Suzuki, *Ther. Res.*, **17**, 1995-1999 (1996).
123. C.E. Copper, R.J. Springett, A. Panagiotopoulou and J. Penrice, *Biochem. Soc. Trans.*, **24**, 448S (1996).
124. M.S. Thorniley, N.J. Lane, S. Manek and C.J. Green, *Biochem. Soc. Trans.*, **21**, 501S (1993).
125. B.R. Soller and S. Zhang, *Proc. SPIE-Int. Soc. Opt. Eng.*, **3259** (Systems and Technologies for Clinical Diagnostics and Drug Discovery), 122-129 (1998).
126. M. Murakami, T. Katsumara, T. Hamaoka, T. Osada, T. Sako, H. Higuchi, K. Esaki, R. Kime and T. Shimomitsu, *J. Biomed. Opt.*, **5**, 406-410 (2000).

127. C. Angus, D. Welford, M. Sellens, S. Thompson and C.E. Cooper, *Adv. Exp. Med. Biol.*, **471**, 283-288 (1999).
128. C.E. Copper and R. Springett, *Philos. Trans. R. Soc. London, Ser. B*, **352**, 669-676 (1997).
129. C.E. Cooper, S.J. Matcher, J.S. Wyatt, M. Cope, G.C. Brown, E.M. Nemoto, and D.T. Delpy, *Biochem Soc Trans*, **22**, 974-980 (1994).
130. C.E. Cooper, M. Cope, V. Quaresima, M. Ferrari, E. Nemoto, R. Springett, S. Matcher, P. Amess, J. Penrice, L. Tyszczuk, J. Wyatt, and D.T. Delpy, 'Measurement of Cytochrome Oxidase Redox State by Near-Infrared Spectroscopy' in "Optical Imaging of Brain Function and Metabolism II", Villringer and Dirnagl (Eds.), Plenum Press, New York, NY, pp. 63-73 (1997).
131. F.F. Jöbsis-vanderVliet and P.D. Jöbsis, *J. Biomed. Opt.*, **4**(4), 397-402 (1999).
132. M.S. Thorniley, Y.A.B.D. Wickramasinghe and P. Rolfe, *Biochem. Soc. Trans.*, **16**, 978-979 (1988).
133. W.N.J.M. Colier, B.E.M. Ringnalda, J.A.M. Evers and B. Oeseburg, *Adv. Exp. Med. Biol.*, **317**, 305-311 (1992).
134. S.J. Matcher, C.E. Elwell, C.E. Cooper, M. Cope, and D.T. Delpy, *Anal. Biochem.*, **227**, 54-68 (1995).
135. M.S. Thorniley, L.N. Livera, Y.A.B.D. Wickramasinghe, S.A. Spencer and P. Rolfe, *Adv. Exp. Med. Biol.*, **277**, 323-334 (1990).
136. M. Tamura, A. Seiyama and O. Hazeki, *Adv. Exp. Med. Biol.*, **215**, 297-300 (1987).

137. K. Kawada, T. Kusaka, K. Isobe, T. Imai, S. Itoh, S. Onishi and K. Hirao, *Ther. Res.*, **17**, 2022-2026 (1996).
138. Y. Hoshi, O. Hazeki, Y. Kakihana, and M. Tamura, *J. Appl. Physiol.*, **83**(6), 1842-1848 (1997).
139. C.E. Cooper, M. Cope, V. Quaresima, M. Ferrari, E. Nemoto, R. Springett, S. Matcher, P. Amess, J. Penrice, L. Tyszczuk, J. Wyatt and D.T. Delpy, *Adv. Exp. Med. Biol.*, **413**, 63-73 (1997).
140. S. Wray, M. Cope, D. D.T., J.S. Wyatt, and E.O.R. Reynolds, *Biochim. Biophys. Acta*, **933**(184-192) (1988).
141. C.E. Cooper, D.T. Delpy, and E.M. Nemoto, *Biochem. J.*, **332**, 627-632 (1998).
142. S. Kuroda, *Hokkaido Igaku Zasshi*, **70**, 401-411 (1995).
143. M. Tsuji, H. Naruse, J. Volpe and D. Holtzman, *Pediatr. Res.*, **37**, 253-259 (1995).
144. A. Tanaka, T. Kitai, A. Tokuka, T. Inomoto, H.J. Kim, K. Tanaka, Y. Yamaoka and K. Ozawa, *Res. Exp. Med.*, **193**, 353-359 (1993).
145. F. Van Bel, P.E.M. Zeeuwe, C.A. Dorrepaal, M. J.N. Benders, M. Van De Bor and R. Hardjowijono, *Biol. Neonate*, **70**, 141-154 (1996).
146. V. Quaresima, R. Springett, M. Cope, J.T. Wyatt, D.T. Delpy, M. Ferrari, and C.E. Cooper, *Biochim. Biophys. Acta*, **1366**, 291-300 (1998).
147. G. Grubhofer, P. Mares, A. Rajek, T. Muellner, M. Haisjackl, M. Dworschak, and A. Lassnigg, *Acta Anaesthesiol. Scand.*, **44**, 586-591 (2000).

148. R.E. Gagnon, F.A. Gagnon, and A.J. MacNab, *Eur. J. Appl. Physiol. Occup. Physiol.*, **74**, 487-495 (1996).
149. M.H. Heise, *Horm. Metab. Res.*, **28**, 527-534 (1996).
150. M.A. Arnold, *Curr. Opin. Biotechnol.*, **7**, 46-49 (1996).
151. D.L. Bodenner and R.C. Eastman, *Curr. Opin. Endocrinol. Diabetes*, **2**, 72-77 (1995).
152. M. Heise, A. Bittner and R. Marbach, *J. Near Infrared Spectrosc.*, **6**, 349-359 (1998).
153. J.J. Burmeister and M.A. Arnold, *Clin. Chem.*, **45**(9), 1621-1627 (1999).
154. R. Marbach, T. Koschinsky, F.A. Gries, and H.M. Heise, *Appl. Spectrosc.*, **47**(7), 875-878 (1993).
155. M.A. Arnold and G.W. Small, *Anal. Chem.*, **62**, 1457-1464 (1990).
156. M.A. Arnold, J.J. Burmeister, and G.W. Small, *Anal. Chem.*, **70**, 1773-1781 (1998).
157. I. Gabriely, R. Wozniak, M. Mevorach, J. Kaplan, Y. Aharon and H. Shamoon, *Diabetes Care*, **22**, 2026-2032 (1999).
158. K.M. Quan, G.B. Christison, H.A. MacKenzie, and P. Hodgson, *Phys. Med. Biol.*, **38**, 1911-1922 (1993).
159. M.H. Heise and A. Bittner, *Proc. SPIE-Int. Soc. Opt. Eng.*, **3257** (Infrared Spectroscopy: New Tool in Medicine), 2-12 (1998).

160. V.A. Saptari and K. Yousef-Toumi, *Proc. SPIE-Int. Soc. Opt. Eng.*, **4163** (Optical Techniques and Instrumentation for Measurement of Blood Composition, Structure and Dynamics), 45-54 (2000).
161. O.J. Rolinski, D.J.S. Birch, L.J. McCartney and J.C. Pickup, *J. Photochem. Photobiol., B*, **54**, 26-34 (2000).
162. V.M. Aristarkhov and I.S. Balakhovskii, *Klin. Lab. Diagn.*, **4**, 18-22 (1998).
163. B. Jung, M. McShane, S. Rastegar and G.L. Cote, *Proc. SPIE-Int. Soc. Opt. Eng.*, **3253** (Biomedical Sensing and Imaging Technologies), 41-46 (1998).
164. H.J. Kim, Y.A. Kim, S.H. Chang, H. Chang, K. Cantrell and E.H. Piepmeier, *Anal. Sci. Technol.*, **11**, 47-53 (1998).
165. G. Lu, X. Zhou, M.A. Arnold and G.W. Small, *Appl. Spectrosc.*, **51**, 1330-1339 (1997).
166. A.J. Berger, Y. Wang, M.S. Feld and G.R. Harrison, *Appl. Opt.*, **35**, 209-212 (1996).
167. K.H. Hazen, M.A. Arnold and G.W. Small, *Appl. Spectrosc.*, **48**, 477-483 (1994).
168. L.A. Marquardt, M.A. Arnold and G.W. Small, *Anal. Chem.*, **65**, 3271-3278 (1993).
169. T. Yano, T. Fanatsu, K.-I. Suehara and Y. Nakano, *J. Near Infrared Spectrosc.*, **9**, 43-48 (2001).
170. T. Yano, H. Matsushige, K.-I. Suehara and Y. Nakano, *J. Biosci. Bioeng.*, **90**, 540-544 (2000).

171. R.E. Shaffer, G.W. Small and M.A. Arnold, *Anal. Chem.*, **68**, 2663-2675 (1996).
172. S. Pan, H. Chung, M.A. Arnold, and G.W. Small, *Anal. Chem.*, **68**(7), 1124-1135 (1996).
173. A.K. Amerov, K.J. Jeon, Y.-J. Kim and G. Yoon, *Proc. SPIE-Int. Soc. Opt. Eng.*, **3599** (Optical Diagnostics of Biological Fluids IV), 33-42 (1999).
174. J.Y. Qu, B.C. Wilson and D. Suria, *Appl. Opt.*, **38**, 5491-5498 (1999).
175. T.W. Koo, A.J. Berger, I. Itzkan, G. Horowitz and M.S. Feld, *Diabetes Technol. Ther.*, **1**, 153-157 (1999).
176. Q. Ding, 'Data Analysis Strategies for quantitative near-infrared spectroscopy: application to the measurement of organic solvents in water and the determination of glucose in biological matrixes'. Unpublished Ph. D. Dissertation, Ohio University, Athens, OH (1998).
177. I. Itzkan, A. Berger, T.-W. Koo, M.S. Feld and G. Horowitz, *Book of Abstracts*, *216th ACS National Meeting, Boston, August 23-27*, I&EC 144 (1998).
178. K.H. Hazen, M.A. Arnold, and G.W. Small, *Anal. Chim. Acta.*, **371**, 255-267 (1998).
179. X. Dou, Y. Yamaguchi, H. Yamamoto, S. Doi and Y. Ozaki, *Vib. Spectroscopy*, **13**, 83-89 (1996).
180. A.J. Berger, I. Itzkan and M.S. Feld, *Spectrochim. Acta, Part A*, **53A**, 287-292 (1997).

181. D.M. Haaland, M.R. Robinson, G.W. Koepp, E.V. Thomas and R.P. Eaton, *Appl. Spectrosc.*, **46**, 1575-1578 (1992).
182. E.V. Thomas, *Anal. Chem.*, **72**, 2821-2827 (2000).
183. M.W. Misner, H. Guthermann and M. Block, *Proc. SPIE-Int. Soc. Opt. Eng.*, **3603** (Systems and Technologies for Clinical Diagnostics and Drug Discovery II), 23-29 (1999).
184. K.J. Schlager and T.L. Ruchti, *Proc. SPIE-Int. Soc. Opt. Eng.*, **2386**, 174-184 (1995).
185. J.J. Burmeister, M.A. Arnold and G.W. Small, *Diabetes Technol. Ther.*, **2**, 5-16, (2000).
186. H.S. Ashton, H.A. MacKenzie, P. Rae, Y.C. Shen, S. Spiers and J. Lindberg, *AIP Conf. Proc.*, **463**, 570-572 (1999).
187. J. Qu and B.C. Wilson, *J. Biomed. Opt.*, **2**, 319-325 (1997).
188. G. Spanner and R. Niessner, *Fresenius' J. Anal. Chem.*, **355**, 327-328 (1996).
189. M. Noda, M. Kimura, T. Ohta, A. Kinoshita, F. Kubo, N. Kuzuya and Y. Kanazawa, *Int. Congr. Ser.*, **1100**, 1128-1132 (1995).
190. H.M. Heise, A. Bittner and R. Marbach, *Clin. Chem. Lab. Med.*, **38**, 137-145 (2000).
191. U.A. Mueller, B. Mertes, C. Fischbacher, K.U. Jageman and K. Danzer, *Int. J. Artif. Organs*, **20**, 285-290 (1997).

192. K. Maruo, M. Oka, K. Shimizu and J.C. Chen, *Kokai Tokkyo Koho*, (2001), Application JP 99-211457.
193. K. Ohkubo, M. Inohara and Y. Yoshimura, *Kokai Tokkyo Koho*, (1999), Application JP 97-310890.
194. R. Quintana, *U.S.* (1996), Application US 94-243756.
195. A. Essen-Moeller, *PCT Int. Appl.*, (1996), Application WO 96-SE327.
196. R.D. Rosenthal, J.J. Mastrototaro, J.K. Frischmann and R. Quintana, *PCT Int. Appl.*, (1995), Application WO 94-US9210.
197. R.D. Rosenthal, *PCT Int. Appl.*, (1993), Application WO 92-US10046.
198. R.D. Rosenthal, *PCT Int. Appl.*, (1992), Application WO 92-US5134.
199. R.D. Rosenthal, L.N. Paynter and L.H. Mackie, *U.S.*, (1992), Application US 90-544580.
200. R.D. Rosenthal, *U.S.*, (1991), Application US 90-565302.
201. R.D. Rosenthal, *U.S.*, (1991), Application US 89-298904.
202. R.D. Rosenthal, L.N. Paynter and L.H. Mackie, *PCT Int. Appl.*, (1990), Application WO 90-US394.
203. K.J. Schlager, *U.S.*, (1989), Application US 88-145459.
204. M. Toida and I. Miyagawa, *Eur. Pat. Appl.*, (1997), Application EP 97-107946.
205. G. Mueller, *Ger. Offen.*, (1997), Application DE 95-19538372.
206. M. Noda and M. Kimura, *Kokai Tokkyo Koho*, (2000), Application JP 99-670079.

207. K. Maruo and M. Oka, *Kokai Tokkyo Koho*, (1999), Application JP 97-353845.
208. R.D. Rosenthal, *PCT Int. Appl.*, (1997), Application WO 97-US2349.
209. K. Abraham-Fuchs and A. Oppelt, *Ger.*, (1999), Application DE 98-19807939.
210. T. Sonehara, Y. Miyanohara, M. Suga and T. Ninomiya, *Jpn. Kokai Tokkyo Koho*, (2000), Application JP 98-198359.
211. A.K. Amerov, K.-J. Jeon, Y.-J. Kim and G.-W. Yoon, *Brit. UK Pat. Appl.*, (1999), Application GB 98-18315.
212. R.T. Kurnik, J.J. Oliver, R.O. Potts, S.R. Waterhouse, T.C. Dunn, Y. Jayalakshmi, M.J. Lesho, J.A. Tamada and C.W. Wei, *U.S.* (2001), Application US 98-163856.
213. T. Haak, *Exp. Clin. Endocrinol. Diabetes*, **107**, S-108-S113 (1999).
214. M.S. Borchert, M.C. Storrie-Lombardi and J.L. Lambert, *Diabetes Technol. Ther.*, **1**, 145-151 (1999).
215. M.A. Arnold and C.V. Eddy, *Book of Abstracts, 216th ACS National Meeting, Boston, August 23-27, I&EC-109*, (1998).
216. J. Qu and B.C. Wilson, *Proc. SPIE-Int Soc. Opt. Eng.*, **2679** (Advances in Laser and Light Spectroscopy to Diagnose Cancer and Other Diseases III: Optical Biopsy), 236-242 (1996).
217. M.J. McShane and G.L. Cote, *Proc. SPIE-Int. Soc. Opt. Eng.*, **3257** (Infrared Spectroscopy: New Tool in Medicine), 86-90 (1998).

218. M.R. Riley, H.M. Crider, M.E. Nite, R.A. Garcia, J. Woo and R.M. Wegge, *Biotechnol. Prog.*, **17**, 376-378 (2001).
219. C.B. Lewis, R.J. McNichols, A. Gowda and G.L. Cote, *Appl. Spectrosc.*, **54**, 1453-1457 (2000).
220. M.R. Riley and H.M. Crider, *Talanta*, **52**, 473-484 (2000).
221. M.R. Riley, C.D. Okeson and B.L. Frazier, *Biothechnol. Prog.*, **15**, 1133-1141 (1999).
222. M.R. Riley, M. Rhiel, X. Zhou, M.A. Arnold and D.W. Murhammer, *Biotechnol. Bioeng.*, **55**, 11-15 (1997).
223. T. Yano, M. Harata, T. Aimi and Y. Nakano, *Anim. Cell Technol.: Dev. 21st Century*, 357-361 (1995).
224. H. Chung, M.A. Arnold, M. Rhiel, and D.W. Murhammer, *Appl. Spectrosc.*, **50**(2), 270-276 (1996).
225. T. Yano and M. Harata, *Anim. Cell Technol.: Basic Appl. Aspects, Proc. Int. Meet. Jpn. Assoc. Anim. Cell Technol. 6th*, 410-405 (1994).
226. H. Chung, M.A. Arnold, M. Rhiel and D.W. Murhammer, *Appl. Biochem. Biotechnol.*, **50**, 109-125 (1995).
227. M.J. McShane and G.L. Coté, *Appl. Spectrosc.*, **52**(8), 1073-1078 (1998).
228. M.J. McShane, G.L. Coté, and C.H. Spiegelman, *Appl. Spectrosc.*, **52**(6), 878-884.
229. G. A. Gaesser and D.C. Poole, *Int. J. Sports Med.*, **9**, 284-287 (1988).

230. J.L. Vincent, P. Dufaye, J. Berre, M. Leeman, P.J. Degaute and R. Kahn, *Crit. Care Med.*, **11**, 449-451 (1983).
231. B.N. Cowan, H.J.G. Burns, P. Boyle and I.M. Ledingham, *Anaesthesia*, **39**, 750-755 (1984).
232. D. Lafrance, L.C. Lands, L. Hornby, C. Rohlicek, and D.H. Burns, *Can. J. Anal. Sci. Spectrosc.*, **45**(2), 36-40 (2000).
233. D. Lafrance, L.C. Lands, L. Hornby, and D.H. Burns, *Appl. Spectrosc.*, **54**(2), 300-304 (2000).
234. L.M. Mitsumori, 'Near Infrared Analysis of Lactate in Solutions and Serum'. Unpublished M.Sc. Dissertation, University of Washington, Seattle, WA (1994).
235. Y. Yamasaki, H. Okuda, K. Matsuoka, and K. Xu, *US patent 5,757,002* (1998).

Chapter 3 Near Infrared Spectroscopic Measurement of Lactate in Human Plasma.

As a marker of the glycolytic activity, quantitative analysis of lactate is of significance during clinical situations when diagnosis is rapidly needed. Measurements of lactate levels have then to be performed by a rapid and robust method. Some studies, which have reported lactate measurements in either simulated or biological matrices and undiluted human plasma using NIRS, suggested the technique could hold significant promise for noninvasive analysis. However, none of these studies were able to quantify lactate accurately enough for clinical purposes. As example, the PLS model was developed from the undiluted human plasma of healthy volunteer at rest. For this reason the model was unable to achieve a precision good enough to be used for real-time monitoring of lactate in clinical situations. Indeed, lactate concentrations were too low in the samples and almost at the detection limit of the technique.

To overcome this limitation, a new approach is proposed. While the lactate concentration in healthy human is usually maintained to 0.7-1 mmol/L, exercise or illness can make lactate level to reach concentration as high as 25 mmol/L. Furthermore, it is also recognized and well accepted that a lactate concentration of less than 2 mmol/L is considered as normal. Techniques that allow rapid and robust measurements of lactate concentration changes above 2 mmol/L are what should be specifically targetted.

To meet this objective, the first step of the approach proposed is to extend to a larger physiological range the lactate concentrations in human plasma. This was accomplished by collecting spectra from different exercising human subjects. Furthermore, because red blood cells were removed from plasma, interference related to scattering was minimized.

However, direct quantitative measurements by NIRS are often useless because of the lack of specificity of NIR bands. Quantification of lactate in biological fluids using NIRS is then only made possible by using multivariate data analytical techniques. Among these techniques, Partial Least Squares (PLS) has shown significant success in the determination of correlation between analyte concentrations and spectral responses in complex media. A more complete description of the method is provided in Appendix A.

3.1 *Abstract*

A method based on near-infrared spectroscopy (NIRS) is presented, which provides a rapid analysis of lactate in plasma. In order to test the technique, NIRS analysis and enzymatic measurements were made on plasma samples taken from exercising humans. A correlation coefficient of 0.995 and a standard error of 0.51 mmol/L were found between the enzymatic and the NIR results. This standard error is within the range needed for real-time monitoring of lactate in plasma for exercise studies. In the future, this technique may provide a valuable tool to assess physiological status for research and clinical use.

3.2 *Introduction*

Elevations in either blood or plasma concentrations of lactate provide evidence of increased glycolytic activity. Therefore, lactate measurements are used for both clinical and research purposes in the assessment of tissue perfusion and oxidative capacity. For instance, aerobic exercise training results in higher exercise capacities and lower lactate levels at similar workloads. The determination of lactate is also important in other clinical situations, during surgery or in emergency trauma situations, where a rapid and easy measurement method is important.⁽¹⁾

Most of the current techniques for clinical lactate measurements are based on electrochemical enzymatic sensors ⁽²⁻⁴⁾, due to the fast time response possible. However, because these methods are invasive and often require substantial sample preparations, they do not offer the possibility to the clinician of *in vivo* monitoring of lactate level in a continuous manner.

From the clinical spectroscopic methods that exist for lactate determination ⁽⁵⁻⁸⁾, near-infrared spectroscopy (NIRS) holds significant promise to achieve noninvasive measurement of lactate in biological fluids. This technique has already shown potential for monitoring other *in vivo* metabolites in biomedical analysis.⁽⁹⁻¹⁵⁾ These successes have made NIRS acceptable as alternative method for clinical measurements.

Few studies report lactate measurements in either simulated or biological matrices using NIRS. Some *in vitro* trials to quantify lactate in simulated biological matrices have been attempted.^(16, 17) However, in these studies, the system was kept simple by controlling parameters such as pH, temperature, and ionic strength using a buffered aqueous solution. It is known that these parameters have an important contribution to the water spectrum^(18, 19) and will normally vary during the monitoring of *in vivo* lactate level. More recently, a study has shown that lactate in cell culture media could be determined.⁽²⁰⁾ A standard error of prediction (SEP) of 0.40 mmol/L with the use of 10 partial least-squares (PLS) regression analysis factors was found for a lactate concentration range varying from 0.08 to 11.00 mmol/L. Finally, a recent study reports simultaneous measurements of five different analytes, including lactate, with the use of NIRS and PLS, in undiluted human plasma⁽²¹⁾ of patients at rest. However, due to the variable background between 2000 and 2400 nm, which is dominated by proteins, the study was not able to quantify lactate accurately.⁽²¹⁾

In this paper, the NIRS approach is extended to a larger human physiological range of lactate concentrations in human plasma. To accomplish this, we used NIR spectra collected from different human subjects to generate a calibration model for lactate. The normal human physiological range for lactate varies from 0.3 to 25 mmol/L. Care was taken so that the lactate concentration in this study covered a large portion of this range. The experimental design was developed to minimize the contribution of glucose or other species to the lactate estimation.

3.3 *Experimental*

3.3.1 **Instrumentation**

Plasma samples were assayed in triplicate for lactate with the use of the YSI Model 1500 Sport Lactate Analyzer (Yellow Springs Instruments, Yellow Springs, OH). This instrument used a proprietary electrochemical enzymatic detection of lactate. The mean of the three results was recorded. Plasma lactate analysis with this device has a standard prediction error of 0.2 mmol/L based on five replicates of a standard. The manufacturer reports that the instrument delivers a linear response for lactate in the 0 to 30 mmol/L concentration range.

Spectra were collected with a Nicolet Magna-IR 550 Fourier transform near-infrared (FT-NIR) spectrometer (tungsten-halogen lamp / quartz beamsplitter) equipped with an InSb detector. The spectral range scanned was from 890 to 2500 nm (11500-4000 cm^{-1}) and 64 interferogram scans at a spectral resolution of 2 cm^{-1} were averaged. Single-beam spectra were computed with a Happ-Genzel apodization and Fourier transformation routines available on the system. Background spectra of air were taken every hour. Sample absorbance in the 2000 - 2500 nm region was optimized with the use of a 1 mm pathlength rectangular Infrasil quartz cell from Starna (Atascadero, CA). Sample temperature was controlled with a copper-jacketed cell holder equipped with a YSI Model 72 temperature controller to $25 \pm 0.1^\circ\text{C}$. Temperature was monitored continuously during data collection with a copper-constantan thermocouple probe placed into the sample holder.

3.3.2 Reagents

To identify lactate contribution to the plasma spectra, we collected a pure lactate spectrum. Sodium lactate was purchased in dry form from Sigma Chemical (St. Louis, MO). Standard solution was prepared by weighing suitable amounts of sodium lactate and diluting with pH 7.2 0.1M phosphate buffer. Phosphate buffer was prepared with reagent-grade water.

3.3.3 Procedures

Ten healthy adult subjects (eight males and two females) were tested during maximal effort made by a 30s sprint on an isokinetic cycle. The cycle was modified to have the pedal speed fixed and effort translated into greater force generation.⁽²²⁾ The study was approved by the Ethics Committee of the Montreal Children's Hospital, in accordance with the Helsinki Declaration of 1975. After signed informed consent, and prior to exercise, an intravenous line was placed in the antecubital fossa, and kept patent with a 0.9% saline solution. Blood was sampled at three time intervals: (1) just prior to exercise; (2) at the end of exercise; (3) 10 min following exercise. This approach was used in an attempt to cover the largest portion of the human physiological lactate concentrations. Blood was drawn into tubes containing lithium heparin beads (Sarstedt Inc., St-Laurent, Quebec) and immediately transferred to prechilled 0.75 mL microvette tubes containing 1 mg/mL of sodium fluoride, to arrest glycolysis. Samples were then centrifuged to separate plasma and analyzed by the proprietary enzymatic method of the Yellow Springs Instruments. The pH of

blood samples was measured prior to centrifuging with the use of a microProbe pH electrode (Fisher Scientific). Plasma was kept on ice between enzymatic and FT-NIR experiments to arrest metabolism and avoid degradation of samples.

Before measurements, samples were put in the thermostated sample holder, and 5 min was given for samples to reach $25 \pm 0.1^\circ\text{C}$. Sample data collection was randomized to avoid correlation between time and lactate level.

To selectively extract lactate information from NIR spectra in the presence of other chemical interferents, we used PLS regression analysis.^(23, 24) The PLS routine has been developed previously.⁽²⁵⁾ The number of significant factors was determined from the prediction error sum of squares (PRESS) values calculated for each factor. The ratios between PRESS values for each factor and the minimum PRESS value were calculated and compared to F-test values. The F-test comparison was used to determine the minimum number of statistically significant factors.⁽²⁶⁾

The second derivatives of the 30 absorbance spectra corresponding to unique plasma samples were divided into calibration and prediction subsets using a leave N-out cross-validation PLS routine. The second-derivative spectra were determined by using the method of discrete differences.⁽²⁷⁾ The leave-N-out procedure uses all the samples but N in the calibration set and estimates the N excluded samples with the calibration results. Rather than using the conventional leave-one-out cross-validation method, we used a block of the three samples from the same volunteer.

Basically, the procedure uses the spectra from nine volunteers to estimate lactate levels in the three samples of the tenth. This procedure has the advantage of allowing the determination of inter-individual variations by estimating lactate at three different levels of concentration. Programs for the input of spectral data and cross-validation were written in Matlab (The Mathworks Inc., South Natick, MA).

3.4 *Results and Discussion*

3.4.1 Spectral Features

The human plasma spectrum is mostly dominated by water and proteins. Water has two absorbance peaks above 1900 nm, centered at 1920 and 2630 nm. The spectral region chosen for the lactate determination extended from 2050 to 2400 nm, as reported in previous studies.^(16, 17, 20, 21) This wavelength range was chosen to reduce interferences from water, since the major lactate absorbance peaks are located between the two water peaks. In Figure 3.1, a series of human plasma spectra from different patients containing lactate concentrations in the normal physiological range are shown, after subtraction of a pure water spectrum. A spectrum of lactate in buffered aqueous solution is also included in Figure 3.1. As illustrated in the figure, the three absorbance peaks related to lactate are centered at 2166, 2254, and 2292 nm. These wavelengths are in agreement with the ones suggested previously.⁽¹⁶⁾ Besides lactate absorbance, Figure 3.1 shows several other peaks. These peaks come from other plasma constituents. To enhance the spectral variations of lactate over the background, we used second-derivative spectra rather than raw spectra. In Figure 3.2,

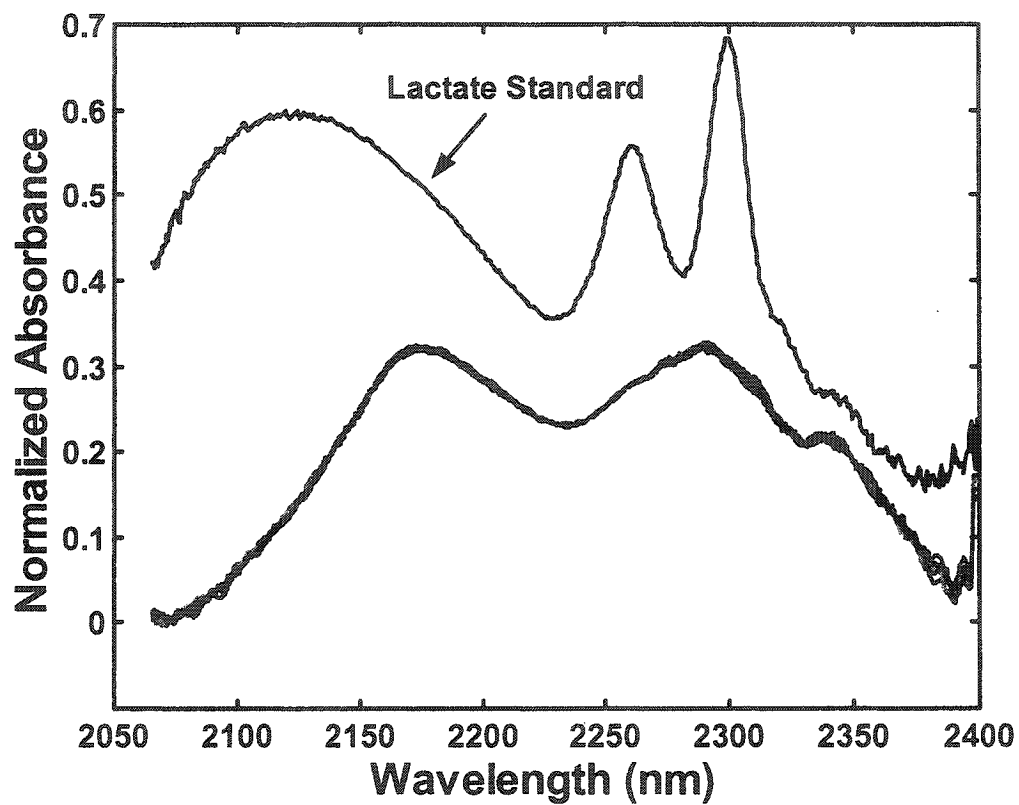


Figure 3.1: NIR absorbance spectra of human plasma specimens and 10 mmol/L lactate standard in aqueous buffered solution after water subtraction. Lactate standard spectrum has been offset for clarity.

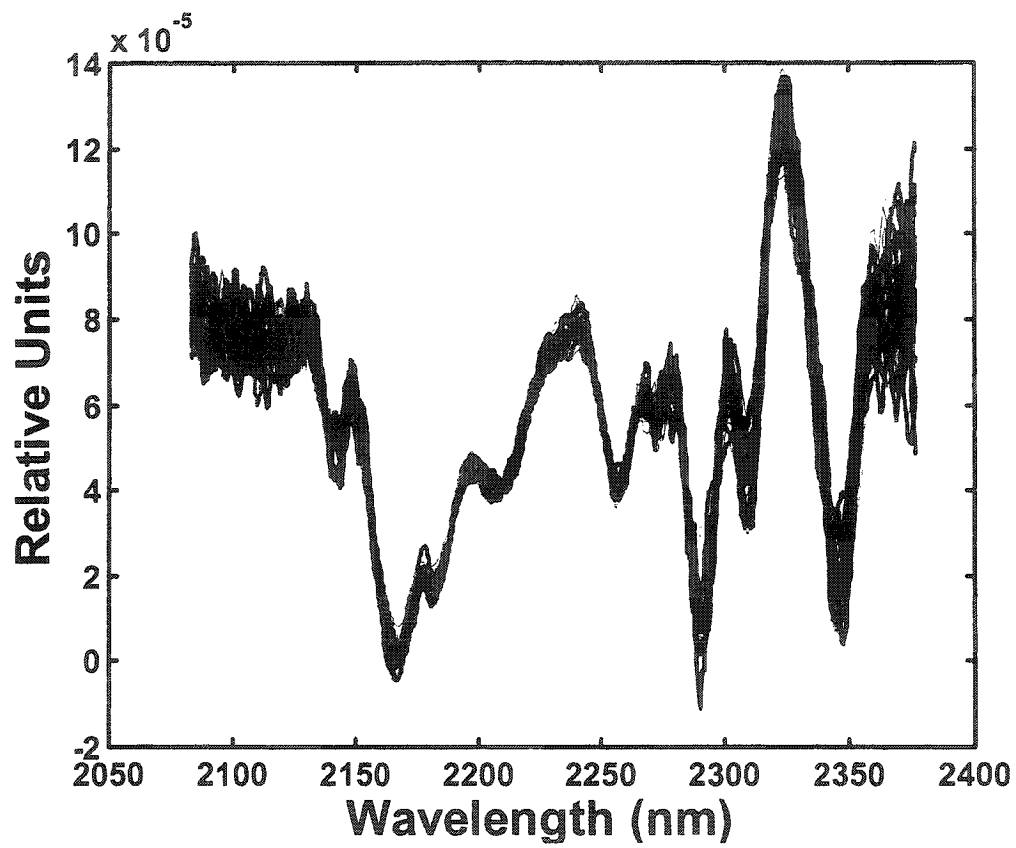


Figure 3.2: Second derivative of NIR absorbance spectra of human plasma specimens.

a series of second-derivative spectra from different patients' plasma samples are shown. The regions where lactate contributes are consistent with Figure 3.2.

3.4.2 Experimental Protocol for Minimal Covariance with Plasma Constituents

An acceptable PLS model requires the absence of covariance between the multiple components of the sample matrix. The experimental design chosen allows the development of a calibration model that isolates lactate contribution from other plasma species, such as glucose, proteins, or pH variation, and minimizes the covariance with them. First, the vast majority of energy required for a 30s sprint comes from anaerobic metabolism of glycogen and hydrolysis of phosphocreatine (PCr).^(28, 29) In fact, the fall in glycogen is accompanied by increases in muscle and blood lactate that amount to > 75% of the expected anaerobic yield of glycogen.⁽²⁸⁾ In other words, almost all the glycogen is metabolized anaerobically. The anaerobic metabolism of glycogen accounts for 50-55% of the ATP requirements and PCr degradation for 23-28%, with aerobic metabolism accounting for 16-28%.⁽²⁹⁾ Therefore, there is little uptake and breakdown of exogenous glucose during a 30s isokinetic sprint, which minimizes the covariance between lactate and glucose. Likewise, proteins are major plasma constituents. To develop a robust calibration, one must also demonstrate the absence of covariance with lactate. Vigorous exertion leads to a net flux of water into the tissues.⁽³¹⁾ This result will cause protein concentration to rise in the plasma. However, this increase in protein concentration will be small compared to lactate variation, as little water is transferred from plasma to tissues in the process.⁽³¹⁾ Together with proteins, water is the main constituent of

plasma. The absence of covariance between water content variation during exercise and lactate level is also shown by the small random baseline shift of the raw human plasma spectra. In addition, the leave-three-out cross-validation routine used includes water variation between individuals to estimate lactate concentration. Finally, since pH variations during exercise have an effect on the water spectrum^(18, 19), blood pH was also monitored for all samples. Some acidosis is observed immediately after exercise for all volunteers with an average of 0.07 pH unit change between samples. However, no significant change was noticed for the samples taken 10 min after exercise for all individuals, although lactate level changes by roughly 50%. Therefore, no linear relationship exists between pH change and lactate concentrations.

3.4.3 Optical Pathlength

A 1 mm pathlength was chosen according to previous studies that report successful quantification of lactate.^(16, 17, 20) However, the optical throughput is limited by the water absorption in the wavelength range picked for the lactate measurement. The root-mean-square (rms) noise of the 100% lines computed across the 2050 – 2400 nm using a linear model is 0.66 mAU. The signal-to-noise ratio (SNR) at 2160 nm is approximately 30, which is enough for lactate measurement.

3.4.4 PLS Calibration Models

While the first factors contribute the most to the PLS model, 10 factors is the minimal number of PLS factors as determined by PRESS and shown in Figure 3.3. However, an F-test at a 95% confidence level shows that no statistically significant

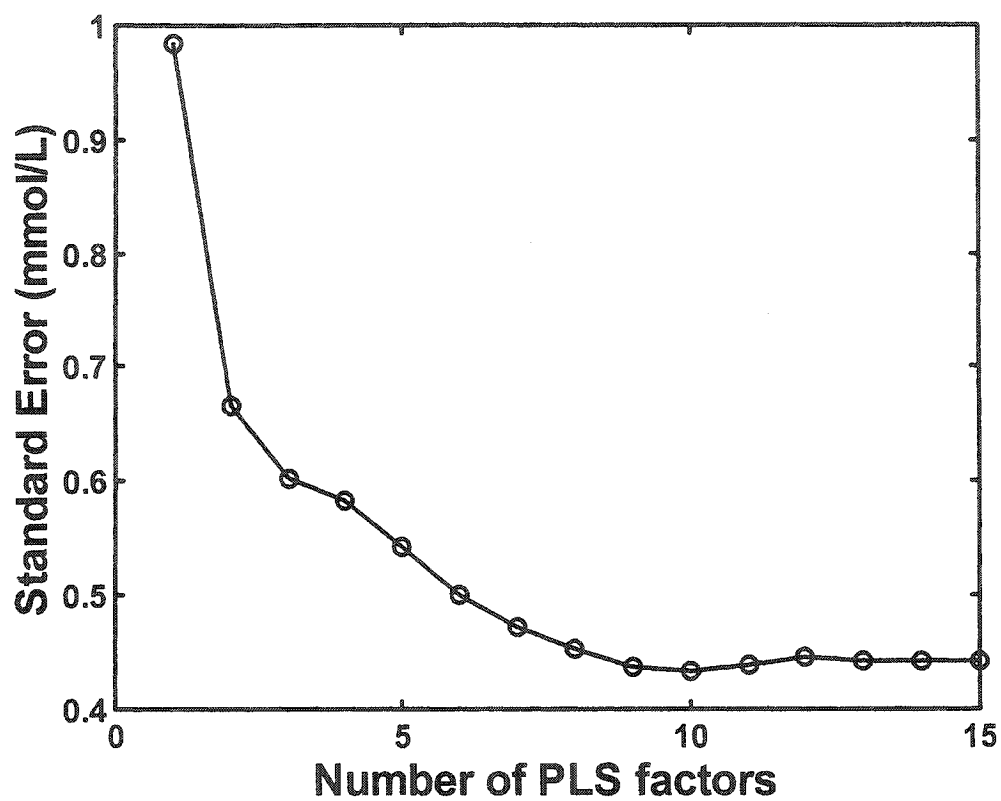


Figure 3.3: PRESS plot for lactate cross-validation model based on the 2050 to 2400 nm spectral range.

difference exists between 6 and 10 PLS factors. Therefore, 6 factors were chosen for analysis. The last 4 factors, out of the 10 chosen by PLS, appear to be associated with smaller changes between individuals, like matrix differences or pH changes during exercise.

Figure 3.4 shows the regression coefficient vector based on a 6 PLS factors model. This represents the calibration coefficients at each wavelength, as determined by PLS. Upon viewing Figure 3.4, it should be noted that the magnitudes of the peaks are the important features, and both positive and negative values are significant. In the figure, several features from the plasma matrix, such as water, proteins, and other plasma constituents, can be distinguished. The peaks at 2250 and 2300 nm contribute to the greatest extent to the calibration model. Several calibration models were developed with the use of smaller windows within the 2050-2400 nm range, in an attempt to achieve a better correlation of the data. However, the best correlation was obtained when the entire range, from 2050 to 2400 nm, was used to build the model, as previously shown.⁽¹⁷⁾

Estimations of lactate concentration in plasma with the use of PLS were obtained by the scalar product of the calibration coefficients vector and each spectrum of the data set. Results with the use of 6 PLS factors are shown in Figure 3.5. Correlation between the data and the line of identity gives a correlation coefficient (r^2) of 0.995. The root-mean-square error of cross-validation (RMSECV) on the linear regression is 0.51 mmol/L. Furthermore, the figure shows an increased spread in the

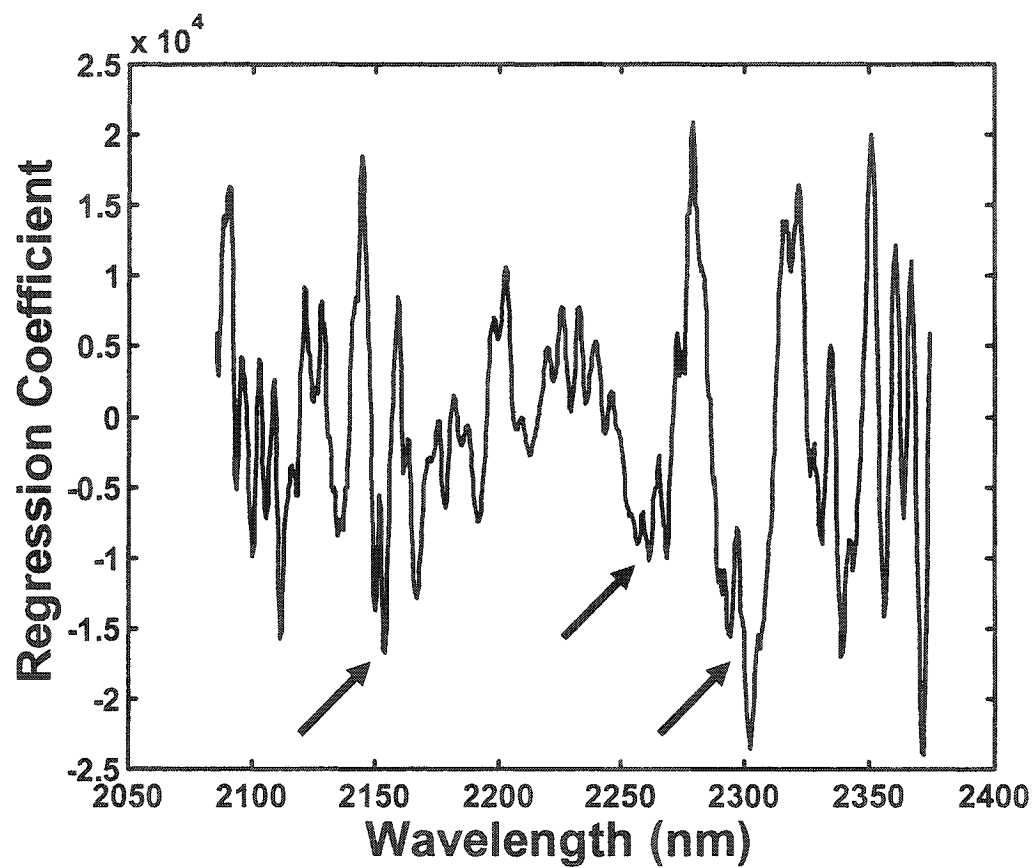


Figure 3.4: Linear regression coefficient plot using 6 PLS factors for the NIR determination of lactate in human plasma. Regions where lactate contributes are identified.

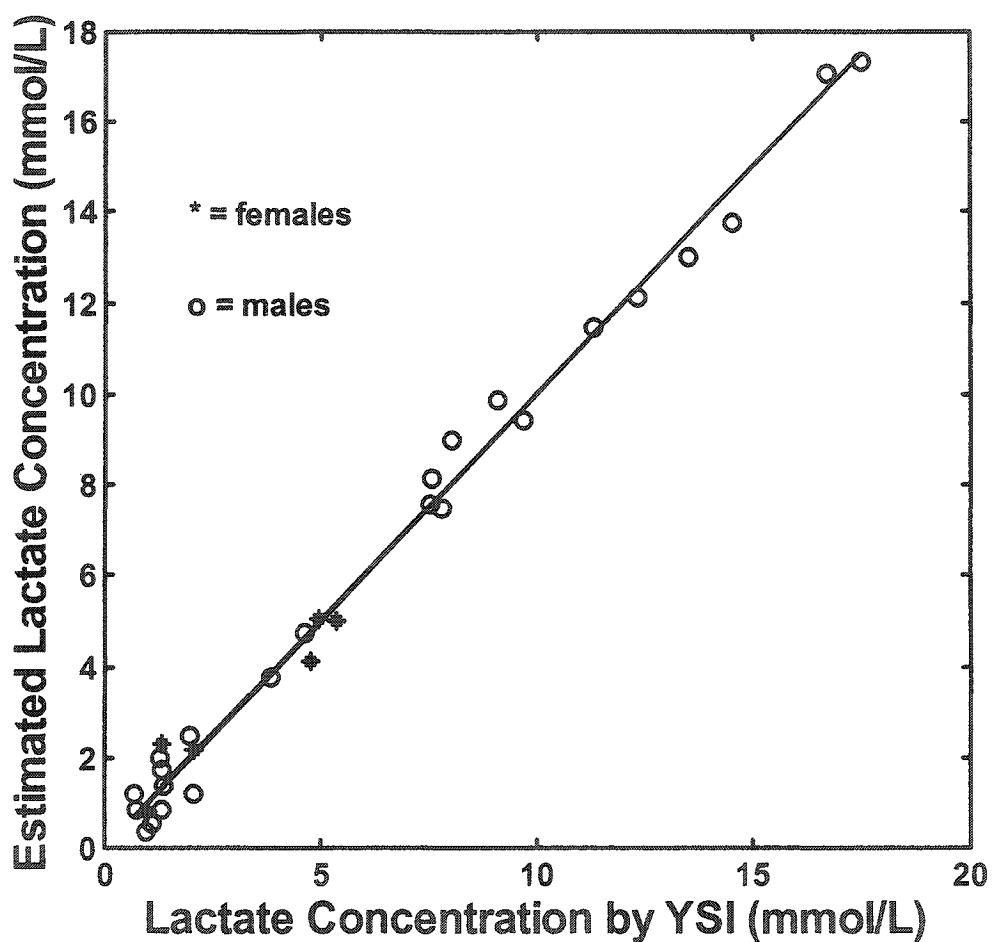


Figure 3.5: NIRS estimated vs. YSI Lactate Analyzer values for human plasma samples for each of the ten subjects. Cross-validation model: 6 PLS factors based on 2050-2400 nm spectral segment.; $n=30$, $r^2=0.995$, RMSCV=0.51 mmol/L using a leave-3-out cross-validation procedure.

data at low lactate concentrations. This result is confirmed when standard error is calculated on the data of each of the three time intervals samples. The spreading of the data indicates the limitation of the model to estimate low lactate levels⁽²¹⁾ when a larger physiological range of lactate concentration is used to build the calibration model. However, no particular grouping in the data is seen. This consideration indicated that possible variation in plasma composition between individuals has little impact on the model. Likewise, Figure 3.5 showed similarities between subjects in data spreading along the line of identity. This result seems to indicate that gender has little or no impact on the data grouping.

3.5 Conclusion

It has been shown that lactate measurement in human plasma is possible with the used of the NIRS in the 2050-2400nm spectral range. Although some spreading in the data is seen at low lactate concentrations, the method achieves a standard error of 0.51 mmol/L, which is well within the range needed for real-time monitoring of lactate in plasma for exercising studies. By extending the work of Hazen et al.⁽²⁵⁾ to a larger human physiological range of lactate concentrations, the results of this work represent an important step toward the development of an NIRS method for the determination of lactate in blood. This method may provide a faster and nondestructive alternative to current enzymatic ones.

3.6 References

1. P. Racine, R. Engelhardt, J.C. Higelin, and W. Mindt, *Med. Instrum.*, **9**, 11-14 (1975).
2. W.P. Soutter, F. Sharp, and D.M. Clark, *Br. J. Anaesth.*, **50**, 445-450 (1978).
3. D.L. Williams, A.R. Doig, and A. Korosi, *Anal. Chem.*, **42**, 118-121 (1970).
4. D.A. Baker and D.A. Gough, *Anal. Chem.*, **67**, 1536-1540 (1995).
5. W.G. Kuhr and J. Korf, *J. Cerebral Blood Flow Metabol.*, **8**, 130-137 (1988).
6. R.J. Henry, D.C. Cannon and J.W. Winkelman, *Clinical Chemistry : Principles and Technics* (Harper and Row, Hagerstown Maryland, 1974), 2nd ed., p.1328.
7. T. Michaelis, K.-D. Merboldt, H. Bruhn, W. Hänicke, and J. Frahm, *Radiology*, **187**, 219-227 (1993).
8. A.F. Mannion, P.M. Jakeman, and P.L.T. Willan, *J. Appl. Physiol.*, **75**, 1412-1418 (1993).
9. L.A. Sodickson and M.J. Block, *Clin. Chem.*, **40**, 1838-1844 (1994).
10. M.R. Robinson, R.P. Eaton, D.M. Haaland, G.Q. Koepp, E.V. Thomas, B.R. Stallard, and P.L. Robinson, *Clin. Chem.*, **38**, 1618-1622 (1992).
11. R. Marbach, Th. Koschinsky, F.A. Gries, and H.M. Heise, *Appl. Spectrosc.*, **47**, 875-881 (1993).
12. M.A. Arnold, "New Developments and Clinical Impact of Noninvasive Monitoring", in *Handbook of Clinical Laboratory Automation, Robotics and knowledge Optimization*, G.R. Kost, Ed. (John Wiley and Sons, New York, 1996), Chap. 26, p.631.

13. C. Fischbacher, K.U. Jagemann, K. Danzer, U.A. Muller, L. Papenkordt, and J. Schuler, *Fresenius' J. Anal. Chem.*, **359**, 78-82 (1997).
14. J. Qu and B.C. Wilson, *J. Biomed. Opt.*, **2**, 319-325 (1997).
15. H.M. Heise and A. Bittner, *SPIE-Int. Soc. Opt. Eng.*, **3257**, 2-5 (1998).
16. H. Chung, M.A. Arnold, M. Rhiel, and D.W. Murhammer, *Appl. Spectrosc.*, **50**, 270-276 (1996).
17. M.J. McShane, G.L. Coté, and C.H. Spiegelman, *Appl. Spectrosc.*, **52**, 878-884 (1998).
18. J. Lin and C.W. Brown, *Appl. Spectrosc.*, **47**, 1720-1727 (1993).
19. M.K. Phelan, C.H. Barlow, J.J. Kelly, T.M. Jinguji, and J.B. Callis, *Anal. Chem.*, **61**, 1419-1424 (1989).
20. M.J. McShane and G.L. Coté, *Appl. Spectrosc.*, **52**, 1073-1078 (1998).
21. K.H. Hazen, M.A. Arnold, and G.W. Small, *Anal. Chim. Acta*, **371**, 255-267 (1998).
22. L.C. Lands, L. Hornby, G. Desrochers, T. Iler, and G.J.F. Heigenhauser, *J. Appl. Physiol.*, **77**, 2506-2510 (1994).
23. K.R. Beebe, B.R. Kowalski, *Anal. Chem.*, **59**, 1007A-1017A (1987).
24. H. Martens and T. Næs, *Multivariate Calibration* (John Wiley and Sons, New York, 1989), p.419.
25. L.S.L. Arakaki, M.J. Kushmerick and D.H. Burns, *Appl. Spectrosc.*, **50**, 697-707 (1996).
26. D.M. Haaland, E.V. Thomas, *Anal. Chem.*, **60**, 1193-1202 (1988).
27. F. Holler, D.H. Burns, and J.B. Callis, *Appl. Spectrosc.*, **43**, 877-882 (1989).

28. N. McCartney, L.L. Spriet, G.J.F. Heigenhauser, J.M. Kowalchuk, J.R. Sutton, and N.L. Jones, *J. Appl. Physiol.*, **60**, 1164-1169 (1986).
29. M.E. Trump, G.J.F. Heigenhauser, C.T. Putman, and L.L. Spriet, *J. Appl. Physiol.*, **80**, 1574-1580 (1996).
30. M.I. Lindinger, G.J. Heigenhauser, M.S. McKelvie, and N.L. Jones, *Am. J. Physiol.*, **262** (1 Pt 2), R126-136 (1992).

Chapter 4 Lactate Measurement in Whole Blood using Near Infrared Spectroscopy.

The demonstration in the previous chapter of the capability of NIRS to quantify lactate in plasma using partial least squares (PLS) regression was an important step towards the development of an *in vivo* method. It showed that lactate within the human physiological range could be estimated by this technique, which minimized the contribution or interference from other plasma constituents. However, although plasma represented a more complex medium compared to simulated matrices, some obstacles still existed that may prevent NIRS to be used for real-time monitoring of lactate in clinical situations or physiological studies.

To determine lactate in plasma by NIRS, there is a need for the samples to be centrifuged to separate plasma from red cells. Erythrocytes (or red cells) account for roughly 44 percent of blood volume and plasma for 55 percent.⁽¹⁾ White cells and platelets account for the rest of the blood volume. Plasma main constituents after water are proteins, which accounts for approximately 7% of the plasma volume and can be divided into three categories: Albumins accounting for about 55% of the total proteins in blood, Globulins for about 40% and Fibrinogen for about 5-6% of the total proteins.⁽¹⁾

As a result of red cells removal, scattering was not significant in the plasma samples analyzed in the previous chapter. However, the scattering coefficient in the

2000-2400 nm wavelength range was measured at 3.0 mm^{-1} in tissues. Potential impacts of scattering on the ability to measure lactate by NIRS in blood samples need to be evaluated.

In this chapter, an initial feasibility study was made to determine the potential of NIRS to measure lactate with a small data set of whole blood samples using the PLS regression approach. Estimates of lactate concentration are made on arterial and venous blood samples from exercising rats.

4.1 Abstract

The objective of the study was to evaluate the potential of Near Infrared Spectroscopy (NIRS) as a technique for rapid analysis of lactate in whole blood. In order to test the NIRS technique, a comparison was made with enzymatic measurements using whole blood samples taken from exercising rats. Spectra were collected over the 2050-2400 nm spectral range with a 1 mm optical path length quartz cell. Reference lactate concentrations in the samples were determined by enzymatic measurements. Estimates and calibration of the lactate concentration with NIRS were made using Partial Least-Squares (PLS) regression analysis and leave-N-out cross validation on second derivative spectra. Regression analysis provided a correlation coefficient of 0.984 and a standard error of 0.29 mmol/L between the enzymatic assay and the NIRS technique. The results suggest that NIRS may provide a valuable tool to assess physiological status for both research and clinical use.

4.2 Introduction

As a key metabolite of glycolytic activity, lactate is an indicator of the energy production of the whole organism. For this reason, lactate is of interest in sports medicine. In this discipline, lactate measurements are used for both clinical and research purposes in the assessment of tissue perfusion and oxidative capacity. For instance, the estimation of lactate levels in biological fluids allows the determination of anaerobic threshold during physical exercise.⁽²⁾ The determination of lactate is also of importance in several clinical situations, as during surgery or in emergency trauma situations, where a rapid and easy method is important for diagnostic assessment.^(3,4)

To achieve fast lactate measurements in critical circumstances, most of the standard clinical methods are based on electrochemical enzymatic sensors.⁽⁵⁻⁷⁾ However, because these methods are invasive and often require substantial sample preparations, they do not offer the possibility to the clinician of *in vivo* monitoring of lactate level in a continuous manner. Of the clinical spectroscopic methods that exist for lactate determination⁽⁸⁻¹¹⁾, Near-Infrared Spectroscopy (NIRS) holds significant promise to achieve non-invasive measurement of lactate in biological fluids. The technique has already shown potential to monitor other *in vivo* metabolites in biomedical analysis.⁽¹²⁻¹⁷⁾ These successes have made NIRS acceptable as alternative method for clinical measurements.

Some studies report lactate measurements in either simulated or biological matrices using NIRS.⁽¹⁸⁻²³⁾ Attempts have been made to quantify lactate in simulated biological matrices with some success.⁽¹⁸⁻²⁰⁾ In these studies, the biosystem used was kept simple by controlling parameters such as pH, temperature and ionic strength using a buffered aqueous solution. Recently we have shown successful measurements of lactate in plasma from exercising humans using NIRS.⁽²³⁾ However, no study has reported quantification of lactate in whole blood using NIRS.

The present study examines the potential of NIRS to estimate lactate concentrations in whole blood. To accomplish this, Near-Infrared (NIR) spectra of whole blood samples collected from exercising rats are used to generate a calibration model for lactate. Acceptable prediction ability is demonstrated for lactate.

4.3 *Materials and Methods*

4.3.1 Instrumentation

Blood samples were assayed for lactate using the YSI model 1500 Sport Lactate Analyzer (Yellow Springs Instruments, Yellow Springs, Ohio). This instrument used a proprietary electrochemical enzymatic method of detection for lactate. The mean lactate reading of three assays was recorded and used as the lactate concentration for the given sample. Blood lactate analysis with this device has a standard error of 0.2 mmol/L based on five replicates of a standard. The

manufacturer reports that the instrument delivers a linear response for lactate in the 0 to 30 mmol/L concentration range, which is within the range of the samples used.

Near Infrared spectra were collected with a Nicolet Magna-IR 550 FTNIR spectrometer equipped with a tungsten-halogen lamp, a quartz beamsplitter and a cryogenically cooled indium antimonide (InSb) detector. Sixty-four interferogram scans at a spectral resolution of 2 cm^{-1} were averaged over the 890 nm to 2500 nm ($11500\text{--}4000\text{ cm}^{-1}$) spectral range. Single-beam spectra were computed using a Happ-Genzel apodization and Fourier transformation routines available on the system. Background spectra of air were taken at hourly intervals. Samples were held in a 1 mm pathlength rectangular Infrasil quartz cell from Starna (Atascadero, CA). Sample temperature was controlled and maintained with a copper-jacketed cell holder equipped with a YSI Model 72 Temperature Controller (Yellow Springs Instruments, Yellow Springs, Ohio) to $25 \pm 0.1^\circ\text{C}$. Temperature was monitored continuously during data collection with a copper-constantan thermocouple probe placed into the sample holder.

4.3.2 Reagents

To identify the spectral characteristics of lactate from other blood constituents, a pure lactate spectrum was collected. Sodium lactate was purchased in dry form (Sigma Chemical, St. Louis, MO). A standard solution was prepared by weighing a suitable amount of sodium lactate and diluting with a 0.1M phosphate buffer (pH 7.2). The phosphate buffer was prepared with deionized water.

4.3.3 Procedure

Three adult male Sprague-Dawley rats were run on a treadmill at a constant speed until exhaustion on separate days. The rats doubled their oxygen consumption, and did sufficient exercise to raise their blood lactate concentrations. Samples of blood were taken at two time intervals: (1) just prior to exercise; (2) at the end of exercise. Lines placed in the superior vena cava-right atrial junction and the ascending aorta were used to ensure arterial and venous sampling respectively. Blood was drawn into tubes containing lithium heparin beads (Sarstedt Inc., St-Laurent, Quebec) and immediately transferred to pre-chilled 0.75 ml microvette tubes containing 1 mg/ml of sodium fluoride, to arrest glycolysis. Samples were analyzed by the enzymatic method. Blood was kept on ice between enzymatic and FTNIR experiments to arrest metabolism and avoid degradation of samples.

Samples were put in the thermostated sample holder and given five minutes to reach $25 \pm 0.1^{\circ}\text{C}$, before collecting spectral responses. Just prior to data collection, samples were stirred using a laboratory vortex mixer. Spectral measurements from randomly selected samples were done to avoid any instrument bias.

4.3.4 Partial Least Squares Analysis.

To selectively extract lactate information from NIR spectra in the presence of other chemical interferents, PLS regression analysis was used.^(24,25) Partial Least Squares Regression Analysis is a multivariate method used to determine correlations between analyte concentrations and spectral responses, assuming a relationship

between the two variables. The method consists of extracting orthogonal factors to model the spectral response that correlates with the analyte concentrations. Each factor describes the co-variance between the calibration spectra responses and the analyte concentrations in decreasing amounts. The algorithm used to extract the information has been developed previously.⁽²⁶⁾ To determine the minimum number of significant factors to describe the calibration set, the Prediction Error Sum of Squares (PRESS) values calculated for each factor was used. The ratios between PRESS values for each factor and the minimum PRESS value were calculated and compared to F-test value to determine the minimum number of significant factors.⁽²⁷⁾

The second derivative of the 10 absorbance spectra corresponding to unique blood samples were divided into calibration and prediction subsets using a leave N -out cross-validation PLS routine. The second derivative spectra were determined using the method of discrete differences.⁽²⁸⁾ The leave- N -out procedure uses all the samples but N in the calibration set and estimates the N excluded samples with the calibration results. Rather than using the conventional leave-one-out cross validation method, a block of two spectra, corresponding to the venous and arterial blood samples from the same rat, was used. Essentially, the procedure uses the spectra from 8 samples to estimate lactate levels in the other two. The method is repeated until all 10 samples have been estimated. This procedure has the advantage of allowing the determination of inter-individual variations by estimating lactate at two different levels of concentration. All routines used in the analysis were written in the MATLAB programming language (The Mathworks Inc., South Natick, MA).

4.4 *Results and Discussion*

4.4.1 *Spectral Features.*

Whole blood spectrum is mostly dominated by two main constituents, water and proteins. To reduce interferences from water in the lactate determination, the 2050 to 2400 nm spectral region was used, as reported in previous studies.⁽¹⁸⁻²³⁾ This range was chosen because water has two absorbance peaks above 1900 nm, centered at 1920 and 2630 nm. The major lactate absorbance peaks are located between the two water peaks. This point is illustrated in Figure 4.1, where a series of whole blood spectra from different rats are shown, after subtraction of a pure water spectrum. A difference spectrum of lactate in buffered aqueous solution is also included in Figure 4.1. As seen in the figure, the three absorbance peaks related to lactate are centered at 2166, 2254 and 2292 nm. Besides lactate absorbance, Figure 4.1 shows several other peaks that are related to other blood constituents. To enhance the spectral variations of lactate over the background and remove the offset and baseline variations, second derivative spectra rather than raw spectra were used. In Figure 4.2, a series of second-derivative spectra from different whole blood samples are shown. The regions where lactate contributes are consistent with Figure 4.1.

4.4.2 *Optical Pathlength*

A 1 mm pathlength was chosen according to previous studies that reported successful quantification of lactate.^(19-21,23) However, the optical throughput is limited by the water absorption in the wavelength range picked for the lactate measurement.

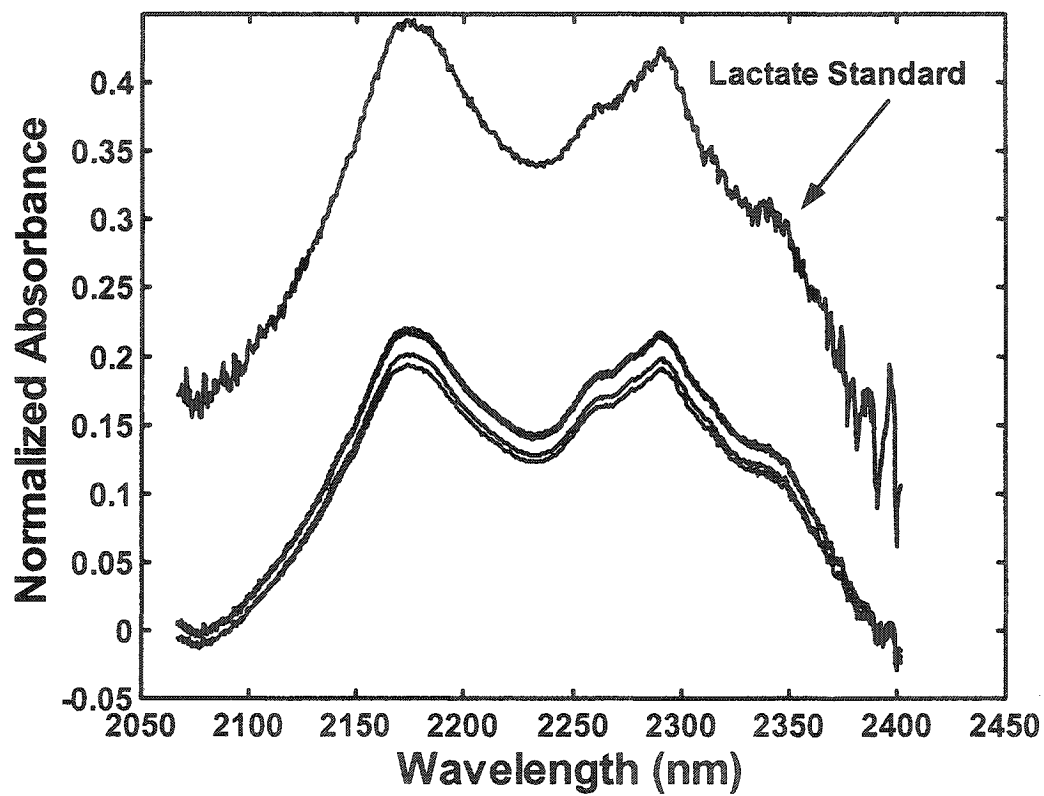


Figure 4.1: NIR absorbance spectra of rat whole blood specimens and 10 mmol/L lactate standard in aqueous buffered solution after water subtraction. Lactate standard spectrum has been offset and identified for clarity.

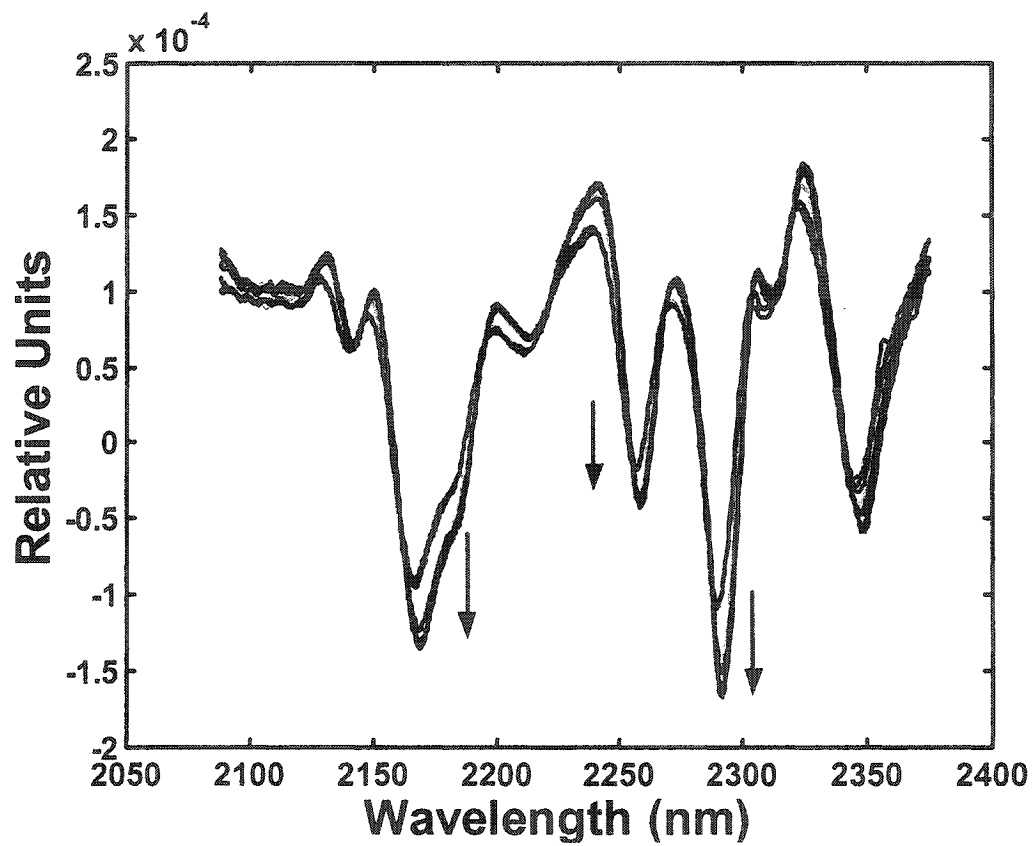


Figure 4.2: Second derivative of NIR absorbance spectra of rat whole blood specimens. Arrows indicate the regions where changes in lactate concentration are contributing.

The root-mean-square (RMS) noise of the 100% lines computed across the 2050–2400 nm using a linear model is 10.2 milli Absorbance Units (mAU). The signal-to-noise ratio (SNR) is approximately 20 at 2166 nm, which appears sufficient for lactate measurement.

4.4.3 PLS Calibration Models.

While the first factors contribute the most to the PLS model, 10 factors is the minimal number of PLS factors as determined by PRESS and shown in Figure 4.3. However, an F-test at a 95% confidence level shows that no statistically significant difference exists between 3 and 10 PLS factors. Therefore, three factors were chosen for analysis. The last seven factors, out of the ten chosen by PLS, appear to be associated with smaller changes between individuals, like matrix differences or pH changes during exercise. The absence of covariance between water content or pH variations during exercise and lactate level has been shown previously.⁽²³⁾

Figure 4.4 shows the linear regression coefficient plot based on a 3 PLS factors model. This represents the calibration coefficients at each wavelength, as determined by PLS. Upon viewing Figure 4.4, it should be noted that the magnitudes of the peaks are the important features and both positive and negative values are significant. In the figure, several features from the plasma matrix, like water, proteins and other plasma constituents can be distinguished. The peaks at 2250 and 2300 nm contribute to the greatest extent to the calibration model. Several calibration models

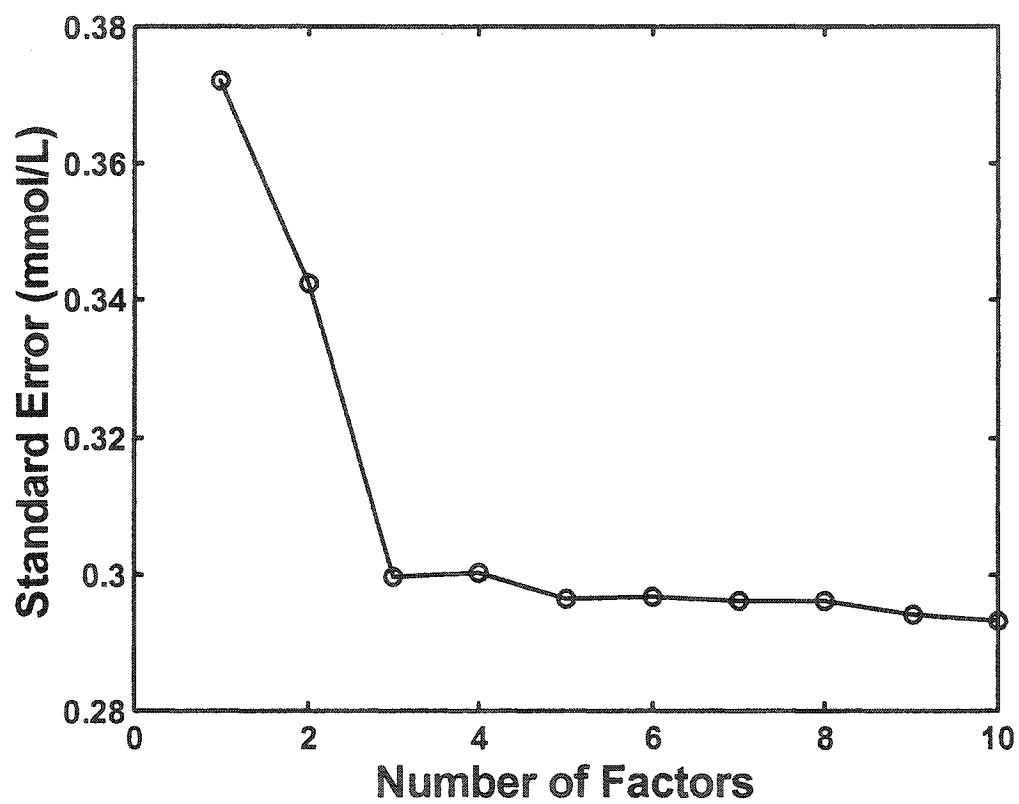


Figure 4.3: PRESS plot for lactate cross-validation model based on the 2050 to 2400 nm spectral range.

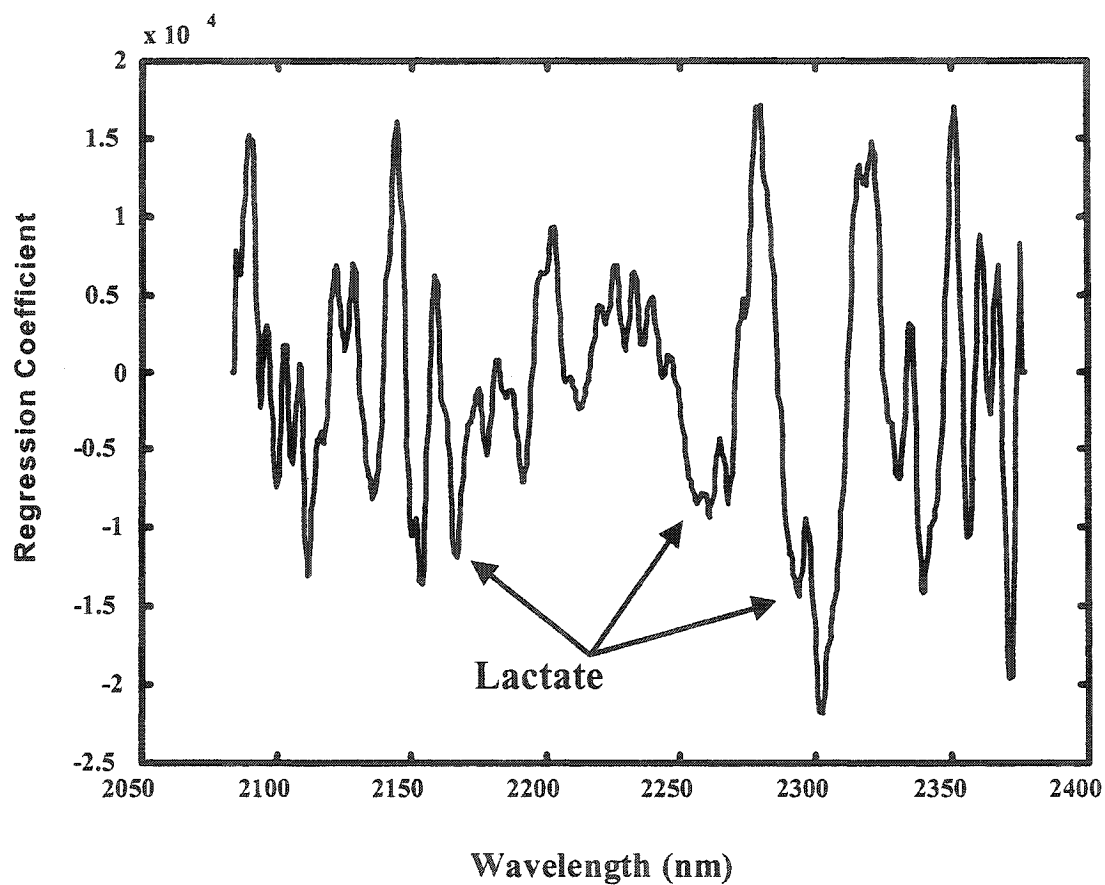


Figure 4.4: Linear Regression Coefficient plot using 3 PLS factors for the NIR determination of lactate in rat whole blood. Regions where lactate contributes are identified.

were developed using smaller windows within the 2050-2400 nm range, in an attempt to achieve a better correlation of the data. However, the best correlation was obtained when the entire range, from 2050-2400 nm, was used to build the model, as previously shown.⁽²⁰⁾

Estimations of lactate levels in blood using PLS were obtained by the scalar product of the calibration coefficient vector and each spectrum of the data set. Results using 3 PLS factors are shown in Figure 4.5. Correlation between the data and the line of identity resulted in a correlation coefficient (r^2) of 0.984. The root mean square error of cross-validation (RMSCV) on the linear regression was 0.29mmol/L. Likewise, Figure 4.5 showed similarities between subjects in data spreading along the line of identity. This indicates that although tight correlation of the data was not apparent at low lactate concentrations, the large change in lactate with exercising rat is easily distinguished.

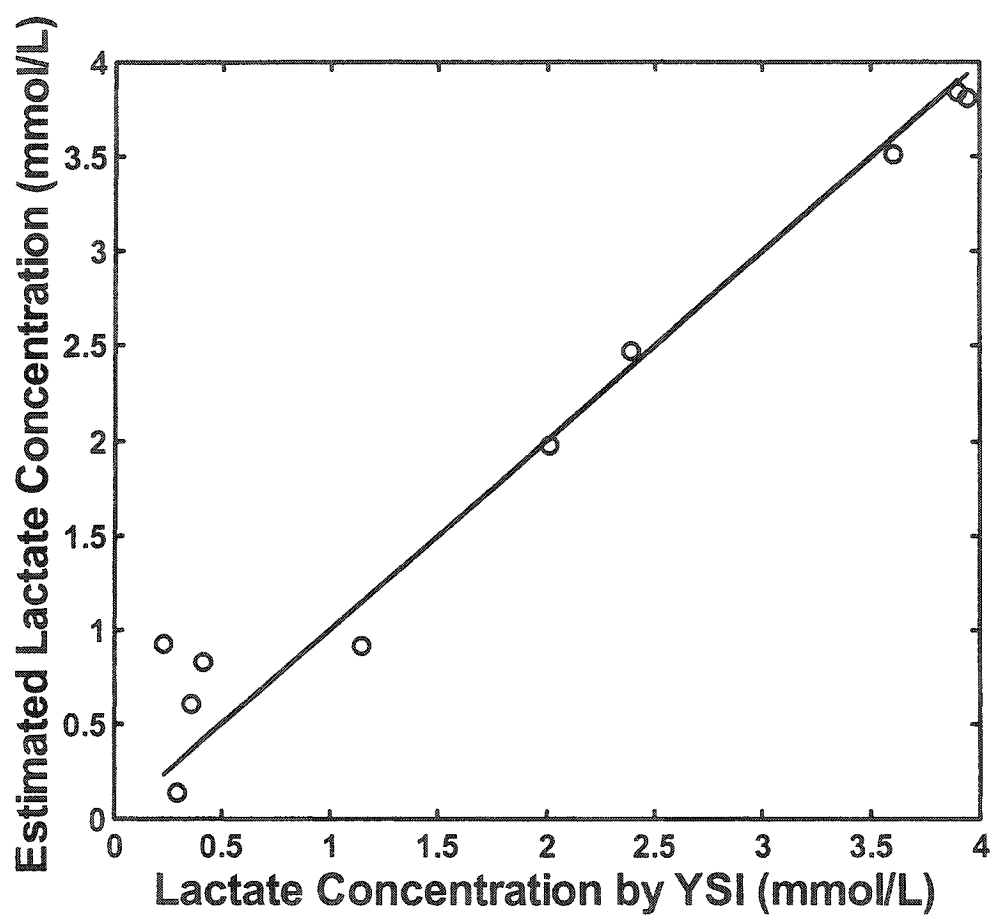


Figure 4.5: NIRS estimated vs YSI Lactate Analyser values for rat whole blood samples for each of the three subjects. Cross-validation model: 3 PLS factors based on 2050-2400 nm spectral segment; $n=10$, $r^2=0.984$, RMSCV=0.29 mmol/L using a leave 2 out cross-validation procedure.

4.5 *Conclusion*

It has been shown that lactate measurement in whole blood is possible using the NIRS in the 2050-2400nm spectral range. A good correlation is observed between estimated and reference lactate levels in blood samples. The method achieves a standard error of 0.29 mmol/L, which is well within the range needed for real-time monitoring of lactate in blood for exercising studies. By extending our previous work ⁽²³⁾ to whole blood, the results represent an important step toward the development of an in vivo NIRS method for the determination of lactate. This method may provide a faster and non-destructive alternative to current enzymatic ones.

4.6 References

1. A. White, P. Handler, E. L. Smith, R. L. Hill and I. R. Lehman, *Principles of Biochemistry 6th edition*, McGraw-Hill. New York, New York, 1978, pp.902-916.
2. G.A. Gaesser and D.C. Poole, *Int. J. Sports Med.*, **9**, 284-288 (1988).
3. P. R. Racine, R. Engelhardt, J.C. Higelin, and W. Mindt, *Medical Instrumentation*, **9**, 11-14 (1975).
4. J. Toffaletti, *Scand. J. Clin. Lab. Invest. Suppl.*, **224**, 107-110 (1996).
5. W. P. Soutter, F. Sharp, and D.M. Clark, *Br. J. Anaesth.*, **50**, 445-450 (1978).
6. D. L. Williams, A.R. Doig, and A. Korosi, *Anal. Chem.*, **42**, 118-121 (1970).
7. D. A. Baker and D.A. Gough, *Anal. Chem.*, **67**, 1536-1540 (1995).
8. W. G. Kuhr and J. Korf, *Journal of Cerebral Blood Flow and Metabolism*, **8**, 130-137 (1988).
9. R. J. Henry, D.C. Cannon, and J.W. Winkelman. *Clinical Chemistry : Principles and Technics 2nd edition*, Harper and Row. Hagerstown Maryland, 1974, p.1328.
10. T. Michaelis, K.-D. Merboldt, H. Bruhn, W. Hänicke, and J. Frahm, *Radiology*, **187**, 219-227 (1993).
11. A. F. Mannion, P.M. Jakeman, and P.L.T. Willan, *J. Appl. Physiol.*, **75**, 1412-1418 (1993).
12. L. A. Sodickson, and M.J. Block, *Clin. Chem.*, **40**, 1838-1844 (1994).
13. M. R. Robinson, R.P. Eaton, D.M. Haaland, G.Q. Koepp, E.V. Thomas, B.R. Stallard, and P.L. Robinson, *Clin. Chem.*, **38**, 1618-1622 (1992).
14. R. Marbach, Th. Koschinsky, F.A. Gries, and H.M. Heise, *Appl. Spectrosc.*, **47**, 875-881 (1993).

15. M. A. Arnold, "New Developments and Clinical Impact of Noninvasive Monitoring". In: *Handbook of Clinical Laboratory Automation, Robotics and knowledge Optimization*, Wiley, New York, 1996, Chapter 26.
16. C. Fischbacher, K.U. Jagemann, K. Danzer, U.A. Muller, L. Papenkordt, and J. Schuler, *Fresenius' J. Anal. Chem.*, **359**, 78-82 (1997).
17. H. M. Heise, R. Marbach, and A. Bittner, *J. Near Infrared Spectrosc.*, **6**, 361-374 (1998).
18. L. M. Mitsumori, "Near Infrared Analysis of Lactate in Solutions and Serum". Master Thesis, University of Washington, Seattle, 1994.
19. H. Chung, M.A. Arnold, M. Rhiel, and D.W. Murhammer, *Appl. Spectrosc.*, **50**, 270-276 (1996).
20. M. J. McShane, G.L. Coté, and C.H. Spiegelman, *Appl. Spectr.*, **52**, 878-884 (1998).
21. M. J. McShane and G.L. Coté, *Appl. Spectr.*, **52**, 1073-1078 (1998).
22. K. H. Hazen, M.A. Arnold, and G.W. Small, *Anal. Chim. Acta.*, **371**, 255-267 (1998).
23. D. Lafrance, L.C. Lands, L. Hornby, and D.H. Burns, *Appl. Spectr.*, **54**, 300-304 (2000).
24. H. Martens and T. Naes. *Multivariate Calibration.*, Wiley, New York, 1989, 419pp.
25. K. M. Beebe and B.R. Kowalski, *Anal. Chem.*, **59**, 1007A-1017A (1987).
26. L. S. L. Arakaki, M.J. Kushmerick, and D.H. Burns, *Appl. Spectr.*, **50**, 697-707 (1996).

27. D. M. Haaland and E.V. Thomas, Part 1 and 2., *Anal. Chem.*, **60**, 1193-1202 (1988).
28. F. Holler, D.H. Burns and J.B. Callis, *Appl. Spectr.*, **43**, 877-882 (1989).

Chapter 5 Measurement of Lactate in Whole Human Blood with Near-Infrared Transmission Spectroscopy.

In Chapter 4, it was demonstrated that NIRS could potentially estimate lactate concentration in whole blood. However, although the experimental arrangement was made to increase lactate concentration, no attempt was made to monitor physiological parameters such as glucose level, pH variation or hematocrit level during the experiment. Therefore, covariance with these parameters may exist when trying to estimate lactate.

To verify that covariance with pH variation and hematocrit was minimized, these parameters were measured in whole blood from exercising humans, using the same exercise protocol developed previously in Chapter 3. In addition, to investigate possible covariance with other blood constituents, standard additions of lactate standard were used to generate an extended data set. With this approach, the capability of NIRS to distinguish lactate concentration variation from the background was confirmed.

The concept of referenced measurement of lactate against baseline level is introduced to investigate the contribution of the background and significantly improve lactate estimate results. By considering the lactate estimate at rest as a baseline for future variation after exercising, it was possible to maximize lactate

concentration variation by subtracting other blood species contribution to the spectrum, since these variations were smaller than that of lactate. In practice, the spectrum of a patient at rest was kept as a reference and all other spectra were taken against the reference. Lactate level at rest for a healthy patient is normally below 2 mmol/L. Therefore, variations of lactate above 2 mmol/L were observed. Results of the referenced method were compared with previous method to estimate lactate in blood.

5.1 Abstract

We have evaluated the potential of near-infrared spectroscopy (NIRS) as a technique for rapid analysis of lactate in whole blood. To test the NIRS technique, a comparison was made with a standard clinical method using whole blood samples taken from five exercising human subjects at three different stage of exercise. To expand lactate concentration within the physiological range, standard additions method was used to generate 45 unique data points. Spectra were collected over the 2050-2400 nm spectral range with a 1 mm optical path length quartz cell. Reference lactate concentrations in the samples were determined by enzymatic measurements. Estimates and calibration of the lactate concentration with NIRS was made using Partial Least Squares (PLS) regression analysis and leave-N-out cross validation on second derivative spectra. Separate calibrations were determined from each of the subject samples and cumulative PRESS was used to determine the number of PLS factors in the final model. The results from the PLS model presented are generated from the five individual calibration coefficient vectors and provided a correlation

coefficient of 0.978 and a standard error of cross validation of 0.65 mmol/L between the enzymatic assay and the NIRS technique. To study the parameters that impact the spectra baseline and the correlation between the calculated model and the data, referenced measurements of lactate against baseline spectrum were made for each individual. A correlation coefficient of 0.992 and a standard error of cross validation of 0.21 mmol/L were found. The results suggest that NIRS may provide a valuable tool to assess physiological status for both research and clinical needs.

5.2 Introduction

As a key metabolite of glycolytic activity, lactate can be used as a marker for the assessment of tissue perfusion and oxidative capacity. Lactate measurements can be used to determine the anaerobic threshold during physical exercise.⁽¹⁾ Likewise, in critical care, an increase in lactate level reflects an imbalance between lactate production and elimination. A lactate concentration less than 2 mmol/L is considered as normal.⁽²⁾ Indeed, if lactate concentration in healthy human is usually maintained to 0.7-1 mmol/L, it can exceed 11 mmol/L for an individual under stress or shock and can go as high as 25 mmol/L.⁽³⁾ Lactate concentrations higher than 4 mmol/L have been found in association with myocardial infarction⁽⁴⁾, cardiac arrest⁽⁵⁾, circulatory failure⁽⁶⁻⁷⁾ and in emergency trauma situations.⁽⁸⁻⁹⁾ In these cases, measurements of lactate levels are of prognostic significance and have to be performed by a rapid and robust method.

Most of the standard clinical methods are based on electrochemical enzymatic sensors.⁽¹⁰⁻¹²⁾ However, these methods are invasive and often require substantial sample preparations. They are limited by the number of analyses that can be performed in a short period of time. Likewise, they do not offer the possibility to the clinician of concurrent *in vivo* or *ex vivo* monitoring of lactate level in a continuous manner.

Previous studies have shown that near (NIRS) and mid infrared spectroscopy can be applied to the determination of lactate in simulated biological matrices, amniotic fluid and human plasma.⁽¹³⁻¹⁷⁾ However, these matrices were low scattering media. The development of an *ex vivo* monitoring method for lactate, using blood loops or small blood extraction with time, needs to consider the potential impact of red cells on the scattering and the absorption of the signal.

The present study examines the potential of NIRS to estimate lactate concentration in whole human blood. Care was taken so that the lactate concentration in this study covered a large portion of the human physiological range, which goes from 0.3 to 25 mmol/L.⁽³⁾ The experimental design was developed to minimize the contribution of glucose or other species to the lactate estimation. Separate calibrations were determined for each of the subject samples using a leave-N-out cross validation procedure. The final model was developed using the cumulative error of all the individual models. Both measurements of total lactate concentration

for all individuals and change in lactate concentration for each individual after spectral subtraction were considered.

5.3 *Experimental*

5.3.1 Instrumentation

Whole blood samples were assayed in triplicate for total blood lactate with the use of a YSI Model 1500 Sport Lactate Analyzer (Yellow Springs Instruments, Yellow Springs, OH). This instrument uses a proprietary electrochemical enzymatic detection of lactate. The mean of three results was recorded. Blood lactate analysis with this device has a standard error of 0.2 mmol/L based on five replicates of a standard. The manufacturer reports that the device delivers a linear response for lactate in the 0 to 30 mmol/L concentration range.

5.3.2 Sample Collection

Five healthy adult subjects (four males and one female) were tested during maximal effort made by a 30-s sprint on a modified isokinetic cycle. The cycle was modified to have the pedal speed fixed and effort translated into greater force generation.⁽¹⁸⁾ The study was approved by the Ethics Committee of the Montreal Children's Hospital, in accordance with the Helsinki Declaration of 1975. After signed informed consent, and prior to exercise, an intravenous line was placed in the antecubital fossa, and kept patent (open) with a 0.9% saline solution. Blood was sampled at three time intervals: (1) just prior to exercise; (2) at the end of exercise;

(3) 10 min. following exercise. This approach was used in an attempt to cover the largest portion of the human physiological lactate concentrations. Blood was drawn into tubes containing lithium heparin beads (Sarstedt Inc., St-Laurent, Quebec) and immediately transferred to pre-chilled 0.75 mL microvette tubes containing 1 mg/mL of sodium fluoride, to arrest glycolysis. Samples were analyzed for lactate by the YSI enzymatic method. The pH of all blood samples was measured with the use of a microProbe pH electrode (Fisher Scientific), since pH variations may have an effect on the water spectrum.⁽¹⁹⁻²⁰⁾ Likewise, to monitor the potential impact on light scattering, blood hematocrit was measured for all samples. For the hematocrit measurement, blood samples were placed in capillary tubes. The tubes were loaded into a centrifuge and spun at 13000 rpm for 1 minute. Hematocrit was measured by reading the volume percentage of the red blood cells in the tubes using a micro-capillary reader. Blood was kept on ice between enzymatic and FT-NIR experiments to arrest metabolism and avoid degradation of samples.

5.3.3 Sample Preparation

The lactate concentrations obtained from the subjects studied range from 0.36 to 8.93 mmol/L. To expand the lactate concentration within the physiological range for this study, each blood sample was divided in three sub-samples. Aliquots of a standard lactate solution were added to two of the three sub-samples to raise the original lactate concentration by 5 and 10 mM respectively. The main advantage of this procedure is that a limited number of samples is required to cover a wider range of lactate concentrations. Likewise, because only lactate is varying in the sub-

samples, it reduces the possible covariance with other blood constituents that may vary during exercise. This method has been shown to provide improved prediction quality and enhanced calibration model robustness in samples with complex background.⁽²¹⁾ Sodium lactate was purchased in dry form from Sigma Chemical (St. Louis, MO). A standard solution was prepared by weighing suitable amounts of sodium lactate and diluting with pH 7.3 0.1M phosphate buffer. Phosphate buffer was prepared with deionized water. The pH of the phosphate solution was close to the blood pH of this study, which ranged from a low of 7.44 to a high of 7.62 for all of the samples. Likewise, the amount of buffered solution added to spike the blood samples was relatively small compared to the blood samples volume (5 μ L of phosphate buffer in 500 μ L of blood sample). No pH changes were seen related to the addition of the phosphate solution into the blood samples. Likewise, an ANOVA test between samples taken at rest and 10 minutes after exercise indicated there was no difference with pH at the 95% confidence level.

Samples were put in the thermostated sample holder and given five minutes to reach $25 \pm 0.1^{\circ}\text{C}$, before collecting spectral responses. Just prior to data collection, respective blood sub-samples were spiked with lactate standard solution. To ensure homogeneity, all samples were gently stirred using a laboratory vortex mixer before measurements. Spectral measurements from randomly selected samples were done to avoid instrument bias.

5.3.4 Data Collection

Spectra were collected with a Nicolet Magna-IR 550 Fourier transform near-infrared (FT-NIR) spectrometer (tungsten-halogen lamp / quartz beamsplitter) equipped with an InSb detector using a 1 mm pathlength rectangular Infracil quartz cell from Starna (Atascadero, CA). The spectral range scanned was from 890 to 2500 nm (11500-4000 cm^{-1}). A total of 64 interferogram scans at a spectral resolution of 2 cm^{-1} were averaged. Single-beam spectra were computed with a Happ-Genzel apodization and Fourier transformation routines available on the system. Background spectra of air were taken every hour. Sample temperature was controlled to $25 \pm 0.1^\circ\text{C}$ with a copper-jacketed cell holder coupled with a YSI Model 72 temperature controller. Temperature was monitored continuously during data collection with a copper-constantan thermocouple probe placed into the sample holder. Likewise, to evaluate the potential impact of the sedimentation of red cells on lactate concentration, spectra were collected in triplicate for each of the samples. No significant differences in lactate concentration were seen between spectra of the same samples. The average spectrum was then used throughout the study.

5.3.5 Data analysis

Two pre-processing steps were used on the spectra. First, all spectra were mean centered. Mean centering emphasized the subtle variations in the spectra due to changing lactate concentrations. To enhance the spectral variations of lactate over the background and minimize baseline variation, the second derivative of all blood sample spectra was calculated using discrete differences.⁽²²⁾ Partial Least Squares

(PLS) regression analysis was then made on the pre-processed data. The PLS method and the second derivative routine have been developed previously and details of the algorithm have been discussed.⁽²²⁻²³⁾ For robust estimation using PLS, a separate calibration and validation data set are required. A cross validation method was used rather than regular calibration and validation data sets, since there were 45 unique samples. To ensure that variations between patients could be determined, a leave-one-individual-out cross-validation approach was used. Because each individual is excluded and estimated by the four others, this approach can be used to demonstrate the model is robust. In this study, blocks of nine samples from the same volunteer were left out. Basically, the procedure uses the spectra from four volunteers to estimate lactate levels in the nine samples of the fifth. Iteration is done to estimate all samples from each individual. The final model is built using the five individual calibration coefficient vectors to estimate the lactate concentration in each of the samples. This type of calibration is more robust than conventional leave-one-out cross validation model, because the model estimates lactate concentration in nine different samples from the same individual at a time rather than one in the leave-one-out cross validation procedure, thus allowing for inter-individual composition differences. The prediction error sum of squares (PRESS) with *F*-test significance comparisons were used to determine the minimum number of statistically significant factors.⁽²⁴⁾ The number of latent variables used in the model presented in this study is determined using the cumulative PRESS calculated from the sum of the five leave-one-individual-out cross validation. All programs for input of spectral data, pre-

processing and cross-validation were written in Matlab (The Mathworks Inc., South Natick, MA).

5.4 *Results and Discussion*

Spectra of whole blood are mostly dominated by two main constituents: water and proteins. To reduce interference from water, the spectral region extending from 2050 to 2400 nm was chosen for the lactate determination.⁽¹³⁻¹⁷⁾ This spectral range includes the major lactate absorbance peaks, which are located between the two water peaks centered at 1920 and 2630 nm.

A 1 mm pathlength was chosen so that absorption due to lactate was sufficient for quantification and to achieve a good signal-to-noise ratio.⁽¹⁷⁾ The root-mean-square (rms) noise of the 100% lines computed across the 2050 – 2400 nm using a linear model is 4.3 milli Absorbance Units (mAU) and the signal is 82.6 mAU. The signal-to-noise ratio (SNR) at 2160 nm was then approximately 20, which was sufficient to distinguish lactate absorption over the background. Likewise, blood hematocrit ranged from a low of 40.0 to a high of 53.7 for all of the samples. Only small variations during exercise and between subjects were seen. An ANOVA test between individuals indicated that hematocrit variation between blood samples taken at rest and 10 minutes following exercise were not statistically significant at a 95% confidence level.

Before the leave N-out cross-validation PLS routine was used, the second derivative of all the raw absorbance spectra was taken. The second derivative enhanced the spectral variations of lactate over the background and minimized baseline variation. In Figure 5.1, a series of second-derivative spectra from different patients' blood samples are shown.

As shown in Figure 5.2, the minimum of the plot is reached with 12 factors. This corresponds to the smallest standard error in the determination of lactate within the 2050 to 2400 nm range. It has been demonstrated that calibration performance depends on the spectral range used.⁽¹³⁾ In an attempt to optimize the calibration, several calibration models were developed using smaller windows within the 2050–2400 nm. No improvement was found. The minimum number of PLS factors to use for lactate determination was calculated using an *F*-test at a 95% confidence level. The result showed that no statistically significant difference exists between 7 and 12 PLS factors. Therefore, the calibration set used to estimate the lactate concentration was constructed using 7 factors.

Estimations of lactate concentration in whole blood were obtained by the scalar product of the regression calibration coefficients vector, from the five individual calibration coefficient vectors, and each spectrum of the data set. Results using 7 PLS factors are shown in Figure 5.3, where unspiked samples have been identified. Correlation between the data and the line of identity gave a correlation coefficient (r^2) of 0.978. The standard error of cross-validation (SECV) on the linear

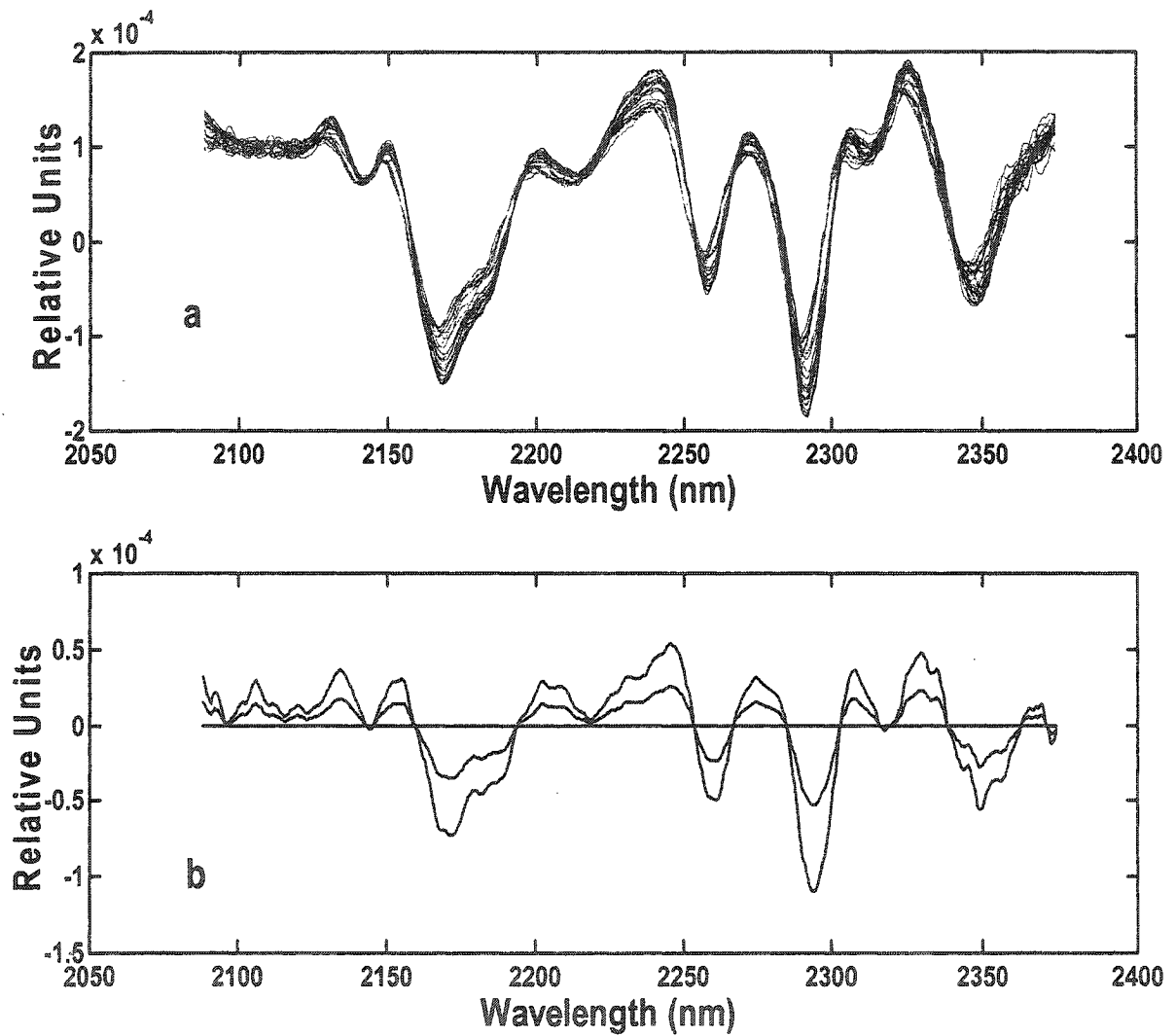


Figure 5.1: Second derivative (a) and second derivative difference between spiked and unspiked samples (b) of NIR absorbance spectra of human whole blood specimens from each of the five subjects.

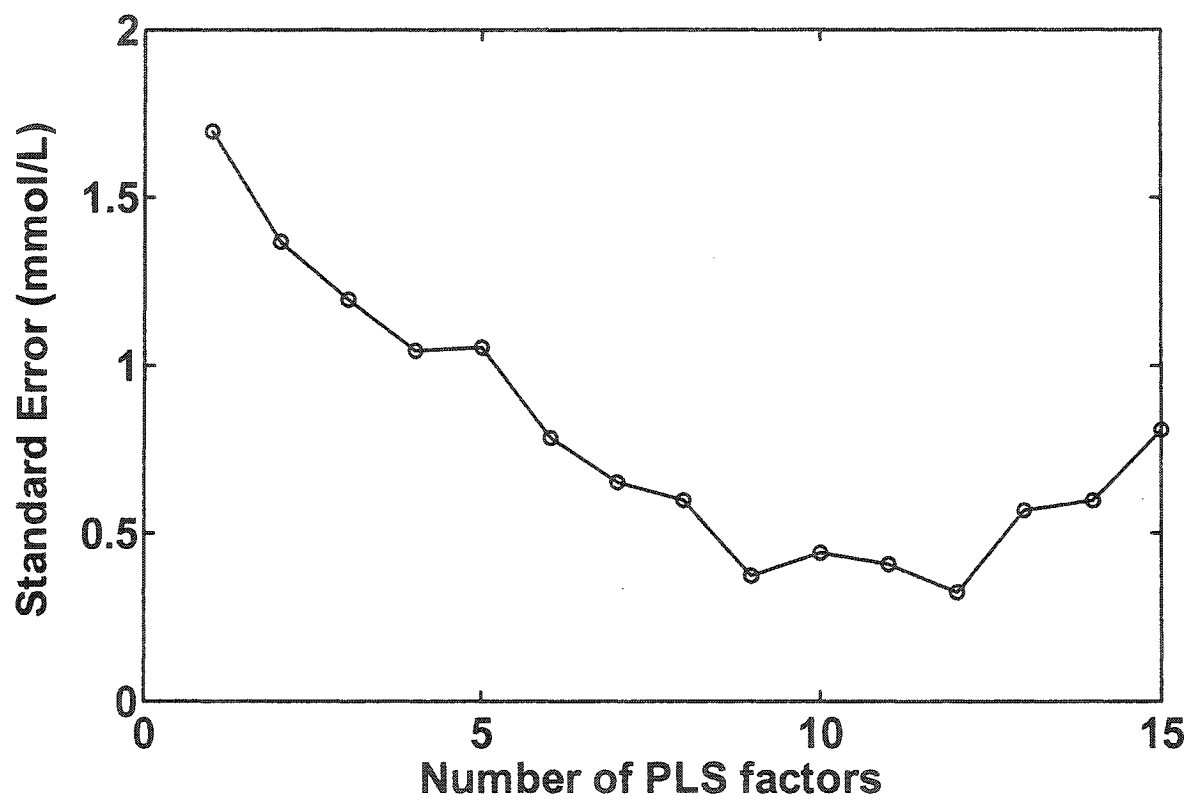


Figure 5.2: Cumulative PRESS plot for lactate cross-validation model based on the 2050 to 2400 nm spectral range.

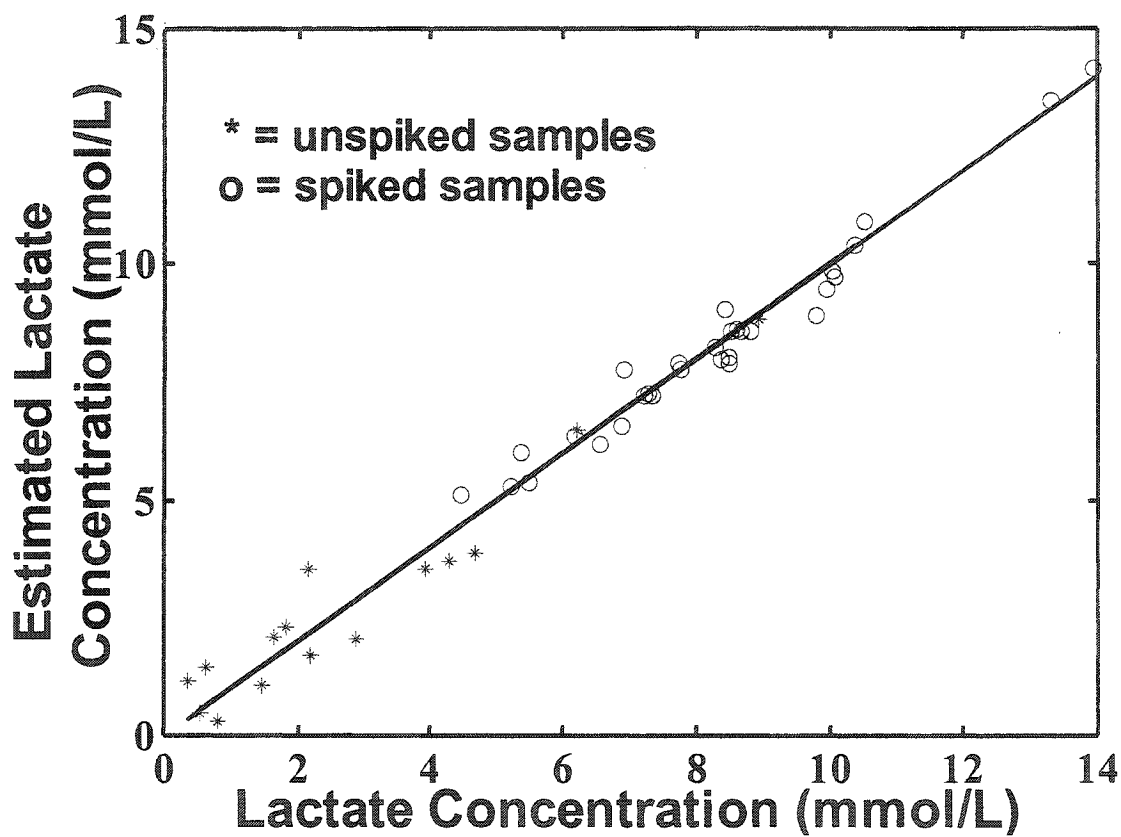


Figure 5.3: NIRS estimated vs. YSI Lactate Analyzer values for whole human blood samples for each of the five subjects. Cross-validation model: 7 PLS factors based on 2050-2400 nm spectral segment; $n=45$, $r^2=0.978$, RMSCV= 0.65mmol/L using a leave-9-out cross-validation procedure.

regression was calculated to be 0.65 mmol/L. There is an increased spread in the data at low lactate concentrations. However, as shown in a previous study where lactate was measured in human plasma, no particular grouping in the data is seen.⁽¹⁷⁾ This consideration indicated that possible variation in blood composition between individuals has little impact on the model. Likewise, Fig. 5.3 showed similarities between subjects in data spread about the line of identity. This indicates that although tight correlation of the data was not apparent at low lactate concentrations, the large change in lactate induced by exercise or sample spiking is easily distinguished. This will also be expected in illness situations.

As mentioned previously, a lactate concentration of less than 2 mmol/L is considered as normal.⁽²⁾ Clinicians are therefore interested in lactate concentration changes above 2 mmol/L. The current model represents the minimum needed to monitor lactate changes that could occur around that threshold value. Most of the variation appears to come from small baseline differences of blood within each subject samples. To test models with reduced blood composition difference, spectra from unspiked samples of subjects at rest were subtracted from the other spectra of each subjects. In fact, five spectra, one from each individual, were then removed from the original 45 samples. This operation is equivalent to a single reference taken at the beginning of the experiment for each of the individuals and allows the observation of trends in lactate concentration changes.

The two pre-processing steps were applied on the resulting spectra and the PLS routine was recalculated. The minimum number of PLS factors to use, calculated with an F -test at a 95% confidence level, was six. Figure 5.4 shows the estimations of referenced lactate concentrations in whole blood using the 6 PLS factors. Correlation between the data and the line of identity gives a correlation coefficient (r^2) of 0.992. The standard error of cross-validation (SECV) on the linear regression is 0.21 mmol/L. The standard error improvement for referenced lactate measurements compared to the absolute measurements is evident. The standard error has decreased by a factor of three. This translates to a significant improvement in the capability of the model to estimate lactate concentration change. These results indicate the potential of referenced lactate measurements for *ex vivo* physiological or clinical assessment when lactate change in an individual is significant such as seen during on-line monitoring of exercise or illness.

5.5 Conclusion

It has been shown that lactate measurement in whole human blood was possible with the use of the NIRS in the 2050-2400nm spectral range. A good correlation is observed between estimated and reference lactate levels in blood samples. The method achieves a standard error of cross validation of 0.65 mmol/L. By spiking the original blood samples, we were able to expand the lactate concentration within the physiological range. Though the spiking is not reproducing exactly what is expected *in vivo*, the agreement of the data between the spiked samples and the naturally varying lactate concentrations is very good. This

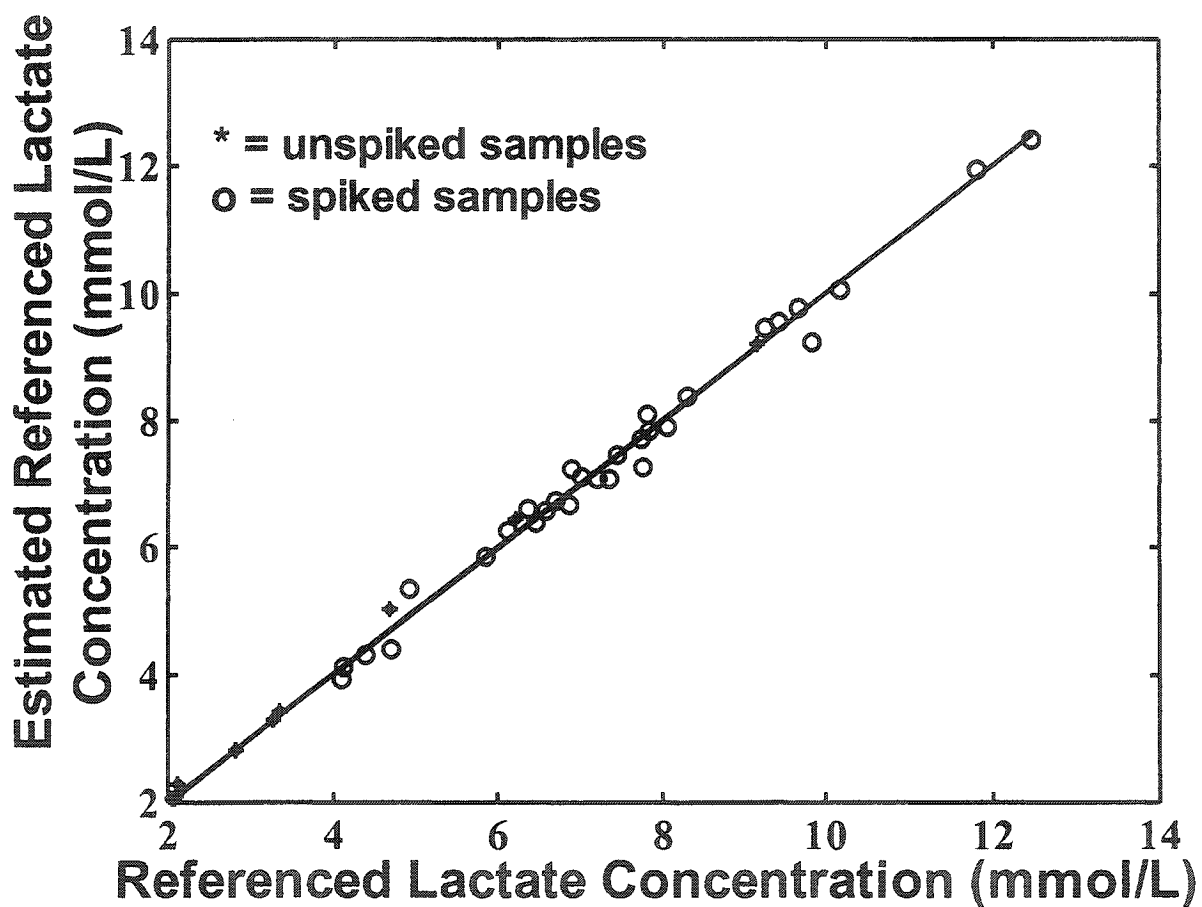


Figure 5.4: NIRS estimated vs. lactate referenced values for whole human blood samples for each of the five subjects. Cross-validation model: 6 PLS factors based on 2050-2400 nm spectral segment; $n=40$, $r^2=0.992$, RMSCV= 0.21 mmol/L using a leave-9-out cross-validation procedure.

indicates that spiking has little impact on the spectra besides lactate increase. However, the model shows some limitation at low lactate concentrations. To improve the precision of the method, referenced measurements of lactate concentration were calculated. The model estimated referenced lactate concentrations higher than 2 mmol/L, with a standard error of cross validation of 0.21 mmol/L.

Likewise, the possible variability of blood specimens was minimized by the experimental design chosen. This experimental design, which includes both the 30-seconds sprint and the standard addition method, allows the development of a calibration model that emphasizes the contribution of lactate over other blood species. As previously mentioned, components such as glucose do not vary significantly during this exercise protocol. Furthermore, by referencing the lactate measurement for each individual, the overall results are improved by mainly minimizing the error seen at low lactate concentration due to baseline variations. The results of this work represent an important step towards the development of an *ex vivo* NIRS method for the determination of lactate. One such potential system would be an *ex vivo* flow through cell to determine referenced lactate concentrations. This in-line system would still require blood to be drawn, but no sample handling would be needed. This approach represents a faster and nondestructive alternative to current enzymatic methods, which could have significant impact in clinical situations or exercise physiological studies.

5.6 References

1. G. A. Gaesser and D.C. Poole, *Int. J. Sports Med.*, **9**, 284-288 (1988).
2. B. A. Mizock and J. L. Falk, *Crit. Care Med.*, **20**, 80-93 (1992).
3. W. Schumer, *Cell Metabolism and Lactate*, in H. Bossart and C. Perret (Ed.), *Lactate in Acute Conditions Int. Symp.*, Basel, 1978, pp.1-9.
4. R. J. Henning, M. H. Weil, and F. Weiner, *Circ. Shock*, **9**, 307-315 (1982).
5. M. H. Weil, C. E. Ruiz S. Michaels, and E. C. Rackow, *Crit. Care Med.*, **13**, 888-892 (1985).
6. G. Broder and M. H. Weil, *Science*, **143**, 1457-1459 (1964).
7. M. H. Weil and A. A. Afifi, *Circulation*, **41**, 989-1001 (1970).
8. J. Aduen, W. K. Bernstein, T. Khastgir et al., *JAMA*, **272**, 1678-1685 (1994).
9. J. Toffaletti, *Scand. J. Clin. Lab. Invest. Suppl.*, **224**, 107-110 (1996).
10. W.P. Soutter, F. Sharp, and D.M. Clark, *Br. J. Anaesth.*, **50**, 445-450 (1978).
11. D.L. Williams, A.R. Doig, and A. Korosi, *Anal. Chem.*, **42**, 118-121 (1970).
12. D.A. Baker and D.A. Gough, *Anal. Chem.*, **67**, 1536-1540 (1995).
13. H. Chung, M.A. Arnold, M. Rhiel, and D.W. Murhammer, *Appl. Spectrosc.*, **50**, 270-276 (1996).
14. M.J. McShane, G.L. Coté, and C.H. Spiegelman, *Appl. Spectrosc.*, **52**, 878-884 (1998).
15. M.J. McShane and G.L. Coté, *Appl. Spectrosc.*, **52**, 1073-1078 (1998).
16. K. Z. Liu and H. H. Mantsch, *Am. J. Obstet. Gynecol.*, **180**, 696-702 (1999).
17. D. Lafrance, L.C. Lands, L. Hornby, and D.H. Burns, *Appl. Spectrosc.*, **54**, 300-304 (2000).

18. L.C. Lands, L. Hornby, G. Desrochers, T. Iler, and G.J.F. Heigenhauser, *J. Appl. Physiol.*, **77**, 2506-2510 (1994).
19. J. Lin and C.W. Brown, *Appl. Spectrosc.*, **47**, 1720-1727 (1993).
20. M.K. Phelan, C.H. Barlow, J.J. Kelly, T.M. Jinguji, and J.B. Callis, *Anal. Chem.*, **61**, 1419-1424 (1989).
21. M. R. Riley, M.A. Arnold, and D.W. Murhammer, *Biotech. Prog.*, **14**, 527-533 (1998).
22. F. Holler, D.H. Burns, and J.B. Callis, *Appl. Spectrosc.*, **43**, 877-882 (1989).
23. L.S.L. Arakaki, M.J. Kushmerick and D.H. Burns, *Appl. Spectrosc.*, **50**, 697-707 (1996).
24. D.M. Haaland and E.V. Thomas, *Anal. Chem.*, **60**, 1193-1202 (1988).

Chapter 6 *In vivo* Lactate Measurement in Human tissue by Near-Infrared Diffuse Reflectance Spectroscopy.

In each of the previous chapters, lactate concentration was estimated from the information extracted from transmittance spectra of fluid samples. Although absorbance and scattering may be significant for some samples, transmittance spectroscopy was feasible by keeping the optical pathlength of light to 1 mm. In this chapter, *in vivo* tissue measurements were investigated. Although, some difficulties exist to do this kind of measurement with a body part offering an optical pathlength of 1 mm or less, some studies have suggested several capillary-rich locations to preferably make *in vivo* analysis by NIR (see section 2.1.2.2.1.1). However, for most of these locations, the sample thickness does not allow near infrared light to penetrate into the tissue to quantify a sufficient volume of the capillaries.

To overcome this problem, a novel approach was evaluated. First, a fingernail was chosen for the *in vivo* measurements, because nail provided an easy access to capillaries of the fingernail bed. Likewise, the wavelength range was changed from 2000-2400 nm to 1500-1750 nm. This region of the electromagnetic spectrum corresponds to the first overtone of O-H, C-H and N-H stretching vibrations. The wavelength range change was motivated by two major advantages: fingernail is almost transparent in this range and penetration depth into tissue is greater, since absorption was less. Figure 6.1 shows a transmittance spectrum from a nail

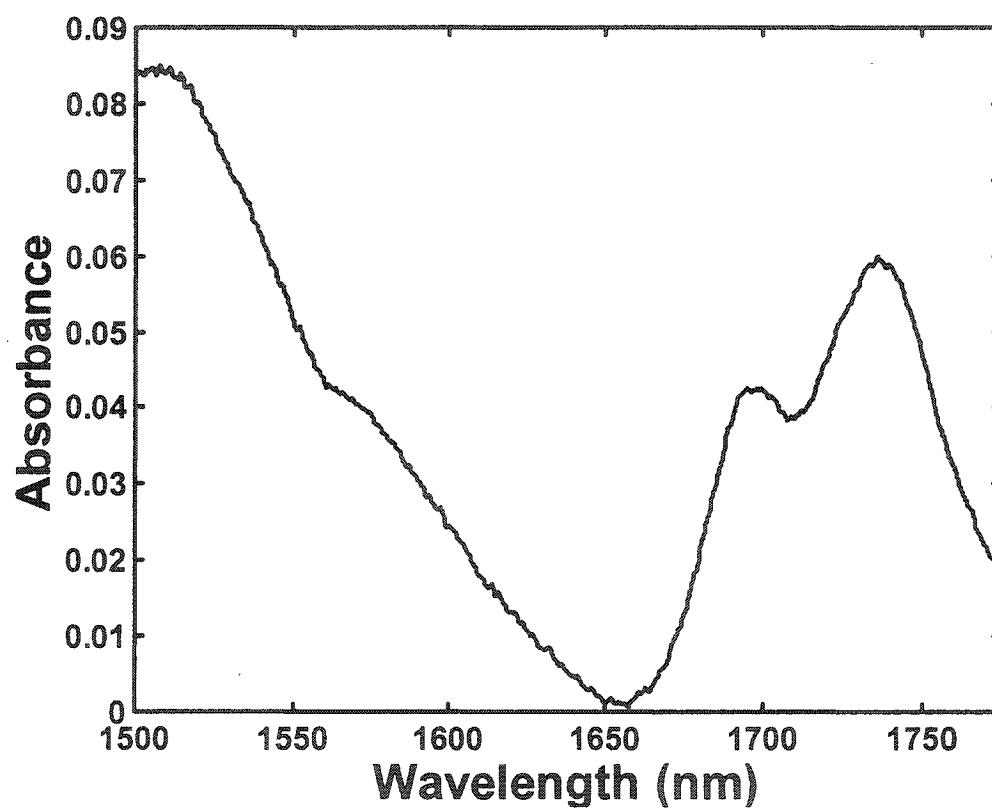


Figure 6.1: NIR transmittance spectrum of a typical human nail of 0.75 mm thickness.

of 0.75 mm thickness in the 1500-1750 nm wavelength range. Finally, diffuse reflectance was chosen as an alternative to the transmittance spectroscopy used previously for this study. While specular reflectance corresponds to the reflected light travelling with the same angle than the one of the incident light, diffuse reflectance is defined as reflectance of light travelling in all directions. Diffuse reflectance has shown its potential and is now widely accepted as a method for quantitative analysis.

To collect diffuse reflectance spectra of a human fingernail bed, there was a need to modify the instrument configuration and develop a sample holder. Furthermore, one objective in this chapter was to investigate spectral variations that take place during *in vivo* measurements and correlate them to changing constituents. 2D correlation spectroscopy was used to achieve this objective. The method is described in Appendix B.

6.1 Instrument Configuration

To successfully take reflectance spectra on human fingernail bed, some modifications of the FT-NIR spectrometer were necessary. As shown on Figure 6.2, an external source was used to provide more light to the sample. Furthermore, because the optical arrangement of the instrument was for transmittance spectroscopy, two flat mirrors were added in the sample compartment (M4 and M5)

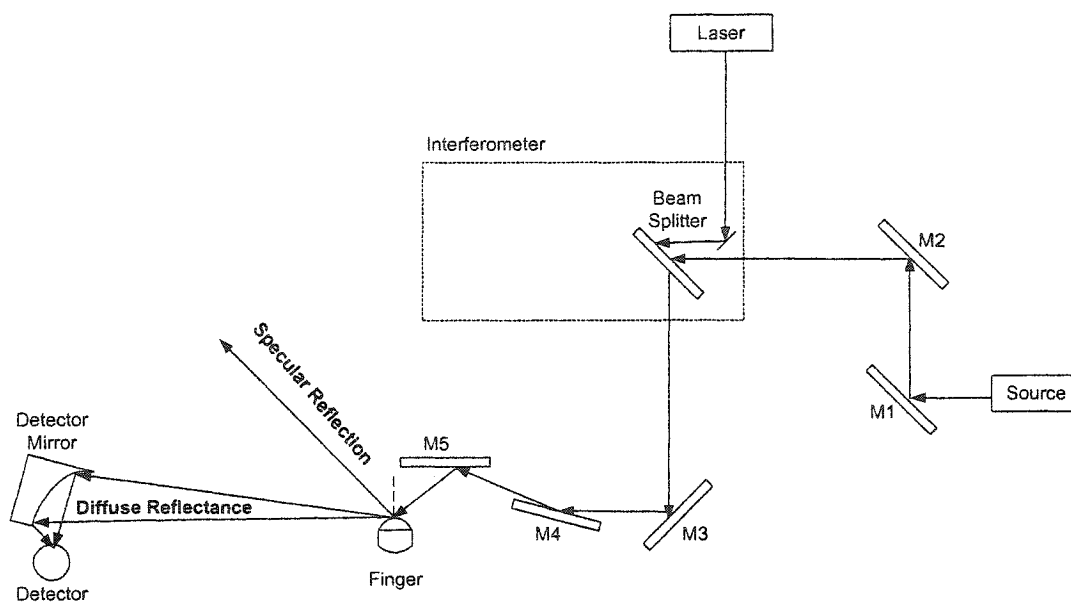


Figure 6.2: Schematic diagram of the modified Nicolet Magna-IR 550 FT-NIR spectrometer to allow diffuse reflectance spectroscopy. M1, M4 and M5 mirrors were added to the original setting of the instrument.

to preferably collect diffuse reflectance. The system was designed to be slightly out of focus at the sample so that measurements were less sensitive to finger movement. Results of a study where the finger was moved (back/forth/left/right) between repeated measurements showed the estimated lactate concentration varying by less than 3%.

Although the variability associated with finger movement was small, a sample holder was designed to minimize them. The sample holder was located at one of the focuses of the Cassegrain mirror to maximize light collection. Figure 6.3 shows the sample holder designed for the diffuse reflectance spectra collection. The finger rested on the small rod. The height of the rod was adjustable so that the fingernail bed was at the center of the beam. Movements of the finger were minimized by a support fasten to the rod. With the new sample holder in place, repeated measurements showed that variability of the signal was below noise level.

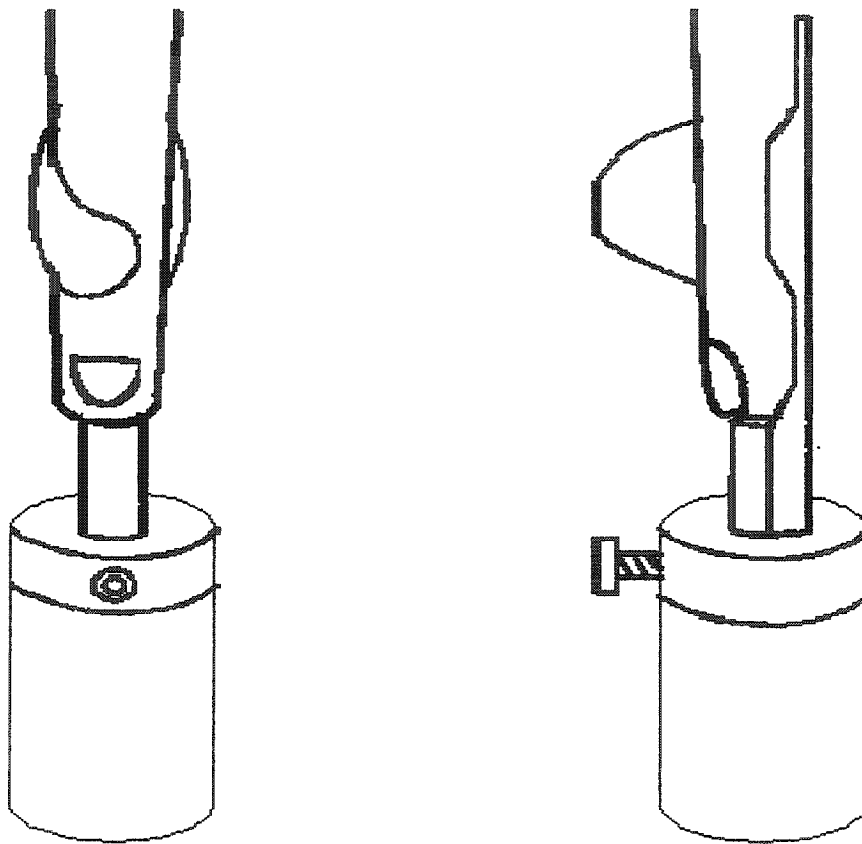


Figure 6.3: Front and left side view of the sample holder (with a finger) designed to minimize finger movement during diffuse reflectance measurements of the fingernail bed.

6.2 Abstract

We have evaluated the potential of near-infrared spectroscopy (NIRS) as a technique for *in vivo* measurement of lactate during exercise in humans. By using 2D correlation spectroscopy, lactate was identified as the primary constituent that was monitored by the *in vivo* measurements. Estimates and calibration of the lactate concentration by NIRS was made using Partial Least Squares (PLS) regression analysis and leave-N-out cross validation on second derivative spectra. Regression analysis provided a correlation coefficient of 0.74 and a standard error of cross validation of 2.21 mmol/L. To study the parameters that impact the spectra baseline and the correlation between the calculated model and the data, lactate spectra were referenced against a baseline spectrum for each individual. For the referenced data, a correlation coefficient of 0.97 and a standard error of cross validation of 0.76 mmol/L between the enzymatic assay and the NIRS technique were found. The results suggest that NIRS may provide a valuable tool to assess *in vivo* physiological status for both research and clinical needs.

6.3 Introduction

In critical care, the continuous monitoring of blood lactate is of significant importance. An increase in lactate level reflects an imbalance between lactate production and elimination. Lactate can then be used as a marker for the assessment of tissue perfusion and oxidative capacity. While a whole blood lactate concentration of less than 2 mmol/L is considered as normal ⁽¹⁾, concentrations higher than

4 mmol/L have been found in association with myocardial infarction⁽²⁾, cardiac arrest⁽³⁾, circulatory failure^(4, 5) and in emergency trauma situations.^(6, 7) Likewise, the change in pattern or the trend towards an increase of blood lactate is a good indicator of survival.^(8, 9) In all these cases, measurements of lactate levels are of prognostic significance and have to be performed by a rapid and robust method.

However, most of the standard clinical methods for lactate analysis are not adapted for continuous lactate monitoring.⁽¹⁰⁻¹²⁾ They often require substantial sample preparations and for this reason, do not offer the possibility to the clinician of concurrent *in vivo* or *ex vivo* monitoring of lactate level in a continuous manner. To achieve at patient monitoring of lactate, several *in vivo* biosensors^(10,13-15), *ex vivo*⁽¹⁶⁻¹⁸⁾ and microdialysis procedures^(19,20) have been developed. Although they overcome some of the problems, these methods suffer from several drawbacks. Biofouling, biocompatibility, thrombi formation, calculation of the recovery and discomfort for the subjects are some of the major disadvantages and problems of these techniques that ultimately remain invasive devices.⁽²¹⁻²⁴⁾

Previous studies have shown the potential of near infrared spectroscopy (NIRS) to monitor non-invasively tissue oxygenation⁽²⁵⁻³⁰⁾ and other metabolites⁽³¹⁻³⁸⁾. Likewise recently, *in vitro* measurement of lactate was also made using Near Infrared Spectroscopy.⁽³⁹⁻⁴¹⁾ The present study investigates the feasibility of *in vivo* monitoring of some physiological markers such as glucose, lactic acid, hematocrit or body temperature using NIRS diffuse reflectance spectroscopy. The experimental

design was developed to minimize covariance between species such as glucose, lactate, pH, water and proteins changes, etc... Separate calibrations were determined for each of the subject samples using a leave-N-out cross validation procedure. Both measurement of total species concentration for all individuals and change in species concentration for each individual after spectral subtraction were considered.

6.4 *Materials and Methods*

6.4.1 Sample Collection

Ten healthy adult subjects (six males and four females) were tested during maximal effort made during a 30-s sprint on a modified isokinetic cycle. The cycle was modified to have the pedal speed fixed and effort translated into greater force generation.⁽⁴²⁾ The study was approved by the Ethics Committee of the Montreal Children's Hospital, in accordance with the Helsinki Declaration of 1975. After signed informed consent, and prior to exercise, an intravenous line was placed in the antecubital fossa, and kept patent (open) with a 0.9% saline solution. Blood was sampled at four time intervals: (1) just prior to exercise; (2) at the end of exercise; (3) 5 min. following exercise; (4) 10 min. following exercise. This approach was used in an attempt to induce changes within the human physiological ranges for lactate, while minimizing covariance with other species. Blood was drawn into tubes containing lithium heparin beads (Sarstedt Inc., St-Laurent, Quebec) and immediately transferred to pre-chilled 0.75 mL microvette tubes containing 1 mg/mL of sodium fluoride, to arrest glycolysis. Samples were then spun at 15 000 rpm at room temperature for 5 minutes in a Eppendorf microcentrifuge Model 5417C (Eppendorf Scientific,

Westbury, NY) to remove plasma for analysis. Plasma samples were each assayed once on a Kodak (Vitros) Model 750 (Orthoclinical Diagnostics, Rochester, NY) for lactate and glucose. Likewise, to monitor the potential impact on light scattering, blood hematocrit was measured for all samples. For the hematocrit measurement, blood samples were placed in capillary tubes. The tubes were loaded into a centrifuge and spun at 13000 rpm for 1 minute. Hematocrit was measured by reading the volume percentage of the red blood cells in the tubes using a micro-capillary reader.

6.4.2 Data Collection

Spectra were collected with a Nicolet Magna-IR 550 Fourier transform near-infrared (FT-NIR) spectrometer (quartz beamsplitter). The instrument was equipped with stabilized external quartz tungsten halogen source (300 W, Oriel) and an InSb detector. A sample holder, that allowed the finger to rest in front of the light beam, was used to minimize finger movement during exercise and data collection. Two flat mirrors (Edmund Scientific Company, Inc., Barrington, NJ, USA) were used in the sample compartment to bring light to the fingernail and allow diffuse reflectance NIR spectra to be obtained. The spectral range scanned was from 1000 to 2500nm ($11500\text{-}4000\text{cm}^{-1}$). A total of 64 interferogram scans at a spectral resolution of 16 cm^{-1} were averaged. Single-beam spectra were computed with a Happ-Genzel apodization and Fourier transformation routines available on the system. Background spectra of air were taken every hour. Skin and body temperatures were monitored during data collection with a copper-constantan thermocouple probe and a

thermometer (Becton and Dickinson, Mississauga, Ont.) placed respectively in the hand and the mouth of the subject. In this study, the spectral range from 1500-1750nm was used to do transcutaneous measurements. There were several reasons that motivated the choice of diffuse reflectance spectroscopy of the human nail bed at these wavelengths. First, the fingernail is relatively transparent in this NIR region with absorption near 1660 and 1740nm.⁽⁴³⁾ With the low absorption, a significant portion of the reflectance signal that arises comes from the nail bed or deeper, where the tissue is rich in capillary blood vessels.⁽⁴³⁾ Furthermore, the root-mean-square (rms) noise of the 100% lines computed across the 1500 –1750nm range using a linear model is 1.38 micro Absorbance Units (μ AU). The signal-to-noise ratio (SNR) at 1690nm is approximately 20, which is sufficient to distinguish species absorption over the background. Finally, several species like lactate or glucose show absorptivities of acceptable magnitude in this spectral range.

6.4.3 Data analysis

To determine the predominant change in the spectra, 2D correlation spectroscopy was used.⁽⁴⁴⁻⁴⁶⁾ The technique of 2D correlation spectroscopy was developed for characterizing differences in spectral responses between elements of a set of spectra with certain variations present among them. Two pre-processing steps were used on the spectra before plotting the 2D correlation spectrum. First, all spectra were mean-centered. Mean-centering emphasized the subtle variations in the spectra due to changing species concentrations. To enhance the spectral variations of

species over the background and minimize baseline variation, the second derivative of all blood sample spectra was calculated using discrete differences.⁽⁴⁷⁾

Following the determination of the predominant species in the spectra, Partial Least Squares (PLS) regression analysis was made on the pre-processed data. The PLS method and the second derivative routine have been developed previously and details of the algorithm have been discussed.^(47, 48) For robust estimation using PLS, a cross validation method was used with the 40 unique samples. In this study, blocks of four samples from the same volunteer were left out. Since each individual is excluded and estimated by the nine others, the leave-one-individual-out cross-validation approach ensures that variations between patients could be determined. The final model is developed using the ten individual calibration coefficient vectors to estimate the concentration in each of the samples. The prediction error sum of squares (PRESS) with *F*-test significance comparisons was used to determine the minimum number of statistically significant factors.⁽⁴⁹⁾ The number of latent variables used in the model presented in this study is determined using the cumulative PRESS calculated from the sum of the ten leave-one-individual-out cross validations. All programs for input of spectral data, pre-processing, 2D correlation plot and cross-validation were written in Matlab (The Mathworks Inc., South Natick, MA).

6.5 *Results and Discussion*

In order to determine wavelengths that mainly correlate over time with spectral changes, a correlation coefficient plot is shown in Figure 6.4. Although it was not possible to assign some of the most correlated wavelengths with a particular species (1586nm, 1593nm, 1626nm and 1716nm), other correlated wavelengths can be assigned to glucose (1612nm and 1689nm) and lactate (1675nm, 1690nm and 1730nm). No correlated wavelengths are related to water. Table I shows changes over time of lactate and glucose concentration for each of the ten individuals.

To better understand what induced spectral changes over the course of time, 2D correlation analysis was used. Figure 6.5 shows the synchronous (bottom) and asynchronous (top) 2D correlation spectra from human nails bed. Both are presented together because they show symmetry with respect to the central diagonal. The synchronous spectrum represents the simultaneous or coincidental changes of spectral intensity variations measured at two different wavelengths during the 10 minutes interval chosen for the experiment. The synchronous spectrum shows correlation peaks appearing at both on and off diagonal. The on-diagonal peaks or “autopeaks” correspond to the autocorrelation of a wavelength. Thus, the evaluation of the synchronous spectrum along its diagonal provides the overall extent of dynamic fluctuations in the spectral intensity. Likewise, the off-diagonal peaks or “cross-peaks” show the simultaneous changes of signals that occur at two different wavelengths. The magnitude and position of cross-peaks can then be useful to

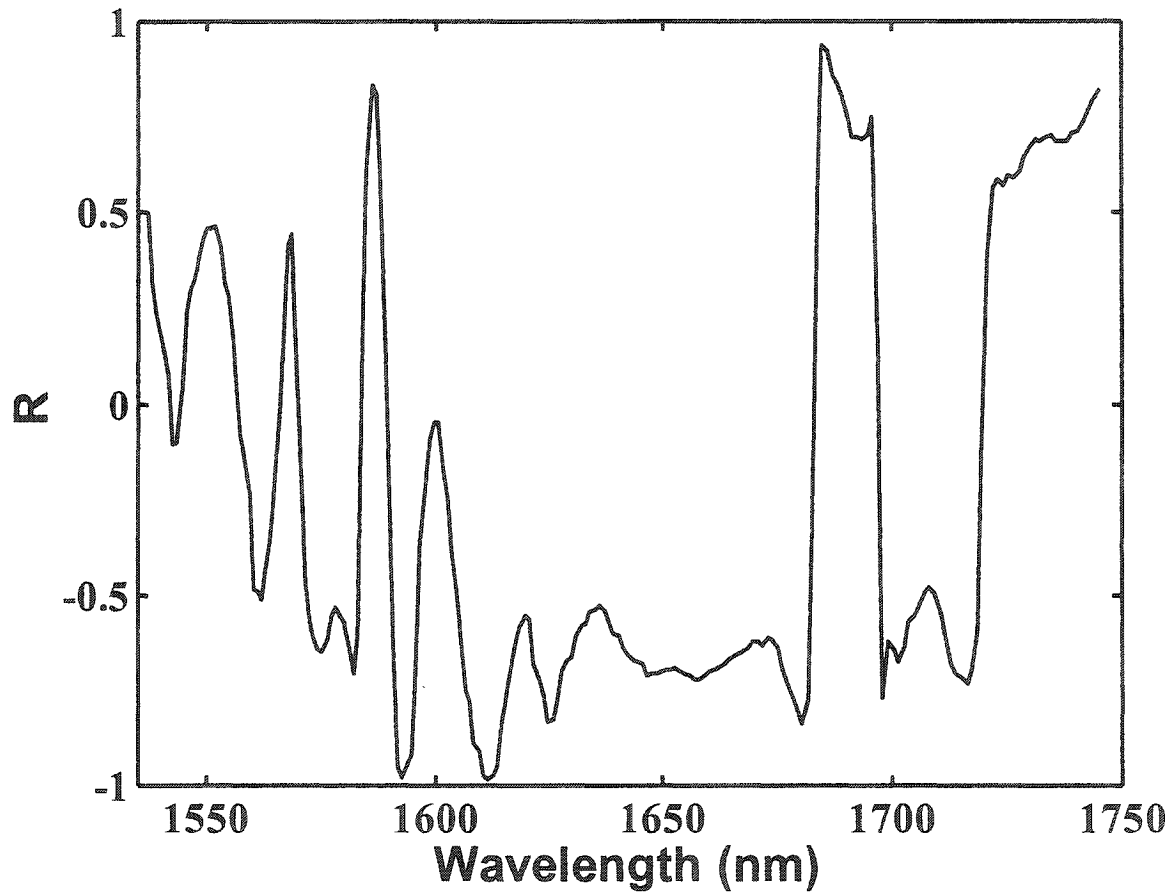


Figure 6.4: Correlation coefficient plot based on diffuse reflectance spectra from the fingernails of each of the subjects.

Table I: Lactate and glucose concentration changes over the course for each of the ten individuals.

	Lactate (mmol/L)				Glucose (mmol/L)			
	At rest	t=0 min	t=5 min	t=10 min	At rest	t=0 min	t=5 min	t=10 min
Subject 1	0.9	1.8	11.2	10.9	5.0	5.4	5.4	5.3
Subject 2	0.7	2.1	5.1	5.4	4.6	4.6	4.6	4.5
Subject 3	0.8	1.2	6.3	6.9	4.6	4.5	4.7	4.7
Subject 4	0.9	1.6	6.0	5.6	4.6	4.8	5.0	4.9
Subject 5	1.0	2.0	8.0	8.3	5.1	5.5	5.1	5.2
Subject 6	0.9	1.6	4.8	4.9	5.2	5.2	5.3	5.3
Subject 7	1.0	2.2	3.1	3.2	4.5	4.4	4.6	4.6
Subject 8	1.5	1.7	5.8	5.7	5.9	5.7	5.7	5.6
Subject 9	1.0	1.4	5.2	4.6	4.9	4.9	4.7	4.7
Subject 10	1.1	1.0	10.1	10.1	4.9	4.7	5.4	5.1

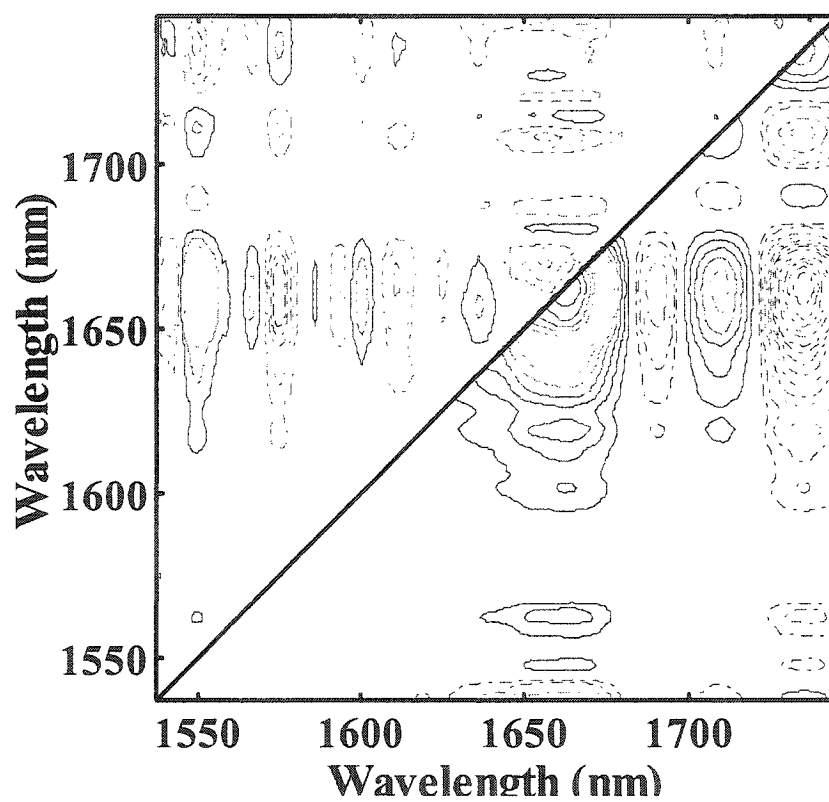


Figure 6.5: 2D-NIR correlation spectra (synchronous and asynchronous) based on diffuse reflectance spectra from the fingernails of each of the subjects.

determine whether simultaneous spectral changes in two wavelength regions are coupled.⁽⁴⁴⁻⁴⁶⁾ The synchronous spectrum in Figure 6.5 shows that the predominant change is centered at 1662nm, but the peak is broad. In an attempt to assign some of the features to species of interest, standard buffered solutions were prepared. It was determined that in the selected spectral range (1500-1750nm) lactate shows absorption at 1675, 1690 and 1730nm, while glucose shows at 1613, 1689 and 1732nm.⁽⁵⁰⁾ The feature at 1662 appears to be a combination of absorption from fingernail (1660nm) and lactate (1675nm). Furthermore, anti-correlated changes appear between 1710nm and 1690nm and 1735nm. While the feature at 1690nm can be assigned to lactate, the feature at 1735 appears to be a combination of absorption from lactate (1730nm), glucose (1732nm) and fingernail (1740nm).

The top part of Figure 6.5 shows the asynchronous spectrum. The asynchronous spectrum represents the sequential or successive information changes in spectral intensities measured at two different wavelengths.⁽⁴⁶⁾ Unlike the synchronous spectrum, the asynchronous plot does not have autopeaks, but only off-diagonal cross-peaks and is antisymmetric with respect to the central diagonal. Furthermore, the sign of the cross-peak can be used to determine the sequential order of the spectral changes that occur. A positive asynchronous cross-peaks at (λ_1, λ_2) indicates that a change at λ_1 occurred predominately before λ_2 in the sequential order of changes. In Figure 6.5, out-of phase changes appear at 1636nm, 1600nm and 1550nm and, but with opposite sign, at 1610nm and 1575nm. While the small out-of-

phase feature at 1610nm can be assigned to glucose, the other features of the asynchronous spectrum have not been assigned, but can be related to other species of human tissues such as proteins. Furthermore, the absence of peaks in the asynchronous spectra at 1710, 1690 and 1735 nm indicate that the peaks arise from the same species.

Since 2D correlation analysis is a method for visualizing the relationship among the variables in multivariate data, it led to the identification of two potential species, lactate and glucose that could be monitored through NIR fingernail diffuse reflectance. To confirm which one of lactate or glucose offers the best potential, PLS models were determined for both species. However, to develop an acceptable PLS model, no covariance between the multiple components of the sample matrix should be seen. Table II lists the correlation coefficients between measured lactate, glucose and the other parameters.

Table II: Correlation coefficients (R) calculated between lactate and other measured parameters.

	<i>Glucose</i>	<i>Hematocrit</i>	<i>Temp. -finger</i>	<i>Temp. - mouth</i>
<i>Lactate</i>	0.2668	0.3793	0.5212	0.2441
<i>Glucose</i>		-0.0633	0.0849	0.0181
<i>Hematocrit</i>			0.2956	-0.1742
<i>Temp. - finger</i>				0.3425

As expected, no significant correlation was found between these parameters. Likewise, it has previously been shown that variable light scattering from red blood cells can be correlated with pH changes in the samples.⁽⁵¹⁾ The correlation with pH is caused by variations in light scatter due to red blood cells shrinking and swelling as a function of pH.⁽⁵¹⁾ However, such correlation is usually seen in experiments where pH variation is much larger (> 1 pH unit) than in a physiological study.⁽³⁹⁾ Furthermore, previous study has shown no correlation between spectral changes and pH variation in samples during a similar protocol to this study.⁽³⁹⁾

As shown in Figure 6.6, the minimum of the plot is reached with 4 factors for lactate. This corresponds to the standard error in the determination of lactate within the 1500 to 1750nm range. Figure 6.7 shows the calibration coefficients plot based on a 4 PLS model. This represents the calibration coefficients at each wavelength, as determined by PLS. Upon viewing Figure 6.7, it should be noted that the peaks magnitude are the important features, and both positive and negative values are significant. In the figure, the peaks at 1680nm (lactate, fingernail), 1690nm (lactate, glucose), 1710nm, 1725nm (lactate, fingernail) and 1740nm (glucose, fingernail) contribute to the greatest extent to the calibration model.

Estimations of lactate concentration in whole blood were obtained by the scalar product of the calibration coefficients vector and each spectrum of the data set.

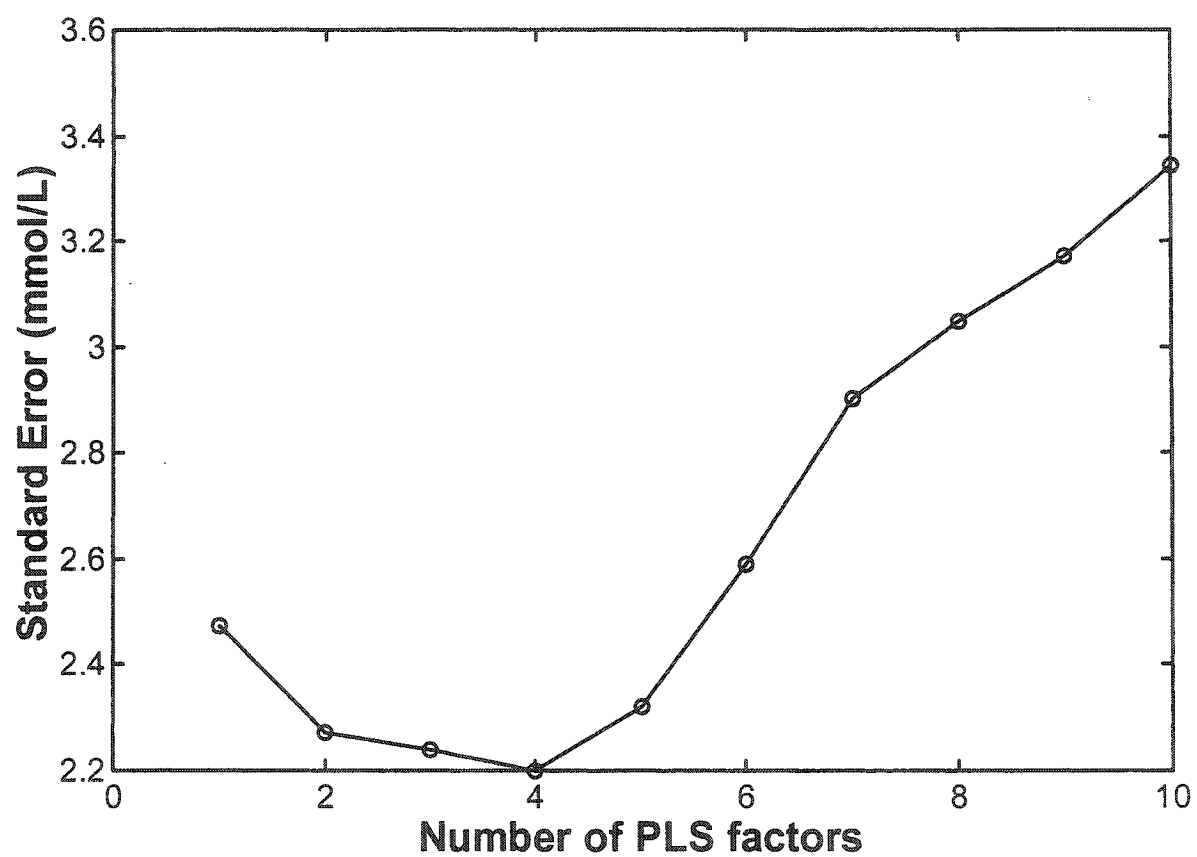


Figure 6.6: PRESS plot for lactate cross-validation model based on the 1500 to 1750nm spectral range.

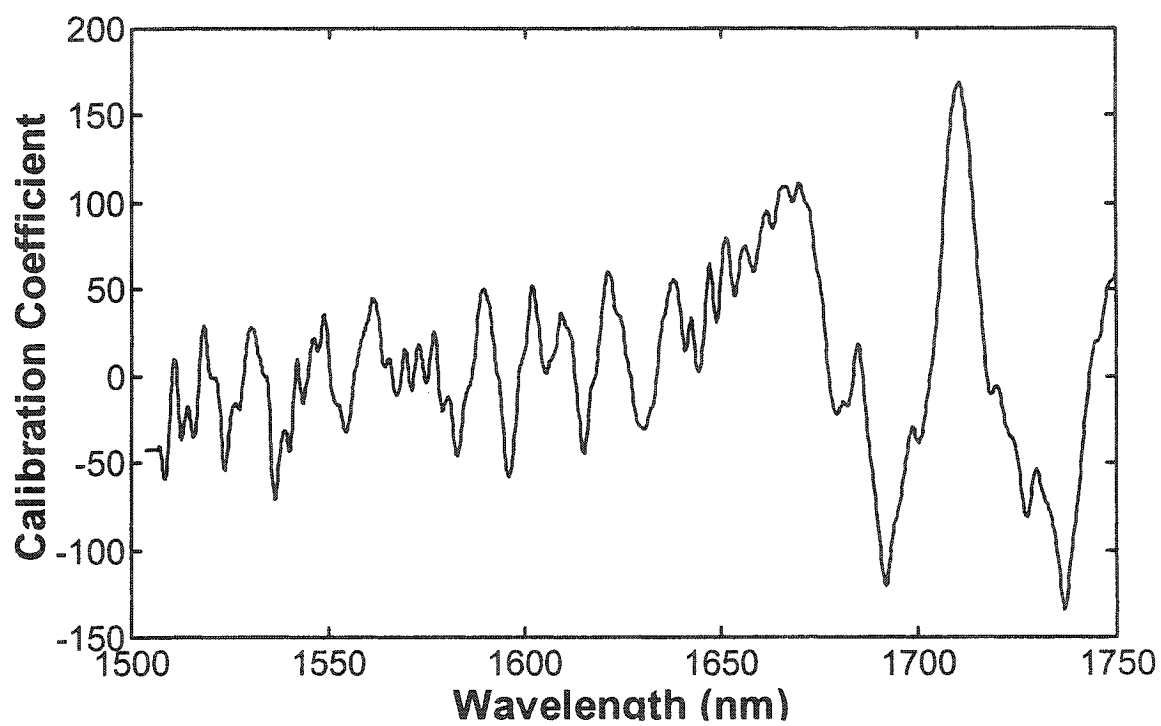


Figure 6.7: Calibration coefficient plot using 4 PLS factors for the *in vivo* determination of lactate.

Results using 4 PLS factors are shown in Figure 6.8. Correlation between the data and the line of identity, resulted in a correlation coefficient (r^2) of 0.74. The standard error of cross-validation (SECV) on the linear regression was calculated to be 2.21 mmol/L. The spread seen in the data possibly comes from small variations in blood composition or in the nail bed during exercise within individuals. However, as shown in a previous studies where lactate was measured in human plasma and blood, no particular grouping in the data is seen.^(39, 41) This consideration indicates that possible variations in blood composition between individuals has little impact on the model. Likewise, Figure 6.8 showed that although tight correlation of the data is not apparent, the large change in lactate induced by exercise is easily distinguished. This will also be expected in illness situations.

The PLS model was also used to estimate glucose concentration. The minimum standard error in the determination of glucose was achieved by using thirteen factors. However, after a *F*-test significance comparison was used to determine the significant number of factors, no difference was found statistically between thirteen and four factors. When four factors are used to build the PLS model for glucose, the correlation coefficient (r^2) gave 0.37 and the standard error of cross-validation (SECV) on the linear regression was calculated to be 1.53 mmol/L. This result indicates that from the two species, lactate is most likely to be the one that can be monitored using the NIR diffuse reflectance of the finger.

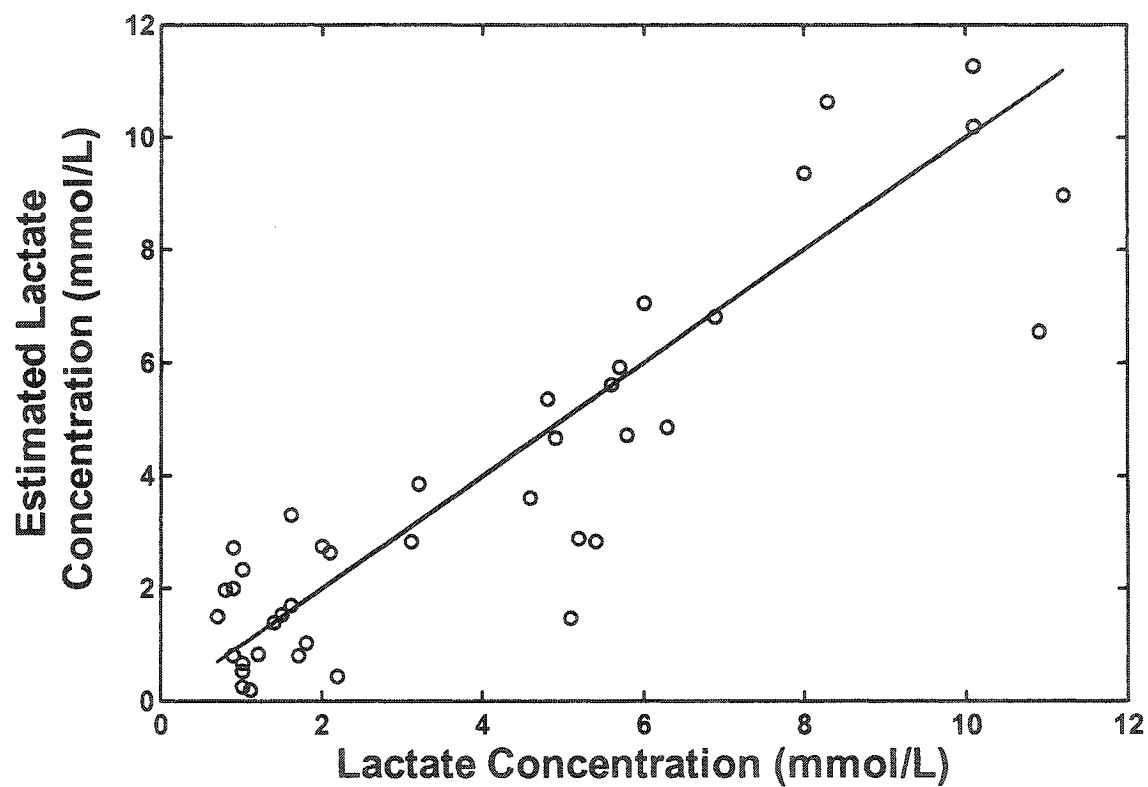


Figure 6.8: NIRS estimated vs. Kodak Vitros values for *in vivo* lactate measurements for each of the ten subjects. Cross-validation model: 4 PLS factors based on 1500-1750nm spectral segment; $n=40$, $r^2=0.74$, RMSCV= 2.21 mmol/L using a leave-4-out cross-validation procedure.

As mentioned previously, a blood lactate concentration of less than 2 mmol/L is considered as normal.⁽¹⁾ Therefore, lactate concentrations changes above 2 mmol/L are of the most importance. The current model represents the minimum needed to monitor lactate changes that could occur around that threshold value. Most of the variation appears to come from baseline differences of blood within each of the subjects and the contribution of the fingernail and the fingernail bed to the spectra. To test models with reduced blood composition difference and fingernail contribution, spectra from volunteers at rest were subtracted from the other spectra of each volunteer with the corresponding measured lactate referenced to the standard. This operation is equivalent to a baseline correction for each individual, which is easily accomplished in the clinic.

The two pre-processing steps were applied on the resulting spectra and the PLS routine was recalculated. The minimum number of PLS factors to use, calculated with an *F*-test at a 95% confidence level, was five. Figure 6.9 shows the estimations of *in vivo* referenced lactate concentrations using the 5 PLS factors. Correlation between the data and the line of identity gives a correlation coefficient (r^2) of 0.97. The standard error of cross-validation (SECV) on the linear regression is 0.76 mmol/L. The standard error improvement for referenced lactate measurements compared to the absolute measurements is evident. The standard error has decreased by a factor of three. This translates to a significant improvement in the capability of the model to estimate lactate concentration change. These results indicate the

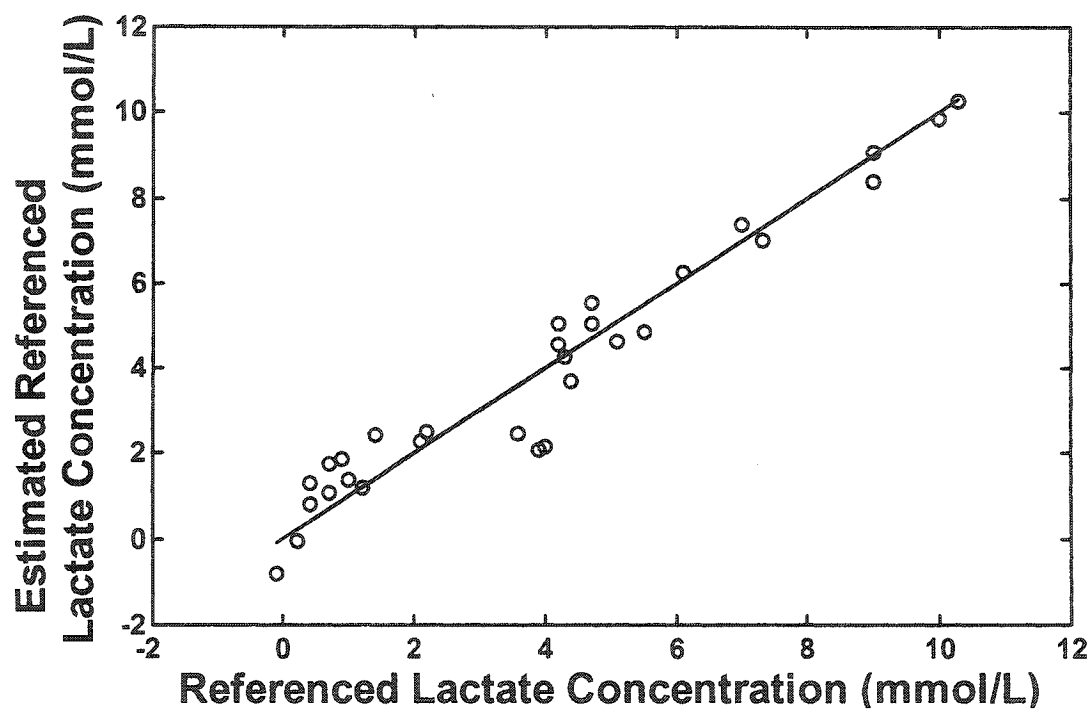


Figure 6.9: NIRS estimated vs. lactate referenced values for *in vivo* lactate measurements for each of the ten subjects. Cross-validation model: 5 PLS factors based on 1500-1750 nm spectral segment; $n=30$, $r^2=0.97$, RMSCV= 0.76 mmol/L using a leave-4-out cross-validation procedure.

potential of referenced lactate measurements for *in vivo* physiological or clinical assessment when lactate change in an individual is significant.

6.6 Conclusion

It has been shown that *in vivo* lactate measurement in exercising humans was possible with the use of the NIRS in the 1500-1750nm spectral range. To improve the precision of the method, referenced measurements of lactate concentration were calculated. The model estimated referenced lactate concentrations higher than 2 mmol/L, with a standard error of 0.76 mmol/L. This approach represents a faster and non-invasive alternative to current enzymatic methods and could have significant impact in clinical situations or exercise physiological studies.

6.7 References

1. B. A. Mizock and J.L. Falk, *Crit. Care Med.*, **20**, 80-93 (1992).
2. R. J. Henning, M. H. Weil and F. Weiner, *Circ. Shock*, **9**, 307-315 (1982).
3. M. H. Weil, C. E. Ruiz, S. Michaels and E. C. Rackow, *Crit. Care Med.*, **13**, 888-892 (1985).
4. G. Broder G and M. H. Weil, *Science*, **143**, 1457-1459 (1964).
5. M. H. Weil and A. A. Afifi, *Circulation*, **41**, 989-1001 (1970).
6. J. Aduen, W. K. Bernstein, T. Khastgir, J. Miller, R. Kerzner, A. Bhatiani, J. Lustgarten, A. S. Bassin, L. Davison and B. Chernow, *JAMA*, **272**, 1678-1685 (1994).
7. J. Toffaletti J, *Scand. J. Clin. Lab. Invest. Suppl.*, **224**, 107-110 (1996).
8. B. N. Cowan, H. J. G. Burns, P. Boyle and I. M. Ledingham, *Anaesthesia*, **39**, 750-755 (1984).
9. J. L. Vincent, P. Dufaye, J. Berre, M. Leeman, P. J. Degaute and R. Kahn, *Crit. Care Med.*, **11**, 449-451 (1983).
10. D. A. Baker and D. A. Gough, *Anal. Chem.*, **67**, 1536-1540 (1995).
11. W. P. Soutter, F. Sharp and D. M. Clark, *Br. J. Anaesth.*, **50**, 445-450 (1978).
12. D. L. Williams, A. R. Doig and A. Korosi, *Anal. Chem.*, **42**, 118-121 (1970).
13. D. Pfeiffer, B. Möller, N. Klimes, J. Szeponik and S. Fischer, *Biosens. Bioelectron.*, **12**, 539-550 (1997).
14. D. L. Wang and A. Heller, *Anal. Chem.*, **65**, 1069-1073 (1993).
15. Q. Yang, P. Atanasov and E. Wilkins, *Biosens. Bioelectron.*, **14**, 203-210 (1999).

16. R. J. Gfrerer, G. A. Brunner, Z. Trijanoski, L. Schaupp, G. Sendlhofer, F. Skrabal, G. Jobst, I. Moser, G. Urban, T. R. Pieber and P. Wach, *Biosens. Bioelectron.*, **13**, 1271-1278 (1998).
17. M. Kyröläinen, H. Håkanson, B. Mattiason and P. Vadgama, *Biosens. Bioelectron.*, **12**, 1073-1081 (1997).
18. C. Meyerhoff, F. Bischof, F. J. Mennel, F. Sternberg, J. Bican and E. F. Pfeiffer, *Biosens Bioelectron.*, **8**, 409-414 (1993).
19. E. Dempsey, D. Diamond, M. R. Smyth, G. Urban, G. Jobst, I. Moser, E. M. J. Verpoorte, A. Manz, H. M. Widmer, K. Rabenstein and R. Freaney, *Anal. Chim. Acta*, **346**, 341-349 (1997).
20. W. A. Kaptein, J. J. Zwaagstra, K. Venema and J. Korf, *Anal. Chem.*, **70**, 4696-4700 (1998).
21. S. R. Ash, J. T. Poulos, J. B. Rainier, W. E. Zopp, E. Janle E and P. T. Kissinger, *ASAIO J.*, **38**, M416-M420 (1992).
22. B. Johne, K. Hansen, E. Mork and J. Holtlund, *J. Immunol. Methods*, **183**, 167-174 (1995).
23. J.B. Justice Jr., Quantitative microdialysis of neurotransmitters *J. Neurosci. Methods* **48**: 263-276, 1993.
24. G. Reach and G. S. Wilson, *Anal. Chem.*, **64**, 381A-386 (1992).
25. R. Boushel and C. A. Piantadosi, *Acta Physiol. Scand.*, **168**, 615-622 (2000).
26. H. Iwai, T. Urakami, M. Miwa, Y. Yamashita and Y. Tsuchiya, *Ther. Res.*, **21**, 1560-1564 (2000).
27. M. Oda, Y. Yamashita and M. Tamura, *Reza Kenkyu*, **25**, 204-207 (1997).

28. M. S. Thorniley, Y. A. B. D. Wickramasinghe and P. Rolfe, *Biochem. Soc. Trans.*, **16**, 978-979 (1988).
29. M. S. Thorniley, N. Livera, Y. A. B. D. Wickramasinghe and P. Rolfe, *Biochem. Soc. Trans.*, **17**, 903-904 (1989).
30. F. Wang, W. Li, F. Lin, G. Wang and H. Ding, *Ziran Kexueban*, **39**, 16-19 (1999).
31. M. A. Arnold, *Curr. Opin. Biotechnol.*, **7**, 46-49 (1996).
32. H. M. Heise, R. Marbach, Th. Koschinsky and F. A. Gries, *Artif. Organs*, **18**, 439-447 (1994).
33. H. M. Heise, *Horm. Metab. Res.*, **28**, 527-534 (1996).
34. H. M. Heise and A. Bittner, *AIP Conf. Proc.*, **430**, 282-285 (1998).
35. H. M. Heise, A. Bittner and R. Marbach, *J. Near Infrared Spectrosc.*, **6**, 349-359 (1998).
36. R. M. Marbach, Th. Koschinsky, F. A. Gries and H. M. Heise, *Appl. Spectrosc.*, **47**, 875-881 (1993).
37. U. A. Mueller, B. Mertes, C. Fishbacher, K. U. Jageman and K. Danzer, *Int. J. Artif. Organs*, **20**, 285-290 (1997).
38. M. R. Robinson, R. P. Eaton, D. M. Haaland, G. W. Koepp, E. V. Thomas, B. R. Stallard and P. L. Robinson, *Clin. Chem.*, **38**, 1618-1622 (1992).
39. D. Lafrance, L. C. Lands, L. Hornby and D. H. Burns, *Appl. Spectrosc.*, **54**, 300-304 (2000).
40. D. Lafrance, L. C. Lands, L. Hornby, C. Rohlicek and D. H. Burns, *Can. J. Anal. Sci. & Spectrosc.*, **45**, 34-38 (2000).

41. D. Lafrance, L. C. Lands and D. H. Burns, *Talanta*. (Submitted June 2002).
42. L. C. Lands, L. Hornby, G. Desrochers, T. Iler and G. J. F. Heigenhauser, *J. Appl. Physiol.*, **77**, 2506-2510 (1994).
43. M. G. Sowa, J. Wang, C. P. Schultz, M. K. Ahmed and H. H. Mantsch, *Vib. Spectrosc.*, **10**, 49-56 (1995).
44. I. Noda, *Bull. Am. Phys. Soc.*, **31**, 520-552 (1986).
45. I. Noda, *J. Am. Chem Soc.*, **111**, 8116-8118 (1989).
46. I. Noda, A.E. Dowrey, C. Marcott, G. M. Story and Y. Ozaki, *Appl. Spectrosc.*, **54**, 236A-248A (2000).
47. F. Holler, D. H. Burns and J. B. Callis, *Appl. Spectrosc.*, **43**, 877-882 (1989).
48. L. S. L. Arakaki, M. J. Kushmerick and D. H. Burns, *Appl. Spectrosc.*, **50**, 697-707 (1996).
49. D. M. Haaland and E. V. Thomas, *Anal. Chem.*, **60**, 1193-1202 (1988).
50. J. J. Burmeister and M. A. Arnold, *Clin. Chem.*, **45**, 1621-1627 (1999).
51. M. K. Alam, M. R. Rohrscheib, J. E. Franke, T. M. Niemczyk, J. D. Maynard and M. R. Robinson, *Appl. Spectrosc.*, **53**, 316-324 (1999).

Chapter 7 Conclusion

7.1 *Conclusions from results obtained*

This dissertation has demonstrated the application of NIR spectroscopy for the non-invasive determination of lactate in biological fluids and tissues. The project began with quantification of lactate in human plasma. It was shown that lactate quantification at physiological concentration in complex biological matrix like human plasma by NIRS was possible. The work was made using PLS chemometrics and a leave- N -out cross-validation routine in the 2050-2400nm spectral range. The method achieved a standard error of 0.51 mmol/L using 6 PLS factors. However, the model did show some limitation for low lactate levels when larger physiological range of lactate concentration was used to build the calibration model. However, no particular grouping in the data was observed, which indicated that possible variation in plasma composition between individuals had little impact on the model. Likewise, similarities between subjects in variance along the line of identity seemed to indicate that gender had little or no impact on the data grouping. Finally, the error level achieved could make possible *ex vivo* monitoring of lactate in plasma for clinical or exercising studies, since this method may provide a faster and nondestructive alternative to current enzymatic ones.

By successfully quantifying lactate in human plasma, blood lactate was then investigated. The development of an in-line instrument to measure lactate would lead to faster diagnosis and cost savings in sample preparation time. Initially, a small data

set of rat blood was used to study the potential of NIRS for lactate quantification. From these measurements, it was shown that lactate assessment in whole blood was possible in the 2050-2400nm spectral range by using PLS chemometrics and a leave-*N*-out cross validation routine. Good correlation was observed between estimated and reference lactate levels in blood samples with the method achieving a standard error of 0.29 mmol/L. However, although tight correlation of the data was not apparent at low lactate concentrations, the large change in lactate with exercising rat was easily distinguished.

To verify that covariance was minimized by the experimental design, an extended data set of human whole blood was used in combination with standard addition of lactate. This experimental design, which included both the 30-seconds sprint and the standard additions of lactate, allowed the development of a calibration model that emphasized the contribution of lactate over other blood constituents. Good correlation was observed between estimated and reference lactate levels in blood samples with the method achieving a standard error of cross validation of 0.65 mmol/L. Furthermore, although the spiking did not reproduce exactly what was expected *in vivo*, the agreement of the data between the spiked samples and the naturally varying lactate concentrations was very good. This indicated that standard additions had little impact on the spectra besides an increase in lactate. However, the model still did show some limitation at low lactate concentrations with an increased variance, although with no particular grouping. Possible variation in blood composition between individuals had little impact on the model, since similarities

between subjects in variance along the line of identity were shown. Moreover, the large change in lactate induced by exercise and sample spiking was easily distinguished. This is also expected in illness situations.

In addition to the experimental design and the use of standard additions, the precision of the method was improved by calculating referenced measurements of lactate concentration. The suggested method minimized the error observed at low lactate concentration due to baseline variations. The model estimated referenced lactate concentrations higher than 2 mmol/L with a standard error of cross validation of 0.21 mmol/L. Based on the results shown with referenced lactate measurements, potential *ex vivo* NIRS method for the determination of lactate can then be developed for in-line monitoring system. This approach would represent a faster and nondestructive alternative to current enzymatic methods, which could have significant impact in clinical situations or exercise physiological studies.

The last part of the dissertation evaluated the potential of NIRS for *in vivo* lactate measurement in exercising humans. A FT-NIR instrument was modified to allow diffuse reflectance spectroscopy of nail finger beds. Results indicated that lactate quantification was possible in the 1500-1750nm spectral range by this method. Using PLS chemometrics and a leave-*N*-out cross validation routine, a correlation of 0.74 was observed between estimated lactate in tissue and reference lactate levels in blood samples. The method achieved a standard error of 2.21 mmol/L. Furthermore, to improve the precision of the method, referenced measurements of lactate

concentration were calculated. The model estimated referenced lactate concentrations higher than 2 mmol/L, with a standard error of 0.76 mmol/L.

7.2 *Future directions*

There are several future directions for this research. First, an assumption was made during the course of this study on Oxygen saturation and blood pH. It was discussed that the range of values of these constituents should not cause significant spectral features in the wavelength region of the analysis. However, since both are important respiratory constituent which might show correlations with the lactate measured, experimental validation of this should be done.

As discussed in Chapter 4 and 5, the referenced measurement method developed has demonstrated that precision in estimated lactate concentration could be improved. This method needs to be investigated further with an extended data set, including ill patients, to demonstrate the robustness of the model when estimating lactate concentration with different pathology. Potentially, direct measurements of lactate concentration changes could be made at patient's bedside in real-time that could improve significantly diagnosis time for medical staff and indirectly chance of survival for the patient.

Another interesting idea to develop is the use of an average spectrum from healthy subjects at rest rather than spectra from individuals as a baseline for the referenced measurement. A potential weakness of the current model would be that

current method works well when lactate level at rest is less than 2 mmol/L. However, in clinical situation, most of the time one individual's lactate level will be higher than 2 mmol/L even at rest. This could have a significant impact on diagnosis. For this reason, the ability to use an average spectrum from healthy individuals rather than the spectrum at rest of an ill patient and referenced the lactate concentration against this baseline would simplify greatly the method. To demonstrate the potential of this approach, some trials were made using an average spectrum of healthy subjects at rest rather than the individual spectra of each of the participants in the referenced measurement method. Figure 7.1 shows the second derivative of an average spectrum from ten healthy individuals. As in the other chapters of this thesis, the average spectrum was first calculated and then PLS and leave-*N*-out cross validation routines were used to estimate referenced lactate concentration. The preliminary results are very encouraging, where referenced lactate concentrations higher than 2 mmol/L, were estimated with a standard error of 1.04 mmol/L. Figure 7.2 shows the estimations of referenced lactate concentration using an average spectrum rather than spectra from each individual at rest. Results obtained are slightly higher than the one reported in Figure 6.9 (0.76 mmol/L). This could be related to the limited number of individuals to calculate the average spectrum.

This approach would especially be of use to monitor lactate level in ill patients or in critical care situations. However, the use of an average spectrum of healthy subjects in the referenced measurement method needs further development to confirm validity for all individuals. One example would be to develop the average

spectrum from a larger group of healthy subjects. Furthermore, independent differences in the fingernail thickness and color should be measured, since this would have an impact on the absolute measurements described.

Finally, the trend in modern analytical instrumentation is for miniaturization, portability and ease of use. Although all the measurements made in this project required great care, a high performance FT-NIR instrument and calibration curves, the findings made through this project will provide a framework for future developments. As example, some portable spectrometers working in the NIR range (1100-1750 nm) are already available in the market. One system (MicroParts – Steag by ALCprecision) was compared to scanning-type spectrometer in a study where skin moisture was measured.⁽¹⁾ Both systems offered similar results when compared to capacitance method to measure moisture level of *stratum corneum*. There are however several advantages to the portable spectrometer. First, spectra are taken within 2 seconds in comparison with 45 seconds for the scanning-type spectrometer. This makes the instrument less sensitive to environmental changes such as moisture or temperature variations while taking measurements. Furthermore, since there are no moving parts, the instrument is less sensitive to shocks. This suggests possible *in vivo* measurements of lactate could be made using one of these portable instruments.

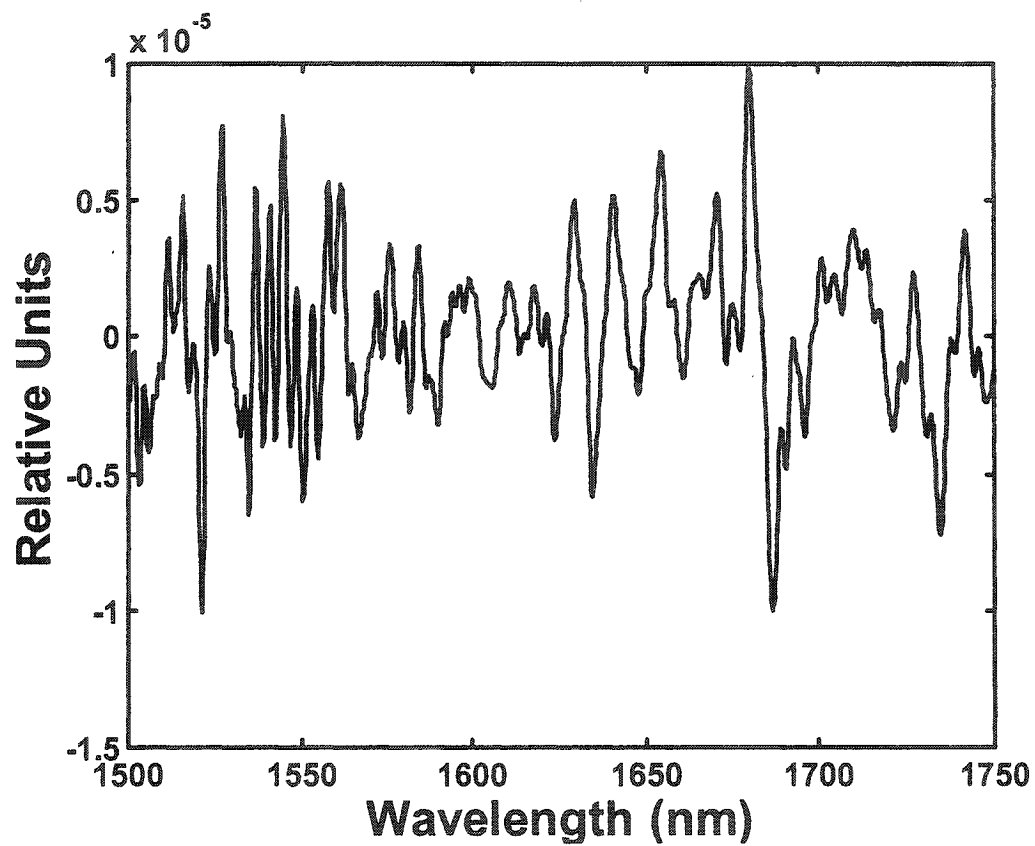


Figure 7.1: Second derivative of an average NIR absorbance spectrum from ten healthy human fingernail beds.

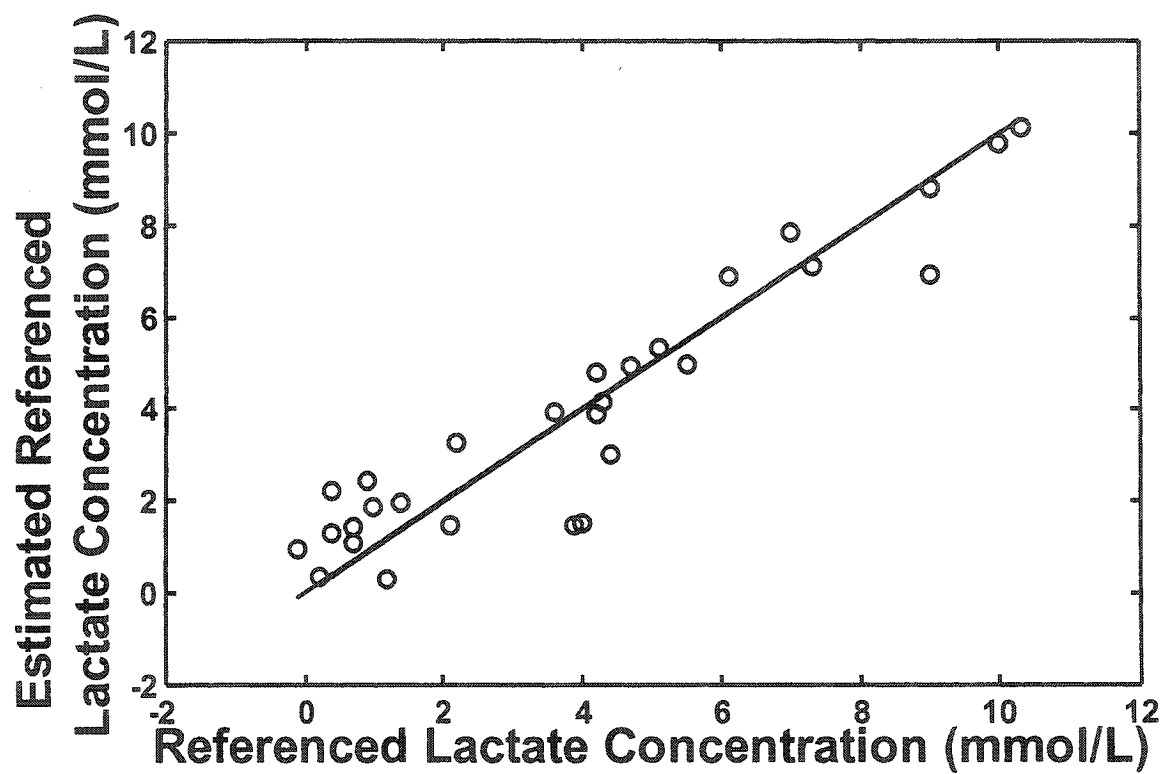


Figure 7.2: NIRS estimated vs. lactate referenced values for *in vivo* lactate measurements using the average spectrum method. Cross-validation model: based on 1500-1750 nm spectral segment; $n=30$, RMSCV= 1.04 mmol/L using a leave-4-out cross-validation procedure.

Overall, the results of this research and the availability of portable instruments suggest that a faster and nondestructive alternative to current enzymatic methods may be developed. This would have significant impact in clinical situations or exercise physiological studies.

7.3 *References*

1. Y.A. Woo, J.W. Ahn, I.K. Chun and H.J. Kim, *Anal. Chem.*, **73**, 4964-4971 (2001).

Appendix A: Partial Least Squares Analysis

The PLS method consists of extracting orthogonal factors to model the spectral response that correlates with the analyte concentrations. PLS creates new orthogonal factors (latent variables) that are linear combinations of the original x -variables. Each factor describes the co-variance between the calibration spectra responses and the analyte concentrations in decreasing amounts. The first factors describe information related to lactate concentration, while later ones are related to irrelevant information and noise in the data. The optimal number of factors is determined by using the Predicted Residual Error Sum of Squares (PRESS) and the PLS prediction of lactate concentration are obtained by multiplying the spectral responses of the test set to the calibration coefficient vector.

Using matrix notation, the “inverse Beer’s law” relationship between the lactate concentration and the measured spectrum can be described as:

$$\mathbf{C} = \mathbf{A}\mathbf{B} \quad (\text{A.1})$$

where \mathbf{C} is a matrix containing of m sample lactate concentrations ($m \times 1$) measured by the enzymatic method, \mathbf{A} contains spectra of n samples ($n \times m$) and \mathbf{B} comprises ($n \times 1$) wavelength calibration coefficients that relates changes in the spectrum to lactate content in the sample. The determination of \mathbf{B} involves writing both \mathbf{C} and \mathbf{A} into a new coordinate system where original data is compressed into loading vectors and intensities. The new coordinate can be represented as:

$$\mathbf{A} = \mathbf{C}\mathbf{W}^t + \mathbf{E} \quad (\text{A.2})$$

where \mathbf{W} is the weight loading vector and \mathbf{E} is error matrices. The weight loading vector using a least squares solution is then represented by:

$$\mathbf{W} = \mathbf{A}^t \mathbf{C} (\mathbf{C}^t \mathbf{C})^{-1} \quad (\text{A.3})$$

After normalizing \mathbf{W} , the score vector \mathbf{T} which corresponds to the contribution of the weight vector to the data set can be calculated.

$$\mathbf{T} = \mathbf{A}\mathbf{W} \quad (\text{A.4})$$

The score vector can be related to the concentration using the following equation:

$$\mathbf{C} = \mathbf{v}\mathbf{T} + \mathbf{e} \quad (\text{A.5})$$

where \mathbf{v} is the vector of coefficient relating the scores to the concentrations. The vector \mathbf{v} can be expressed as:

$$\mathbf{v} = \mathbf{T}^t \mathbf{C} (\mathbf{T}^t \mathbf{T})^{-1} \quad (\text{A.6})$$

the PLS loading vector for \mathbf{A} can then be calculated as:

$$\mathbf{A} = \mathbf{T}\mathbf{b}^t + \mathbf{E} \quad (\text{A.7})$$

$$\mathbf{b} = \mathbf{A}^t \mathbf{T} (\mathbf{T}^t \mathbf{T})^{-1} \quad (\text{A.8})$$

the spectral and concentration residuals are calculated using the equations:

$$\mathbf{E} = \mathbf{A} - \mathbf{T}\mathbf{b}^t \quad (\text{A.9})$$

$$\mathbf{e} = \mathbf{c} - \mathbf{v}\mathbf{T} \quad (\text{A.10})$$

The iteration is done by substituting \mathbf{E} for \mathbf{A} and \mathbf{e} for \mathbf{c} in equation A.2 until the desired numbers of loading vectors is reached.

The final calibration coefficient vector can be determined using the following equation:

$$\mathbf{B} = \mathbf{W}^t (\mathbf{b}\mathbf{W}^t)^{-1} \mathbf{v}^t \quad (\text{A.11})$$

The algorithm generates a series of factors, which describes decreasing amounts of variance correlating to \mathbf{C} . The optimal number of factors is determined by using the Predicted Residual Error Sum of Squares (PRESS), which is calculated as:

$$\text{PRESS} = \frac{1}{n} \sum_{i=1}^n (\mathbf{C}_i - \mathbf{A}\mathbf{B}_{(i)}^t)^2 \quad (\text{A.12})$$

and the PLS prediction of lactate concentration are obtained by multiplying the spectral responses of the test set to the calibration coefficient vector \mathbf{B} .

References

1. A. Lorber, L.E. Wangen, B.R. Kowalski, *J. Chemom.*, **1**, 19-27 (1987).
2. P. Geladi, B.R. Kowalski, *Anal. Chem. Acta*, **185**, 1-17 (1986).
3. K.R. Beebe, B.R. Kowalski, *Anal. Chem.*, **59**, 1007A-1017A (1987).
4. D.M. Haaland, E.V. Thomas, *Anal. Chem.*, **60**, 1193-1202 (1988).

Appendix B: 2D Correlation Spectroscopy

The 2D correlation spectroscopy was originally developed to analyze vibrational spectra and simplify their visualization, when dynamic spectral variations induced by an external perturbation are investigated in complex spectra.⁽¹⁻⁵⁾ Correlation analysis yields information about the similarity between two functions, that vary with respect to time as the dynamic variable t .⁽⁵⁾ In this study, the correlation between any two measured responses can be seen with respect to a given perturbation induced by the 30 second sprint on the isokinetic cycle.

According to the generalized mathematical formalism of Noda⁽³⁾, spectra intensity variation in this study can be expressed as a function of wavelength (λ) and an index τ in the time domain as $y(\lambda, \tau)$ observed during a period T . The static components and the series of dynamic spectra $\tilde{y}(\lambda, \tau)$ were calculated by subtracting a reference spectrum from each spectrum $y(\lambda, \tau)$.⁽³⁾ In this study, the first spectrum recorded at rest just before beginning the 30 second sprint was chosen as the reference spectrum. The dynamic spectra was then expressed as⁽³⁾

$$\tilde{y}(\lambda, \tau) = y(\lambda, \tau) - y(\lambda, 0) \quad (\text{B.1})$$

The correlation function $R_{\lambda_1 \lambda_2}(\tau)$ is the product of the two functions for which one function is shifted by a time constant t , with respect to the other function.⁽⁵⁾

$$R_{\lambda_1 \lambda_2}(\tau) = \int_{-\infty}^{\infty} y(\lambda_1, \tau) y(\lambda_2, \tau + t) d\tau \quad (\text{B.2})$$

The integral will be large for functions that are highly correlated with one another at a given τ . Inverse relationship will yield negative numbers.⁽⁵⁾ Integrals that are relatively small in magnitude will be obtained for functions that are varying nearly independently of one another. Finally, the correlation function evaluated at a τ of 0 measures the covariance between λ_1 and λ_2 .⁽⁵⁾

To obtain generalized 2D correlation spectra, time domain dynamic spectra needed to be converted into the frequency domain using Fourier transform.⁽³⁾ The complex two-dimensional correlation was then defined as⁽³⁾

$$\Phi(\lambda_1, \lambda_2) + i\Psi(\lambda_1, \lambda_2) = \frac{1}{\pi T} \int_0^\infty \tilde{Y}_1(\omega) \tilde{Y}_2^*(\omega) d\omega \quad (\text{B.3})$$

where $\tilde{Y}_1(\omega)$ represented the Fourier transform of the spectral intensity variations $\tilde{y}(\lambda_1, \tau)$ and $\tilde{Y}_2^*(\omega)$ was the related conjugate of the Fourier transform of $\tilde{y}(\lambda_2, \tau)$. The real part contains information about the correlations in the response variables that occur in-phase. The imaginary part contains information about correlations that occur out-of-phase, which means that change in values of one variable lags behind the changes of the other.⁽⁵⁾ After integration of the non-negative frequencies, the real part of the equation B.2 is called the synchronous 2D correlation intensity, while the imaginary part is called the asynchronous.⁽¹⁻⁵⁾ It should be noted that the synchronous and asynchronous spectra exhibit only features that are correlated at the same frequency.⁽⁵⁾

As mentioned earlier, the synchronous spectrum represents the simultaneous or coincidental changes of spectral intensity variations measured at two different wavelengths (λ_1, λ_2) during the 10 minutes interval chosen for this experiment. Similarly, the synchronous 2D correlation intensity for N dynamic spectra was given by the equation:⁽³⁾

$$\Phi(\lambda_1, \lambda_2) = \frac{1}{N-1} \sum_{j=1}^N \tilde{y}_j(\lambda_1) \cdot \tilde{y}_j(\lambda_2) \quad (\text{B.4})$$

where $\tilde{y}_j(\lambda_i)$ was the spectral intensity at a wavelength λ_i and a time interval t_j .

In contrast, the asynchronous spectrum represents the sequential or successive information changes in spectral intensities measured at two different wavelengths (λ_1, λ_2) .^(3,4) However, unlike the synchronous spectrum, the asynchronous 2D correlation intensity is more complicated to compute. An efficient way to determine N dynamic spectra was given by the expression:⁽³⁻⁴⁾

$$(\lambda_1, \lambda_2) = \frac{1}{N-1} \sum_{j=0}^N \tilde{y}_j(\lambda_1) \cdot \sum_{k=1}^N M_{jk} \cdot \tilde{y}_k(\lambda_2) \quad (\text{B.5})$$

where M_{jk} corresponds to the j th row and the k th column element of the discrete Hilbert-Noda transformation matrix given by:⁽⁴⁾

$$M_{jk} = \begin{cases} 0 & \text{if } j = k \\ 1/\pi (k - j) & \text{otherwise} \end{cases} \quad (\text{B.6})$$

References

1. I. Noda, *Bull. Am. Phys. Soc.*, **31**, 520-552 (1986).
2. I. Noda, *J. Am. Chem Soc.*, **111**, 8116-8118 (1989).
3. I. Noda, *Appl. Spectrosc.*, **47**, 1329-1336 (1993).
4. I. Noda, A.E. Dowrey, C. Marcott, G. M. Story and Y. Ozaki, *Appl. Spectrosc.*, **54**, 236A-248A (2000).
5. P. de B. Harrington, A. Urbas and P.J. Tandler, *Chem. Intel. Lab. Sys.*, **50**, 149-174 (2000).

Appendix C: Ethic Committee Approval



GLUTATHIONE STATUS IN CYSTIC FIBROSIS

Department of Respiratory Medicine
The Montreal Children's Hospital

The goal of this study is to test whether individuals with Cystic Fibrosis have altered blood chemistry because of an inability to cope with the damaging effects of oxygen free radicals. Oxygen free radicals are produced as a result of increased metabolism, as can occur with infection and inflammation. This study will also examine whether a nutritional supplement, based on cow's milk whey protein, can improve the body's ability to cope with oxygen free radicals. Participants for this study must be over the age of 18 years and be diagnosed with cystic fibrosis (CF). Participants must not be severely malnourished (weight > 80% ideal), or have a history of intolerance to cow's milk protein. Participants with CF must have relatively mild lung disease and not have been admitted to hospital in the previous two months prior to the study.

This study involves baseline measurements made during 2 visits, which are repeated after 12 weeks of nutritional supplementation for a total of 4 visits.

Baseline: Participants will have a standardized breakfast (one glass of low fat milk, two slices unbuttered toast with jam, one glass of juice) and will not have engaged in strenuous exercise or consumed any alcoholic beverage in the previous 48 hours, or caffeine in the previous 12 hours.

During the first session, you have their height and weight measured. Body fat percentage will be determined by measuring the thickness of skinfolds on your arm, back and stomach. You will do breathing tests to look at lung capacity. A small amount of blood (15 mL or 1 Tbsp) will be taken from your arm after the intravenous line has been placed. Fifteen minutes later, you will perform an exercise session on a cycle. During this session the amount of work you do will be steadily increased until you are too tired to continue, usually in less than 15 minutes. You will wear a nose clip and breathe through a mouthpiece throughout the session so that your breathing can be measured and your exercise capacity determined. Your heart rate and rhythm will also be closely monitored and recorded by an electrocardiogram. Two more blood samples (15 mL or 1 Tbsp each) will be taken, one immediately following the test, and the other 5 minutes later. The total amount of blood removed for the four tests will be 45 mL (3 Tbsp). The other measure will be done on chest secretions. We know that some people have trouble bringing up their secretions. We will loosen and help the secretions to come up by first giving you a bronchodilator medication called Ventolin (a drug which opens the air passages, making it easier to breathe), from a disk inhaler. You will then inhale 5% sterile saline (salty water) being delivered by a nebulizer. Throughout the inhalation, you will be encouraged to cough, and the inhalation will actually be interrupted every 3 minutes for you to rinse out your mouth with water and then to forcefully cough up lung secretions into a separate container. The inhalation procedure will continue until the quantity of sputum is satisfactory, which should be achieved in less than 20 minutes.

During the second session, the same procedure will be repeated except that you will cycle as hard as you can for 30 seconds on another cycle, 3 hours after the first blood test. As you cycle, your heart rate and rhythm will be closely monitored and recorded by an electrocardiogram. Your leg strength and your total work output will also be determined. A second blood test will be performed immediately following exercise, and 5 minutes later (total 45 ml or 3 Tbsp). After a rest period of at least 30 minutes, you will then go back on the cycle and will be asked to maintain a force output of 80% of your previously achieved maximum for as long as you can. Again, as described above you will be asked to breathe 5% saline and cough up chest secretions.

Each session will take approximately 3 hours to complete.



Appendix D: Copyright Clearance


Work With RLS Order

Account#: 2000126289

Order ID	Document Reference	Title	Circulation/Distribution	Republication Format	Request Date
880962	DOCTORAL THESIS	NEAR INFRARED DETERMINATION OF LACTATE IN BIOLOGICAL FLUIDS AND TISSUES	10	Other Book	8/16/2002

[Cancel Order](#) [Credit Line Information](#) [Order Item From Another Publication](#) [Pre-Invoice Information](#)**Permission Request Details (Click here for Help)**

Choose an item to view or modify by clicking on the Order Detail ID.

	Title of Publication	Type of Content	Content Description	Response Status
	APPLIED SPECTROSCOPY	Full Article	NEAR INFRARED SPECTROSCOPY MEASUREMENT O	Yes
Order Detail ID: 8684256		Cancel Item Add Another Item From This Same Publication	Total Fee: 0.00	

Choose an item to view or modify by clicking on the Order Detail ID. You may now click the [Search](#) button at the top or bottom of the page to request permission to use another publication.

Copyright © 1995-2002, Copyright Clearance Center, Inc. 222 Rosewood Drive, Danvers, MA 01923 USA.
Phone 978-750-8400 Fax 978-750-4470 [Online Privacy Policy](#) | [Contact Us](#)



Terms and Conditions

Account#: 2000126289

Please review the terms and conditions for reproducing copyrighted content you have requested from *APPLIED SPECTROSCOPY*. CCC's standard RLS Terms and Conditions are available at the link lower on this page. For your protection and to ensure your complete satisfaction, your order will not be placed until you have accepted the terms and conditions.

To place your order, please click "accept" at the bottom of the terms and conditions.

Permission Availability : Yes

Total Fee: \$0.00

[RLS Terms and Conditions](#)

Copyright Clearance Center, Inc.
Republication Licensing Service (RLS) Terms and Conditions
(which apply to all RLS license transactions)

1. Licenses are granted by Copyright Clearance Center, Inc. ("CCC"), as agent for the rightsholder identified on the Order Confirmation (the "Rightsholder"), and are for republication of a copyrighted work as described in detail on the Order Confirmation (the "Work"). "Republication," as used herein, generally means the inclusion of the Work, in whole or in part, in a new work which is also described on the Order Confirmation. CCC provides this license through its Republication Licensing Service (or